If the whole process of modeling has succeeded, something will have happened in our head, namely that an understanding of the relationships has emerged.

- Volker Grimm

University of Alberta

LINEAR FEATURES IMPACT PREDATOR-PREY ENCOUNTERS: ANALYSIS WITH FIRST PASSAGE TIME

by

Hannah White McKenzie 

A thesis submitted to the Faculty of Graduate Studies and Research in partial fulfillment of the requirements for the degree of **Master of Science**

in

Mathematical and Statistical Biology

Department of Mathematical and Statistical Sciences
Department of Biological Sciences

Edmonton, Alberta
Fall 2006

Your file Votre référence
ISBN: 978-0-494-22322-2
Our file Notre référence
ISBN: 978-0-494-22322-2

Abstract

Landscapes are heterogeneous and animals respond to this heterogeneity by altering their movement patterns. This thesis was motivated by the need to understand the impact of a particular type of heterogeneity, anthropogenic linear features, on wolf (*Canis lupus*) movement in the central east slopes of the Rocky Mountains (Alberta, Canada). First passage time refers to the length of time taken to first encounter an object, such as a prey item. Novel first passage time analysis methods for animal movement were developed and applied to wolves in the presence of linear features. The underlying movement model was parameterized using paths obtained from GPS collars. These animal movement paths were confounded by measurement error. I developed a mechanistic, empirically-based method for buffering linear features that minimized the underestimation of animal use of linear features introduced by GPS measurement error. Mean first passage time analysis showed that wolves found prey faster in landscapes with higher densities of linear features, resulting in an increased functional response, which was most prominent at low prey densities. These findings have implications for management of species at risk in highly developed landscapes.

Acknowledgements

I am greatly appreciative to NSERC, Alberta Ingenuity, and the University of Alberta who provided financial support for this research. I would also like to recognize the funding partners for the CESES project. MITACS provided a travel grant which allowed me to collaborate with researchers at the University of Saskatchewan.

My co-supervisors Dr. Mark Lewis and Dr. Evelyn Merrill who's unique perspectives, support, and encouragement were instrumental in the completion of this thesis and my growth as a scientist and a person. To my committee members Dr. Colleen Cassady St. Clair and Dr. Subhash Lele for being active members of my committee.

The Lewis lab, especially Alex for numerical advice; Amy for being my partner in wolf movement crime; Bill for being a dedicated and supportive mentoring post-doc; Cecelia for administrative support; Caroline, Chris, and Marjorie for all the kinds of support necessary to get through a thesis alive; Hawthorn for priceless GIS assistance; Mark D and Caspar for indispensable technical assistance; Marty and Peter for their positive philosophy; Tomas for invaluable Mathematica and Latex tips.

The Merrill lab, especially Darcy for his humour and general handyness; Doris, and later Shevenell for their administrative support; Maria for her laughter; Nate for his field knowledge and the fact that he was always ready to help in any way he could; Phil for random ArcMap tidbits; Stephen for interesting discussion; and to Mark H. and Jacqui for their guidance.

To Julia who was my guide and companion through happy winter days of fieldwork, and everyone else at the Nordegg field house.

To Jim Allen and everyone at the Nordegg ranger station for their assistance. Dr. Ray Spiteri for his guidance regarding all things numerical. Thomas Hillen for giving me "life-counselling", which came in quite handy in the last few weeks of thesis writing!

To those who foster the non-academic side of my life (without you I would simply disappear into geek-dome...) Courtney, Caley, and Bella for getting me settled in Edmonton. Jen, John, Smoke, Samwise, and Checkov for their company and support. Lea for many wonderful dinners.

To my parents, who's support has, and will continue to be, one of the most important parts of my life.

Finally, I wish to acknowledge everyone I have crossed paths with during my lifetime, as they have contributed in some small way to making me the person I am today.

This thesis is dedicated to Beverly and John Mckenzie.

Contents

List of Tables

List of Figures

Chapter 1

Introduction

Natural landscapes are spatially heterogeneous. Variation in landscape structure and composition influences animal movement rates and directionality (Weins, 2001). Because movement is a fundamental component of many animal interactions spatial heterogeneity must be considered. One question about animal movement is: At what rate do animals encounter features of their landscape? This question, which has not previously been addressed using mechanistic movement models, is the topic of this thesis. The theoretical work is motivated by a need to understand the predator-prey relationship between wolves and ungulates in the central east slopes of the Rocky mountains, Alberta, Canada, where anthropogenic linear features create a heterogeneous landscape.

Chapter 1 develops a method necessary for the subsequent analysis of wolf movement data in Chapter 3 by addressing the problem of GPS measurement error in the wolf locations. Ignoring GPS measurement error may result in incorrect calculation of movement distributions (Jerde and Visscher, 2005), and misinterpretation of movement behaviours (Hurford, 2005) or habitat selection patterns (Samuel and Kenow, 1992; Rettie and McLoughlin, 1999; Frair et al., 2004). I develop and demonstrate a mechanistic, empirically-based method for buffering linear features that minimizes the underestimation of animal use of linear features introduced by GPS measurement error.

Chapter 2 reviews and expands current mathematical approaches to modeling animal movement. I show that mean first passage time, the average time taken for an animal to reach a specified site (or set of sites) in the landscape for the first time (Berg, 1993; Redner, 2001), provides a way of understanding how landscape heterogeneity affects search times. Using the random walk framework, I derive a

new equation for the mean first passage time in a heterogeneous landscape. The ability of mean first passage time to capture the effect of changes in small-scale animal movements on landscape-level processes is illustrated with a simple model of a territorial predator searching for prey. Solutions to the mean first passage time equation are used to extend Holling's disk equation by including different searching movement behaviours.

The focus of Chapter 3 is understanding the potential effects of increasing linear feature development on wolf-ungulate interactions. Previous studies have found linear features alter animal movement (Jalkotzy et al., 1997). Although most species experienced negative impacts, positive effects were observed for predators. For example, wolves used seismic lines and trails as travel corridors (James and Stuart-Smith, 2000; Whittington et al., 2005) and moved over two times faster on seismic lines than in the forest (James, 1999). In contrast, seismic lines were associated with a higher risk of predation for ungulates (James and Stuart-Smith, 2000; Frair et al., 2005). These observations suggest linear features, and seismic lines in particular, may alter wolf-ungulate interactions. I quantified wolf movement in relation to seismic lines by considering how characteristics of a wolf's movement path changed as a function of distance from seismic lines. I used the mean first passage time model developed in Chapter 2, parameterized with wolf movement data, to determine the potential effects of small-scale response to seismic lines on the time to find a prey, and potential impact on the wolf's functional response.

In my concluding remarks I draw connections between chapters and indicate areas of future work.

Literature cited

Berg, H. 1993. Random Walks in Biology. Princeton University Press.

Frair, J., E. Merrill, D. Visscher, D. Fortin, H. Beyer, and J. Morales. 2005. Scales of movement by elk (Cervus elaphus) in response to heterogeneity in forage resources and predation risk. Landscape Ecology **20**:273–287.

Frair, J., S. Nielsen, E. Merrill, S. Lele, M. Boyce, R. Munro, G. Stenhouse, and H. Beyer. 2004. Removing GPS collar bias in habitat selection studies. Journal of Applied Ecology **41**:201 – 212.

Hurford, A., 2005. Wolf movement within and beyond territory boundary. Master's thesis, University of Alberta.

Jalkotzy, M., P. Ross, and M. Nasserden, 1997. The Effects of Linear developments on Wildlife: A Review of Selected Scientific Literature. Technical report, Arc Wildlife Services Ltd.

James, A., 1999. Effects of Industrial Development on the Predator-Prey Relationship Between Wolves and Caribou in Northeastern Alberta. Ph.D. thesis, Universtiy of Alberta.

James, A., and A. Stuart-Smith. 2000. Distribution of caribou and wolves in relation to linear corridors. Journal of Wildlife Management **64**:154–159.

Jerde, C., and D. Visscher. 2005. GPS measurement error influences on movement model parameterization. Ecological Applications **15**:806 – 810.

Redner, S. 2001. A Guide to First-Passage Processes. Cambridge University Press.

Rettie, W., and P. McLoughlin. 1999. Overcoming radiotelemetry bias in habitat-selection studies. Canadian Journal of Zoology **77**:1175 – 1184.

Samuel, M., and K. Kenow. 1992. Evaluating habitat selection with radiotelemetry triangulation error. Journal of Wildlife Management **56**:725 – 734.

Weins, J., 2001. Dispersal, Chapter the landscape context of dispersal, pages 96–109. Oxford University Press.

Whittington, J., C. St. Clair, and G. Mercer. 2005. Spatial responses of wolves to roads and trails in mountain valleys. Ecological Applications **15**:543 – 553.

Chapter 2

Assessing linear feature use in the presence of GPS measurement error

2.1 Introduction

Global Positioning System (GPS) collars are used frequently by ecologists to collect location data for animals moving across a landscape. The data can be used to classify animal locations into habitats or to recreate movement paths for the purposes of testing hypotheses about habitat use, movement, and behavior. However, location data is subject to measurement error (Thomas et al., 1993). As such, it is necessary to incorporate location error into analysis techniques to ensure correct biological inference. For example, if measurement error is ignored, habitat selection patterns may be misinterpreted (Samuel and Kenow, 1992; Rettie and McLoughlin, 1999; Frair et al., 2004), movement distributions miscalculated (Jerde and Visscher, 2005), or behaviors misinterpreted (Hurford, 2005).

A number of studies have addressed the measurement error associated with telemetry data (Nams and Boutin, 1991; Samuel and Kenow, 1992; Rettie and McLoughlin, 1999; D'eon and Delparte, 2005; Jerde and Visscher, 2005), but see Saltz (1994)). The most commonly used approach is to buffer locations by replacing the point location with an area of fixed radius. The buffer accounts for the imprecision in the location by assuming the animal is located within an area rather than at an exact point location. A uniform distribution of measurement error is usually implicitly assumed without obtaining support from observed data (but see Samuel and Kenow (1992)). Furthermore, there is no consistent method for choosing

the buffer radius, leading to widely varying buffer sizes (e.g., Dickson and Beier (2002), McLoughlin et al. (2002), and Dickson et al. (2005)). It is not clear how sensitive the biological conclusions in the above studies were to the choice of buffer radius, or whether it is reasonable to compare results from studies where different buffer radii were used.

Linear anthropogenic features, such as roads, seismic lines, and pipelines, are ubiquitous in many North American landscapes (Timoney and Lee, 2001) and are known to alter animal distribution, movement, and behaviour (Thurber et al., 1994; James, 1999; Dyer et al., 2001, 2002; Whittington et al., 2005). Measurement error creates a particularly difficult problem for detecting animal use of linear features because the width of a linear feature is generally less than the measurement error (McLoughlin et al., 2002). Consequently, there is increased probability the location will be classified as off a linear feature when in truth it is on the linear feature (Type I error), resulting in a bias towards underestimating linear feature use (McLoughlin et al., 2002; Rettie and McLoughlin, 1999).

Here we develop a mechanistic, empirically-based method of buffering linear features addressing the underestimation bias caused by GPS measurement error. We illustrate how to select an appropriate buffer radius that accounts for both the error distribution and the width of the linear feature such that bias introduced by measurement error is minimized. This method is an advancement over previous approaches because it is based on an empirical distribution of measurement error and an *a priori* accepted level of location misclassification. We also show how to test for the robustness of the location classification against the two types of error. Here Type I error is the misclassification of a location off a linear feature when the true location is on, and Type II error is the misclassification of a location on a linear feature when the true location is off. We demonstrate the effectiveness of the method at reducing the Type I error using simulated location data and illustrate how considering measurement error changes our inference of linear feature use.

2.2 Exposition of the theoretical approach

Quantifying the error distribution. The distribution of GPS measurement error describes the probability of observing a location $\hat{\mathbf{x}} = (\hat{x}, \hat{y})$ at a given distance from the true location $\mathbf{x} = (x, y)$. The error $|\hat{\mathbf{x}} - \mathbf{x}|$, which follows a distribution, reflects the precision of locations obtained by the GPS collar. For example, a leptokurtic error distribution, such as the Laplace, has a larger number of short and long

measurements than an equivalent normal distribution with the same variance (Kot et al., 1996).

We propose symmetric two-dimensional normal (Eq 2.1a), exponential (Eq 2.1b), and Bessel (Eq 2.1c) distributions as potential models for the distribution of GPS measurement error. We write the two-dimensional distributions in one dimension by transforming locations to Euclidean distances using the substitution $r = \sqrt{(\hat{x}-x)^2 + (\hat{y}-y)^2}$. To compare the models to the observed measurement error, it is necessary to multiply each of Eq 2.1a-c by $2\pi r$ to account for the transformation from one to two-dimensions.

$$\text{(a) } f_\sigma(r \mid \mathbf{x}) = \frac{1}{2\pi\sigma^2} e^{-\frac{r^2}{\sigma^2}} \quad \text{(b) } f_\beta(r \mid \mathbf{x}) = \frac{1}{2\pi\beta^2} e^{-\frac{r}{\beta}} \quad \text{(c) } f_\rho(r \mid \mathbf{x}) = \frac{\rho^2}{2\pi} K_0(\rho r) \tag{2.1}$$

Here σ, β, and ρ are parameters and K_0 is the modified Bessel function of the second kind (Appendix 2.A). These models were chosen because they represent a range of shapes from mesokurtic to leptokurtic (Figure 2.1A). We considered only symmetric models because the acquisition of GPS locations is not directionally biased (Moen et al., 1996). Model selection techniques are used to determine which of the three models is the best representation of the GPS measurement error.

Selecting the buffer. The best model of the error distribution is used to select a buffer for the linear features, which reduces the location misclassification introduced by the measurement error. We derive a method for choosing the appropriate buffer radius in a hypothesis testing framework. The radius is chosen by finding the rejection region of the test of the null hypothesis that the true location is somewhere on the linear feature against the alternate hypothesis that the true location is not on the linear feature, where the test statistic is the observed location $\hat{\mathbf{x}}$. Under the null hypothesis, the distribution of the observed location $f_\Theta(\hat{x})$, where Θ is a generalized parameter, is derived in Appendix 2.B. The amount of acceptable Type I error (α) is specified *a priori* and corresponds to the proportion of location estimates classified as off the linear feature when the true location is actually on the linear feature. The choice of α fixes the position of the rejection region, and thus the half-width of the buffered linear feature (Figure 2.2). The rejection region is found by solving

$$\int_0^B f_\Theta(\hat{x})\, d\hat{x} = \alpha/2 \tag{2.2}$$

for the quantity B, which is the half-width of the buffered linear feature.

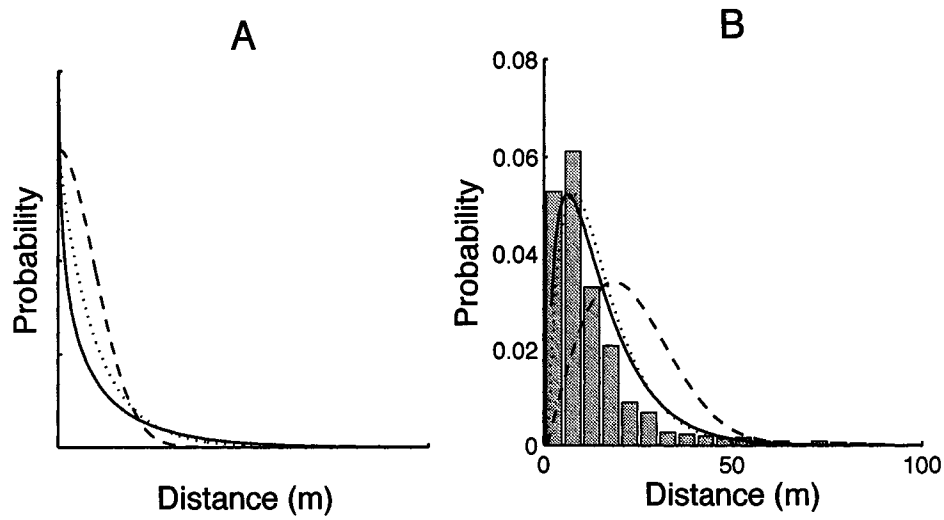

Figure 2.1: A) Candidate models for the distribution of GPS measurement error. Normal (dashed), exponential (dotted), and Bessel (solid) distributions are shown with comparable variances. B) Maximum likelihood fits of the candidate models to the data (gray bar).

Assessing robustness to Type I and Type II error. The robustness of the location classification is evaluated using the power function $\beta(\mathbf{x})$ (Appendix 2.C), which shows the expected Type I and Type II errors for location on and near the linear feature. Formally, the power function represents the probability that the null hypothesis will be rejected given a true location, $\mathbf{x}$, and is particularly useful because it graphically represents both Type I (α) and Type II (β) errors simultaneously. The Type I error described by $\beta(\mathbf{x})$ is different from the Type I error specified by α in Eq 2.2 because the hypotheses under consideration are slightly different. Previously we knew only the true location was on the linear feature, whereas for $\beta(\mathbf{x})$ we know the true location, leading to a different value of α. The types of error can be calculated directly from the graph of the power function. For a location $\mathbf{x}$ on the linear feature, the Type I error is the value of the power funtion at $\mathbf{x}$. If $\mathbf{x}$ is off the linear feature the Type II error is 1 minus the value of the power function at $\mathbf{x}$. Ideally the power function would be 0 for any $\mathbf{x}$ that is on the linear feature and 1 for any $\mathbf{x}$ that is off the linear feature. In other words, for a true location on the linear feature

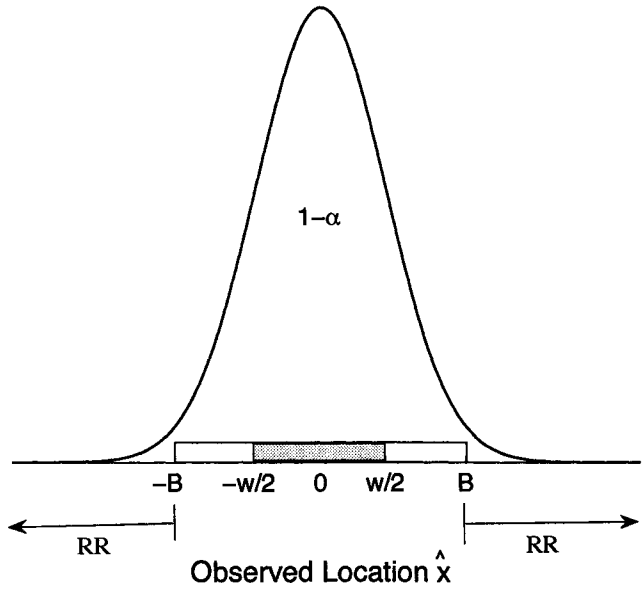

Figure 2.2: Rejection regions (RR) for testing the hypothesis that the true location is on the linear feature of width w, based on the distribution of the observed location $f_\Theta(\hat{x} \mid x \in \Omega)$, where Θ represents the parameter of the distribution and Ω corresponds to the region on the linear feature. The linear feature is shown in gray and the buffer in white.

we should never observe a location estimate off the linear feature, and vice versa. It is not possible to achieve this ideal because of the measurement error, but an appropriate buffer will have a power function near 0 for all $\mathbf{x}$ on the linear feature and close to 1 for all $\mathbf{x}$ off the linear feature (Casella and Berger, 2002).

2.3 Methods

Data. Two sets of GPS data were collected in the central east slopes of the Rocky Mountains, Alberta, Canada (52°27′ N, 115°45′ W) using a Lotek GPS_3300 collar (Lotek Wireless, Ontario, Canada). To select between candidate models for the distribution of GPS measurement error, location data were collected from a GPS collar placed in closed conifer forest 1 m off the ground recording location estimates

at 5-minute intervals over 4 days in February 2005 (n = 1422). The law of large numbers states that if observations are independent, then the sample mean is a consistent estimator for the population mean in the absence of bias (Casella and Berger, 2002). We assume there is no directional bias in location estimates (Moen et al., 1996), so given the large sample size, we use the mean to estimate the true location.

To assess the performance of the best model for the GPS error distribution, data were collected from a collar placed at 9 consecutive locations along a transect perpendicular to a 6.2 m wide linear feature. Locations were recorded at 5-minute intervals for 24 hours at the center and edges, as well as 25, 50, and 75 meters on either side of the linear feature. These distances were chosen from estimated standard deviations of GPS collars (D'eon and Delparte, 2005) so as to vary the amount of overlap between the error distribution and the linear feature.

Model selection and validation. To determine the best model for the error distribution of the Lotek GPS_3300 collar, the three candidate models for measurement error distribution were fit to the location data using maximum likelihood. Maximum likelihood estimates for the parameters of the normal and exponential distributions are

$$\hat{\sigma} = \sqrt{\frac{\sum_{i=1}^{n} r_i^2}{2n}} \quad \text{and} \quad \hat{\beta} = \sqrt{\frac{\sum_{i=1}^{n} r_i}{2n}}. \tag{2.3}$$

The maximum likelihood estimate for the Bessel distribution parameter was found numerically by maximizing the log likelihood function,

$$LL(\rho \mid r_1, \ldots, r_n) = \sum_{i=1}^{n} \log\left(\frac{\rho^2}{2\pi} K_0(\rho r_i)\right), \tag{2.4}$$

using the BFGS quasi-Newton method implemented by Mathematica (Wolfram Research, Inc.). In all likelihood estimates, r_i is the distance of the i^{th} location from the true location and n is the sample size. Confidence intervals for the parameter estimates were constructed using the parametric bootstrap (Efron and Tibshirani, 1993). The best model was selected using Akaike Information Criterion (AIC) (Burham and Anderson, 1998).

To validate the model, for each transect location we found the proportion of observed locations on the linear feature and compared this with the proportion predicted by the model. The relevant measure for calculating the proportion of locations predicted by the model to be on the linear feature is the marginal

distribution $f_\Theta(\hat{x} \mid x)$ of the model $f_\Theta(r \mid \mathbf{x})$. The marginal distribution describes the univariate distribution of $\hat{x}$ for all values of $\hat{y}$. Thus, the proportion of locations predicted by the model to be on the linear feature, for each transect location, is the integral of $f_\Theta(\hat{x} \mid x)$ from $-w/2$ to $w/2$, where w is the width of the linear feature and x is the transect location. We compare the observed proportions to the model predictions using non-parametric bootstrapped confidence intervals (Efron and Tibshirani, 1993). It was possible to do this only for the three central transect locations because all others had fewer than 25 locations observed on the linear feature (Efron and Tibshirani, 1993). We used Bonferroni adjusted 90% confidence intervals to protect experiment-wide error.

2.4 Results

The distribution of measurement error. All collars had fix rates (i.e. # successful locations/total # attempted locations) of greater than 97%. The observed distribution of GPS error was peaked with several long distance outliers (Figure 2.1B), and the Bessel model was the best representation of the empirical distribution of GPS measurement error (Table 2.1). The marginal distribution of the Bessel model is the Laplace distribution (Broadbent and Kendall, 1953). Therefore, the predicted proportion of locations on the linear feature given the transect location x, is

$$\hat{p} = \int_{-w/2}^{w/2} \frac{\rho}{2} e^{-\rho|\hat{x}-x|}\, d\hat{x}. \tag{2.5}$$

The closer the true location was to the center of the linear feature, the greater the proportion of location estimates observed and predicted to be on the linear feature (Figure 2.3). In all cases the predicted proportion was either within or near ($< 1\%$) the Bonferroni adjusted 90% confidence intervals, indicating that the Bessel model is a good representation of the observed GPS error distribution.

Buffer selection and assessment. Based on the Bessel model of error distribution, we derived the formula for the half-width of the buffered linear feature using (Eq 2.2) and replacing the general distribution $f_\Theta(\hat{x})$ with $f_\rho(\hat{x})$ (see Appendix 2.A). For the case where $\int_0^{w/2} f_\rho(\hat{x})\, d\hat{x} < \alpha/2$, meaning the probability of observing a location between the center and edge of the linear feature is less than $\alpha/2$, the half-width of

Table 2.1: Results of maximum likelihood parameter estimation and model selection. Confidence intervals for the parameters are shown in brackets.

Model	Parameter Estimates (95% C.I.)	ΔAIC
normal	$\hat{\sigma} \rightarrow 17.7213\ (17.2694, 18.1979)$	2617
exponential	$\hat{\beta} \rightarrow 7.0157\ (6.7588, 7.2522)$	190
Bessel	$\hat{\rho} \rightarrow 0.1123\ (0.1072, 0.1175)$	0

the buffered linear feature is given by

$$B = -\frac{\log\left\{\frac{1}{2}(1-\alpha)w\rho\,\mathrm{csch}\left(\frac{w\rho}{2}\right)\right\}}{\rho}. \tag{2.6}$$

Recall ρ is the parameter of the Bessel distribution and α is the specified amount of Type I error. For the case where $\int_0^{w/2} f(\hat{x}, \rho)\, d\hat{x} \geq \alpha/2$, meaning the probability of observing a location being between the center and edge of the linear feature is greater than $\alpha/2$, (Eq 2.2) must be solved numerically. Once the half-width of the buffered linear feature is chosen, the power function for assessing the Type I and Type II error associated with the buffer is derived in Appendix 2.B to be

$$\beta(x) = \begin{cases} 1 - e^{\rho x}\sinh(\rho B) & \text{if } x < -B, \\ e^{-\rho b}\cosh(\rho\, x) & \text{if } -B < x < B, \\ 1 - e^{-\rho x}\sinh(\rho B) & \text{if } x > B. \end{cases} \tag{2.7}$$

2.5 Example data analysis

In this section we demonstrate how to apply our approach using location data simulated with ArcGIS (ESRI) and Mathematica (Wolfram Research, Inc.). "True" locations were randomly placed in a landscape containing 9 m wide linear features, and constrained so that 250 points fell on the linear features and 750 points fell off the linear features. For each true location, an "observed" location was generated using the Bessel error distribution for the Lotek GPS_3300 collar. Buffer selection included three steps. (1) Choice of *a priori* Type I error rate. For this analysis we selected an α-level of 0.05, which means we are willing to accept a misclassification of a location off the linear feature 5 times out of 100. The choice of α will vary depending on the biological question under consideration and knowledge of the study system. The implications of the choice of α are further considered in the discussion. (2) Quantification of the error distribution. For this example, we used

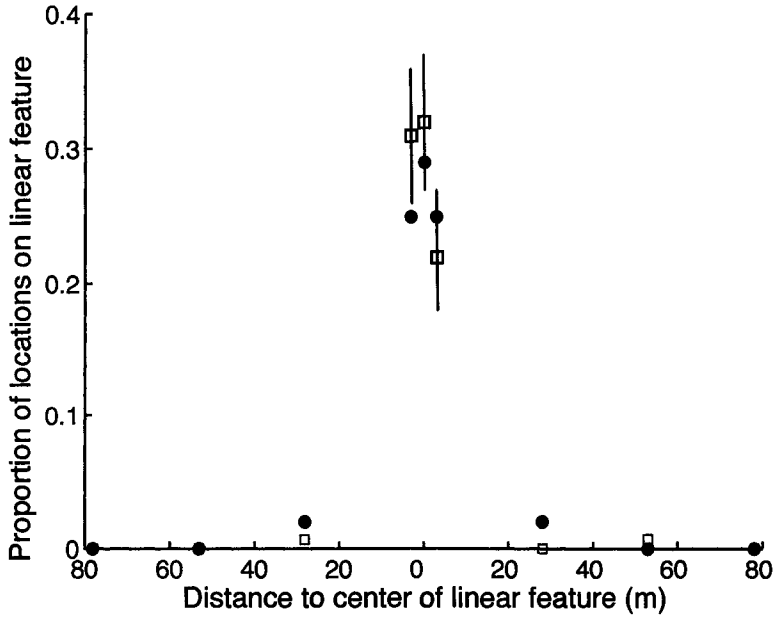

Figure 2.3: Validation of the Bessel model for GPS measurement error using a transect accross a linear feature. Circles represent the theoretical probability of being on the linear feature. Boxes represent the observed probability of being on the linear feature, shown with 90% Bonferroni adjusted C.I. where possible.

the error distribution obtained from the Lotek GPS_3300 collar, which followed the Bessel distribution with parameter $\rho = 0.1123$. (3) Calculation of the buffer. From Eq 2.6, $B = 27$ m for a linear feature width of 9 m. B represents the half-width of the buffered linear feature, so the total width of the buffered linear feature is 54 m. The buffer calculation must be repeated for each linear feature of different width. Once the buffer is selected, we graphically assess the robustness of the buffer to classification error by computing the power function (Eq 2.7) and graphing it (Figure 2.4C). The probability of Type I error ranged from 4.8% for locations at the center to 5.5% for locations at the edge. For true locations off the linear feature the probability of Type II error was high near the edge (94.5%), but dropped to 50% at the edge of the buffer (22.5 m from the edge of the linear feature), and was trivial ($< 1\%$) at 60 m from the edge of the linear feature. When the true locations are know we can directly assess the performance of the buffering method (Table 2.2).

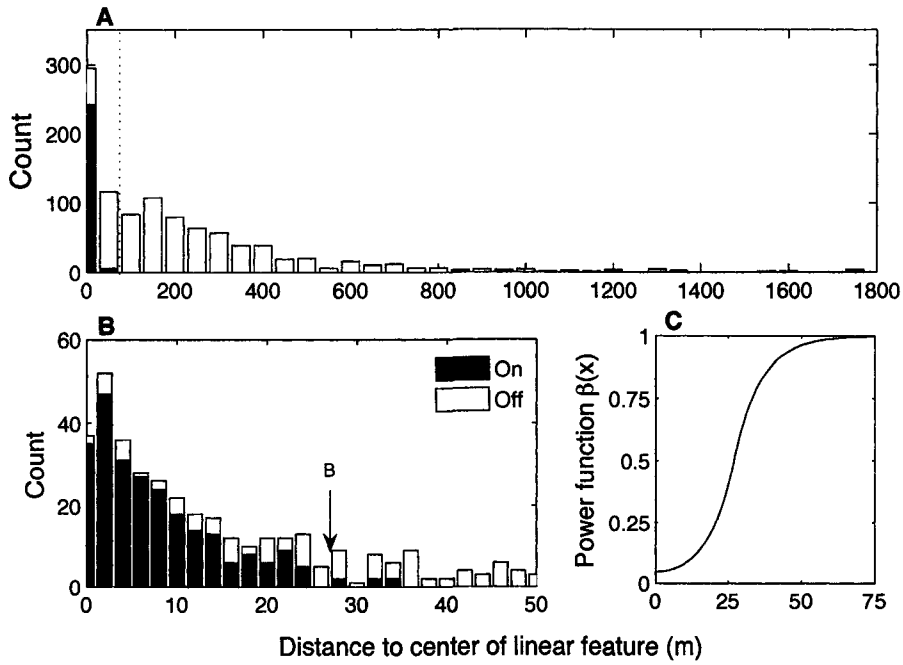

Figure 2.4: A) The distribution of distances of the simulated location data to the nearest linear feature. The region from 0 m to the dotted line is enlarged in B). The arrow labeled B indicates the edge of the buffer. C) The power function (solid line) of the buffer chosen for the example data analysis.

Table 2.2: Results of location classification for the example data. The first four columns show the number of points classified as the first habitat type, given that they are truly located in the second.

Classification	on | on	off | on	on | off	off | off	Type I Error	Type II Error	Proportion of use
Truth	250	-	-	750	-	-	0.25
No Buffer	101	149	8	742	0.60	0.01	0.11
Buffer	243	7	56	649	0.03	0.08	0.30

For example, the total number of correctly classified locations in these example data increased with the addition of the buffer from 843 to 937. Correct classification of locations on linear features increased by 57% and misclassification of locations on linear features increased by only 5%. Significant reduction in Type I error caused only a small increase in Type II error. However, the estimate of the proportion of locations on linear features changed from 0.11 to 0.30, while the true proportion was 0.25. This particular example highlights both the effectiveness and the limitations of the buffering method. The implications of these results are further addressed in the discussion.

2.6 Discussion

Measurement error is common in biological studies and often confounds our ability to detect ecological mechanisms (Rettie and McLoughlin, 1999). Here we considered the effect measurement error in GPS locations has on the classification of animal locations relative to linear features. Because linear features are usually small relative to GPS measurement error, there is a bias to underestimate animal use of linear features (McLoughlin et al., 2002). We developed a general framework for addressing measurement error and showed that incorporating measurement error into location classification reduces this bias. Our method advances previous approaches because it incorporates empirical measures of the error distribution, allowing for robust statistical inference.

We found that the Bessel distribution best represented the measurement error of the Lotek GPS_3300 collar in a closed conifer forest (Table 2.1). This result differs from previous studies where normal distributions (Jerde and Visscher, 2005; Samuel and Kenow, 1992) or uniform distributions (Conner et al., 2003) for measurement error were assumed, but were not validated. Collar type and habitat variables may affect the distribution of GPS measurement error (Moen et al., 1996; Frair et al., 2004; Cain et al., 2005), therefore researchers should quantify error distributions for each collar and habitat type. If habitat type is heterogeneous within the study area, it may be necessary to use GPS measurement error distributions specific to each habitat type. However habitat-specific distributions may increase the complexity of applying the method. Therefore, the effect of habitat type on the GPS measurement error distribution should be investigated before adopting this approach.

Adding buffers increases the area of linear features, thereby reducing bias in misclassification. While past studies have employed buffers (Dickson and Beier,

2002; McLoughlin et al., 2002; Dickson et al., 2005), there was no standard method for selecting the buffer radius. If buffer radii are chosen arbitrarily, their effects on location classification and biological inference are unknown. Our approach produces a known level of Type I error, which permits flexibility in the choice of buffer size depending on the research question. Recall that Type I error corresponds to classifying a location as off a linear feature, when in truth it is on a linear feature. For example, when it is important for conservation to understand the value of specific corridors (Haddad et al., 2003), animal behaviours associated only with linear features Dyer et al. (2001), or predator-prey interactions on linear features James (1999), a researcher is likely to choose a conservative Type I error rate to avoid underestimating linear feature use.

While our method ensures that location classification achieves a specified level of Type I error, there is no direct control of Type II error (i.e. classifying a location as on a linear feature, when in truth it is off a linear feature). Because the level of Type II is not constrained in the method, it may remain constant or increase after the application of the buffers. The probability of making a Type II error depends on the distribution of animal locations relative to the linear features. For example, if animals are found either on linear features or quite far away from linear features, buffering is unlikely to cause a large increase in Type II error. However, if the animals are often found off linear features, but near the edges, then Type II error will increase with buffering. In the latter case, the importance of the edge habitat will be missed and the importance of the linear feature overestimated. Therefore, buffers may not always lead to better estimates of habitat use since total error (i.e. the sum of the Type I and Type II errors) may increase or decrease.

Two approaches can be used to gain insight into the Type II error. First, the distribution of animal locations can be used to help determine whether Type II error is likely to remain constant or increase significantly after buffering. If there are relatively few animal locations between the edge of the linear feature and the edge of the buffer, as compared to the total number of locations, it is unlikely Type II error will increase significantly with buffering. This is not the case in our example, where locations are more uniformly distributed relative to linear features, with numerous locations occurring between the edge of the linear feature and the edge of the buffer (Figure 2.4A,B). As a result, buffering leads to an overestimation of the proportion of use of linear features (Table 2.2). This result suggests animal location data should be assessed before applying the buffering method in order to determine if Type II

error is likely to be a significant problem. Second, by inspecting the graph of the power function (Figure 2.4C), it is possible to evaluate where the probability of making a Type II error becomes small. Using these approaches to examine the data, researchers can make decisions about the trade-off between Type I and Type II error by varying the chosen value of α and comparing the corresponding power functions.

A focus on GPS measurement error and animal use of linear features is timely because GPS technology is now commonly used to acquire animal location data, linear feature densities are likely to increase in the future (Timoney and Lee, 2001), and linear features effect several aspects of animal ecology (Thurber et al., 1994; James, 1999; Dyer et al., 2001, 2002; Whittington et al., 2005). We showed that ignoring GPS measurement error may lead to location misclassification and subsequent confounded inference about animal linear feature use. We developed and demonstrated a new method of buffering linear features that reduces the Type I errors in classification of locations on linear features due to GPS measurement error. Although GPS telemetry is more accurate than traditional radio telemetry, access to more precise location data has stimulated biological inquiry at increasingly finer scales (Deutsch et al., 1998). As technology advances, it is necessary to acknowledge that limitations still exist. Rigorous methods for quantifying and addressing measurement error are needed to ensure biological investigation occurs at an appropriate scale given the measurement error inherent in the data (Ryan et al., 2004). We are confident that appropriate use of buffers to correct for GPS measurement error will lead to more accurate, consistent, and informed inference about animal use of linear features.

Appendix

2.A The modified Bessel function of the second kind

After Abramowitz and Stegun (1972), the modified Bessel function of the second kind, $K_n(x)$, is one of the solutions to the modified Bessel differential equation. For the special case where $n = 0$ it can be written as

$$K_0(x) = \int_0^\infty \frac{\cos(xt)}{\sqrt{t^2+1)}}\, dt. \qquad \text{(2.A-1)}$$

2.B The distribution of the observed locations

We derive the distribution of the observed locations $\hat{\mathbf{x}}$ where the true location $\mathbf{x}$ is on the linear feature. Given no prior information regarding the distribution of true locations, we assume a uniform distribution for $\mathbf{x}$ such that

$$\phi(x) = \begin{cases} \frac{1}{w} & x \in [-w/2, w/2], \\ 0 & \text{elsewhere.} \end{cases}$$

If prior information is available indicating that animals prefer using certain regions of the linear features, such as the edges, the procedure could be adjusted to account for this by assuming an alternate distribution for $\mathbf{x}$. Using Bayes' Rule, the marginal distribution of $\hat{\mathbf{x}}$ is given by

$$f_\Theta(\hat{x}) = \frac{1}{w}\int_{-w/2}^{w/2} f_\Theta(\hat{x} \mid x)\, dx. \tag{2.B-1}$$

Replacing the general error distribution with the Bessel model,

$$\begin{aligned} f_\rho(\hat{x}) &= \int_{-w/2}^{w/2} \frac{\rho}{2w} e^{-\rho|\hat{x}-x|}\, dx \\ &= \begin{cases} \frac{e^{\rho\hat{x}} \sinh\left(\frac{\rho w}{2}\right)}{w} & \text{if } \hat{x} < -w/2, \\ \frac{1-e^{-\frac{\rho w}{2}} \cosh(\rho\hat{x})}{w} & \text{if } -w/2 < \hat{x} < w/2, \\ \frac{e^{-\rho\hat{x}} \sinh\left(\frac{\rho w}{2}\right)}{w} & \text{if } \hat{x} > w/2, \end{cases} \end{aligned} \tag{2.B-2}$$

where the solution is found using a change of variable as in Kot et al. (1996).

2.C Derivation of the power function

Given a buffered linear feature of half-width B, the rejection region (RR) for the hypothesis test is $(-\infty, -B] \cup [B, \infty)$. The power function $\beta(x)$ is defined to be

$$\begin{aligned} \beta(x) &= P_x(\hat{x} \in RR) \\ &= \begin{cases} P(\text{Type I Error}) & \text{if } x \in [-w/2, w/2], \\ P(1 - \text{Type II Error}) & \text{otherwise} \end{cases} \\ &= 1 - \int_{-B}^{B} f_\Theta(\hat{x} \mid x)\, d\hat{x}. \end{aligned} \tag{2.C-1}$$

Replacing the general error distribution with the Bessel model and following Kot et al. (1996),

$$\begin{aligned}\beta(x) &= 1 - \int_{-B}^{B} \frac{\rho}{2} e^{-\rho|\hat{x}-x|}\, d\hat{x} \\ &= \begin{cases} 1 - e^{\rho x}\sinh(\rho B) & \text{if } x < -B \\ e^{-\rho b}\cosh(\rho x) & \text{if } -B < x < B \\ 1 - e^{-\rho x}\sinh(\rho B) & \text{if } x > B. \end{cases}\end{aligned} \tag{2.C-2}$$

Literature cited

Abramowitz, M., and I. Stegun, editors, 1972. Handbook of Mathematical Functions with Formulas, Graphs, and Mathematical Tables, 9th printing, Chapter Modified bessel functions I and K, pages 374–377 . Dover.

Broadbent, S., and D. Kendall. 1953. The random walk of the Trichostrongylus-Retortaeformis Biometrics **9**:460 – 466.

Burham, K. P., and D. R. Anderson. 1998. Model Selection and Multinomial Inference 2nd Edition. Springer.

Cain, J., P. Krausman, B. Jansen, and J. Morgart. 2005. Influence of topography and GPS fix interval on GPS collar performance. Wildlife Society Bulletin **33**:926 – 934.

Casella, G., and R. L. Berger. 2002. Statistical Inference. 2 edition. Duxbury.

Conner, L., M. Smith, and L. Burger. 2003. A comparison of distance-based and classification-based analyses of habitat use. Ecology **84**:526 – 531.

D'eon, R., and D. Delparte. 2005. Effects of radio-collar position and orientation on GPS radio-collar performance, and the implications of PDOP in data screening. Journal of Applied Ecology **42**:383 – 388.

Deutsch, C., R. Bonde, and J. Reid. 1998. Radio-tracking manatees from land and space: Tag design, implementation, and lessons learned from long-term study. Marine Technology Society Journal **32**:18 – 29.

Dickson, B., and P. Beier. 2002. Home-range and habitat selection by adult cougars in southern California. Journal of Wildlife Management **66**:1235 – 1245.

Dickson, B., J. Jenness, and P. Beier. 2005. Influence of vegetation, topography, and roads on cougar movement in southern California. Journal of Wildlife Management **69**:264 – 276.

Dyer, S., J. O'neill, S. Wasel, and S. Boutin. 2001. Avoidance of industrial development by woodland caribou. Journal of Wildlife Management **65**:531 – 542.

Dyer, S., J. O'neill, S. Wasel, and S. Boutin. 2002. Quantifying barrier effects of roads and seismic lines on movements of female woodland caribou in northeastern Alberta. Canadian Journal of Zoology **80**:839 – 845.

Efron, B., and R. Tibshirani. 1993. An Introduction to the Bootstrap. Chapman and Hall/CRC.

Frair, J., S. Nielsen, E. Merrill, S. Lele, M. Boyce, R. Munro, G. Stenhouse, and H. Beyer. 2004. Removing GPS collar bias in habitat selection studies. Journal of Applied Ecology **41**:201 – 212.

Haddad, N. M., D. R. Bowne, A. Cunningham, B. J. Danielson, D. J. Levey, S. Sargent, and T. Spira. 2003. Corridor use by diverse taxa. Ecology **84**:609–615.

Hurford, A., 2005. Wolf movement within and beyond territory boundary. Master's thesis, University of Alberta.

James, A., 1999. Effects of Industrial Development on the Predator-Prey Relationship Between Wolves and Caribou in Northeastern Alberta. Ph.D. thesis, Universtiy of Alberta.

Jerde, C., and D. Visscher. 2005. GPS measurement error influences on movement model parameterization. Ecological Applications **15**:806 – 810.

Kot, M., M. Lewis, and P. vandendriessche. 1996. Dispersal data and the spread of invading organisms Ecology **77**:2027 – 2042.

McLoughlin, P., R. Case, R. Gau, H. Cluff, R. Mulders, and F. Messier. 2002. Hierarchical habitat selection by barren-ground grizzly bears in the central Canadian Arctic Oecologia **132**:102 – 108.

Moen, R., J. Pastor, Y. Cohen, and C. Schwartz. 1996. Effects of moose movement and habitat use on GPS collar performance. Journal of Wildlife Management **60**:659 – 668.

Nams, V., and S. Boutin. 1991. What is wrong with error polygons. Journal of Wildlife Management **55**:172 – 176.

Rettie, W., and P. McLoughlin. 1999. Overcoming radiotelemetry bias in habitat-selection studies. Canadian Journal of Zoology **77**:1175 – 1184.

Ryan, P., S. Petersen, G. Peters, and D. Gremillet. 2004. GPS tracking a marine predator: the effects of precision, resolution and sampling rate on foraging tracks of African Penguins. Marine Biology **145**:215 – 223.

Saltz, D. 1994. Reporting error measures in radio location by triangulation - a review. Jouranal of Wildlife Management **58**:181 – 184.

Samuel, M., and K. Kenow. 1992. Evaluating habitat selection with radiotelemetry triangulation error. Journal of Wildlife Management **56**:725 – 734.

Thomas, D., D. Stram, and J. Dwyer. 1993. Exposure Measurement Error: Influence on Exposure-Disease Relationships and Methods of Correction. Annual Review of Public Health **14**:69–93.

Thurber, J., R. Peterson, T. Drummer, and S. Thomasma. 1994. Gray wolf response to refuge boundaries and roads in Alaska. Wildlife Society Bulletin **22**:61 – 68.

Timoney, K., and P. Lee. 2001. Environmental management in resource-rich Alberta, Canada: first world jurisdiction, third world analogue? Journal of Environmental Management **63**:387 – 405.

Whittington, J., C. St. Clair, and G. Mercer. 2005. Spatial responses of wolves to roads and trails in mountain valleys. Ecological Applications **15**:543 – 553.

Chapter 3

Animal movement in a heterogeneous environment: space use and first passage time

3.1 Introduction

Ecological processes such as dispersal, territorial defence, resource acquisition, and reproduction often occur on spatially heterogeneous landscapes in nature. Variation in landscape structure and composition has been shown to influence animal movement rates and directionality (Weins, 2001). Because movement is often an inherent component of ecological processes, these seemingly obvious observations have profound implications for dispersal, distribution, species interactions, and population dynamics (Kareiva et al., 1990; Turchin, 1991; Lima and Zollner, 1996; Weins, 2001). For example, the distribution of wolves is influenced by variation in topography, presence of conspecifics, and local prey densities (Moorcroft and Lewis, 2006). Similarly, Tewksbury et al. (2002) found that pollination and seed dispersal depended on the connectedness of the landscape. These examples highlight two central questions in spatial ecology: How are animals distributed in space? and At what rate do animals encounter features of their landscape? Answers to these questions emerge from considering how landscape heterogeneity affects animal movement.

Empirical studies of animal movement typically use qualitative observations or phenomenological models to describe how animals interact with and respond to landscape features at a small scale (Crist et al., 1992; Schultz and Crone, 2001; Frair et al., 2005; Whittington et al., 2005). While empirical studies are central

to ecologists' understanding of individual movement mechanisms, the problem of understanding the effect of changes in small-scale movement at landscape or population scales remains (but see Kareiva and Odell (1987)).

Mechanistic, or behaviourally-based, movement models present one method to address the problem of scaling up observations of small-scale movement patterns to larger-scale ecological processes (Turchin, 1998; Okubo and Levin, 2001). These models directly incorporate detailed small-scale empirical observations while offering predictions about large-scale ecological processes. For example, from a spatially explicit model for wolf territoriality, that included wolf movement and scent marking only, Lewis and Murray (1993) predicted the existence of the observed buffer zones between adjacent wolf packs, which acted as prey refuges. Behaviourally-based movement models connect individual movement mechanisms and advection-diffusion equations using the diffusion approximation of the random walk (Skellam, 1991; Turchin, 1998; Okubo and Levin, 2001). The random walk was first used to describe movement by Pearson (1905). Subsequently, the random walk framework was used by Pearson and Blakeman (1906) to describe the migration of animals and by Brownlee (1911) to model the spread of epidemics. Skellam (1955) advanced the use of diffusion processes for ecological questions, such as population growth and competition between two species in heterogeneous habitats, the spread of invaders, and the study of critical patch size. Diffusion models continue to be applied to many ecological processes (Holmes et al., 1994; Turchin, 1998; Okubo and Levin, 2001), with increasing attention to the connection between animal behaviour and the random walk (Moorcroft and Lewis, 2006).

For example, the behaviourally-based mechanistic approach to modeling animal movement has frequently been used to address the first central question: How are animals distributed in space (Turchin, 1998; Okubo and Levin, 2001; Moorcroft and Lewis, 2006)? Under the assumption of random (Brownian) motion, the mean squared displacement of an animal grows linearly with time at rate $2d$, where d is the diffusion coefficient for the animal with units $\frac{\text{ditance}^2}{\text{time}}$ (Turchin, 1998). The location of an animal undergoing Brownian motion is a random variable, indexed by time, and so is a stochastic process (Taylor and Karlin, 1998). The probability density function for the location at any given time t, denoted $u(x,t)$, satisfies the diffusion equation

$$\frac{\partial u}{\partial t} = d\frac{\partial^2 u}{\partial x^2}, \quad u(x,0) = u_0(x), \tag{3.1}$$

on $0 < x < L$, where L is the length of the domain on which the animal is moving and $u_0(x)$ is the possible probability density function specifying the possible initial locations of the animal. If the animal is known with certainty to be initially located at $x = x_0$, then $u_0(x) = \delta(x - x_0)$, where δ is the delta-distribution or "impulse function" with area one and all its mass at the single point $x = x_0$. To solve Eq 3.1 boundary conditions on u or its spatial derivative must be specified at $x = 0$ and $x = L$. We consider two cases where an animal is moving under Brownian motion on the domain of length L: (i) the animal is captured as soon as it touches either end of the domain ($x = 0$ or $x = L$), (ii) the animal is captured as soon as it touches one end of the domain ($x = 0$), but reflected when it touches the other end of the domain ($x = L$). As soon as the animal is captured, it is removed from the domain. Boundary conditions for Eq 3.1 that correspond to case (i) above are $u(0,t) = u(L,t) = 0$, and those corresponding to case (ii) above are $u(0,t) = \frac{\partial u}{\partial t}(L,t) = 0$. In physics, Eq 3.1 with the first set of boundary conditions can be use to describe the temperature distribution in a rod where both ends of the rod are kept at zero degrees. The boundary conditions in (ii) modify the problem to account for insulation of the rod at $x = L$. The solutions to these problems (Appendix 3.A), shown in Figure 3.1, illustrate the increasing likelihood of capture as time progresses. The area under the curve, $\int_0^1 u(x,t)\ dx$, denotes the probability of no capture by time t. In both cases the distribution of animals spreads out over time, eventually becoming zero as the animals are absorbed at the boundaries (Figure 3.1). For more complex animal movement behaviour in heterogeneous landscapes, the distribution of animals is described by the Fokker-Planck, or 'space use' equation, with variable coefficients (Moorcroft and Lewis, 2006),

$$\frac{\partial u}{\partial t} = \frac{\partial}{\partial x}[c(x,t)u] + \frac{\partial^2}{\partial x^2}[d(x,t)u]. \tag{3.2}$$

Now we return to the second central question: At what rate do animals encounter features of their landscape? This was first addressed mathematically in an ecological context by Berg (1993) who calculated the 'mean time to capture' of a randomly moving bacteria by a sticky disk at the center of a homogeneous Petri dish. Mean time to capture is more generally known as the mean first passage time, and defined as the length of time on average taken by an animal to reach a specified site (or set of sites) in the landscape for the first time (Redner, 2001). Mean first passage time has been widely applied to many stochastic processes such diffusion-limited

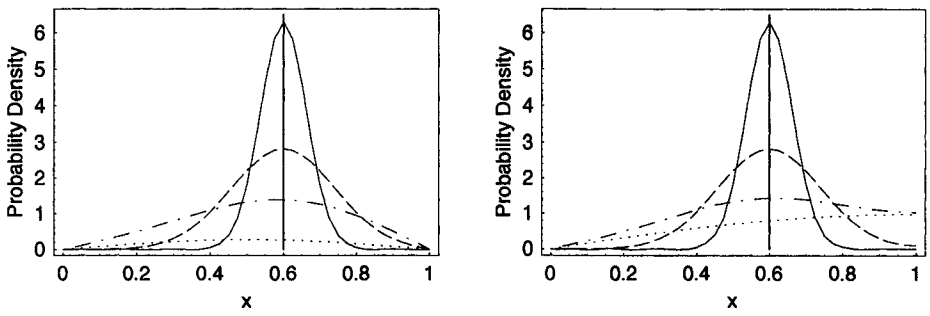

Figure 3.1: Solutions to the simple diffusion equation on a one-dimensional homogeneous domain, $[0, L]$. Lines represent the solution for different times, $t = 1$ (solid), $t = 5$ (dashed), $t = 20$ (dot-dashed), and $t = 100$ (dotted). (a) Boundary conditions are absorbing at both ends (Eq 3.A-1-3.A-2). (b) Boundary conditions are absorbing at $x = 0$ and reflecting at $x = L$ (Eq 3.A-3-3.A-4). The initial condition is $f(x) = \delta(x - 0.6)$, the diffusion coefficient is $d = 0.002$, and $L = 1$.

aggregation, neuron firing, the triggering of stock options, and DNA binding (Berg, 1993; Redner, 2001).

Ecologists have adopted a narrower definition of mean first passage time as the time required for an animal to first cross a circle of given radius centered at the origin of the movement (Johnson et al., 1992), but see Benichou et al. (2005). In ecology, mean first passage time has been used as an alternate summary statistic to the mean squared displacement (Johnson et al., 1992), to measure search time along a path (Fauchauld and Tveraa, 2003), and to distinguish between movement behaviours at different spatial scales (Frair et al., 2005). I suggest that mean first passage time, as defined more generally outside the ecology literature, offers ecologists a framework in which to address questions about animal encounter rates with landscape features.

In a homogeneous landscape the mean first passage time for an animal starting at location x, $w(x)$, is described by the differential equation (Berg, 1993)

$$d\frac{d^2w}{dx^2} + 1 = 0, \tag{3.3}$$

where the diffusion coefficient d is the same as in the corresponding space use equation (Eq 3.1). On a domain of length L Eq 3.3 has solution

$$w(x) = \frac{1}{2d}(Lx - x^2) \tag{3.4}$$

if the animal is captured at the edges of the domain, and

$$w(x) = \frac{1}{2d}(2Lx - x^2) \tag{3.5}$$

if the animal is captured at $x = 0$ and reflected at $x = L$ (Appendix 3.B). An animal starting closer to the point of capture will on average always become captured sooner than an animal beginning further (Figure 3.2).

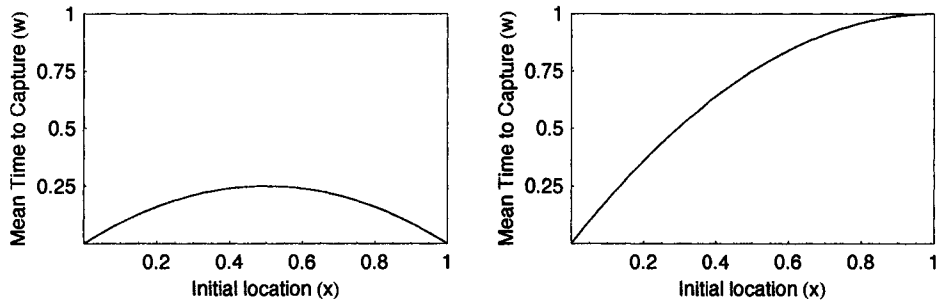

Figure 3.2: Solutions of the mean first passage time equation (Eq 3.3) for two types of boundary conditions. (a) Dirichlet conditions, the animal is captured at $x = 0$ and $x = L$ (Eq 3.4). (b) Neumann conditions, the animal is captured at $x = 0$ and reflected at $x = L$ (Eq 3.5). The other parameter values are $L = 1, d = 0.5$.

In Section 3.2 I review the derivations of the space use and mean first passage time equations in a one-dimensional homogeneous environment (Okubo and Levin, 2001; Berg, 1993) and draw connections between the mathematical methods and the biological interpretations. Using similar methods, in Sections 3.3 and 1.4 I extend the mathematical theory by deriving new equations for the mean first passage time in one- and two-dimensional heterogeneous environments where animal movement is more complex, with movement rates and distributions of movement directions varying in space. In Section 3.5 the potential of the mean first passage time to capture the effect of small-scale movement on landscape-level processes is illustrated using a model of red fox (*Vulpes vulpes*) movement. Here the model is based on the Holgate-Okubo formulation of random movement with a bias towards a den site (Okubo and Levin, 2001). The effects of this movement pattern on the length of time taken to find a prey item at various distances from the den site are calculated.

The mean first passage time is also connected to the functional response, which describes the number of prey consumed by a single predator as a function of prey

density and predator behaviour (Solomon, 1949; Holling, 1959). In the derivation of the Holling disk equation, Holling (1959) assumed that predators moved at a constant speed and searched a constant area per unit time, resulting in a linear prey encounter rate and asymptotic functional response when the time associated with handling a prey was included. This directed searching movement is similar to advection. How does the underlying predator movement change the form of the functional response? Mean first passage time, derived from individual movement, can be used to derive a functional response which incorporates the effect of different types of movement. In Section 3.6 I derive functional responses without and including handling time for pure advection and simple diffusion in a homogeneous landscape, and discuss their biological interpretations.

3.2 Models for space use and mean first passage time in a homogeneous environment

Space use. Diffusion describes how a group of individual particles spread out due to the irregular motion of each particle (Okubo and Levin, 2001). When applied to animals, diffusion may alternatively be viewed as describing the distribution of a large population of animals or the expected location of an individual animal in space and time. Because diffusion is the continuous limit of a random walk, individual small-scale movement can be translated into a diffusion equation (Skellam, 1991).

Although the diffusion-advection equation (Fokker-Planck) equation is a very general model for animal movement, the simplest derivation comes from a random walk with time steps τ and space steps δ. Suppose the probability the animal is located at x at time t is given by the function $u(x,t)$. During each time interval τ the animal may jump a step δ to the right or left with equal probability, $1/2$. Then the probability an individual is at location x at time $t+\tau$ is the sum of the probabilities of arriving at x from all other possible previous locations and can be written as

$$u(x,t+\tau) = \frac{1}{2}u(x-\delta,t) + \frac{1}{2}u(x+\delta,t). \tag{3.6}$$

Eq 3.6 summarizes the movement rules depicted in Figure 3.3(a) using mathematical notation and is often called the *master equation.* Expanding $u(x-\delta)$ and $u(x+\delta)$ using Taylor series, which approximates the functions as sums of powers of x, and taking the diffusion limit, Eq 3.6 can be translated into Eq 3.1 (Appendix 3.C).

The diffusion approximation relates movement in discrete and continuous space by assuming that the animal takes shorter and shorter steps δ in shorter and shorter time intervals τ, so that δ and τ approach zero. As a consequence of the limit, it is theoretically possible for the animal to move with infinite speed and change direction infinitely many times during one time interval (Turchin, 1998). However, the probability of travelling arbitrarily far in an arbitrarily short time period is very small and the average animal takes a long time to travel long distances, which is more consistent with our intuition about movement (Holmes et al., 1994). The diffusion approximation of the random walk has been shown to adequately describe the distribution of animals in time and space for many ecological systems (Holmes et al., 1994; Okubo and Levin, 2001).

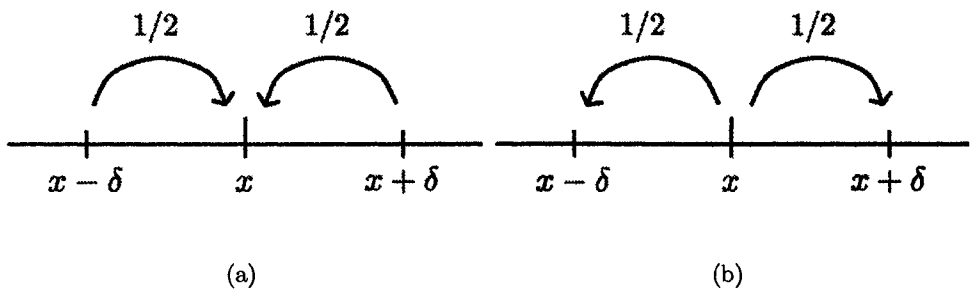

Figure 3.3: Pictorial representation of the random walks corresponding to the (a) space use and (b) mean first passage time equations in a one-dimensional homogeneous landscape.

Mean first passage time. The random walk framework can be used to derive an equation describing the mean first passage time (Berg, 1993; Redner, 2001). Unlike the equation for space use, which describes how the distribution of animals changes over time, the mean first passage time equation describes the time taken for an animal to arrive at some specified final location as function of the starting location. I derive the mean first passage time equation corresponding the the space use equation derived above, meaning that they are based on the same movement rules. Suppose $w(x)$ is the mean first passage time from location x. An animal located at x has equal probability $1/2$ of jumping a step δ to the left or right (Figure 3.3(b)). Then the mean first passage time from the current location x is equal to the sum of the mean first passage times from all possible next locations,

multiplied by the probability of moving to those locations, plus the time taken to move, τ. This is summarized by the master equation,

$$w(x) = \tau + \frac{1}{2}w(x-\delta) + \frac{1}{2}w(x+\delta). \tag{3.7}$$

Using a similar approach as for the space use equation, Eq 3.7 can be translated into Eq 3.3 (Appendix 3.D). In contrast to the space use equation, which can be solved on an infinitely large domain, in order for the mean first passage time problem to be well-defined the animal must be moving in some finite domain. This restriction is natural, because otherwise the animal could potentially wander away from the specified final location indefinitely. Therefore we must define *boundary conditions*, or rules governing animal movement at two places in the domain: at the specified final location and at the edges of the domain. The final location in Berg's example was a sticky disk. Because we assume the animal's movement terminates once it arrives at the specified end location, the disk 'absorbs' the animal. Intuitively the mean first passage time for an animal beginning on the edge of the disk is zero, since the animal is already at the end location. Mathematically this called is a Dirichlet boundary condition and can be written as $w(e) = 0$, where e is the end location. When the animal reaches the edges of the domain, it is reflected back into the domain. Therefore, at the edge of the domain, the mean first passage time does not change with space. This type of boundary condition is called a Neumann condition and is written as $\frac{dw}{dx} = 0$. Domains often can be chosen so that reflecting boundary conditions are biologically reasonable. Islands, lakes, home ranges, or habitat patches with impermeable boundaries are all examples of biologically reasonable domains. Once boundary conditions are defined, solutions to Eq 3.3 can be found analytically (for example Eqs 3.4 and 3.5). For different diffusion coefficients $d_1 < d_2$, the mean first passage time is always shorter for animals with the larger diffusion coefficient d_2 (Figure 3.4). This is consistent with the intuition that on average, faster moving animals will arrive at the specified final location sooner then slower moving animals.

The review of the derivations of the space use and mean first passage time equations in a one-dimentional homogeneous landscape highlights three major results. First, an equation for mean first passage time can be derived from movement behaviour specified by a random walk. This is done by taking the diffusion approximation of a master equation, which gives rise to a differential equation. Additionally, the diffusion coefficient of the mean first passage time equation is the

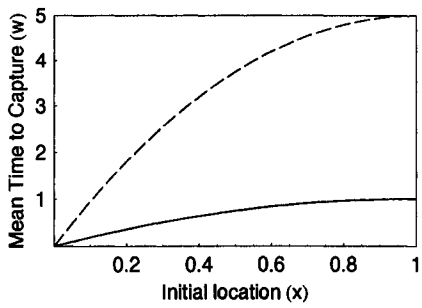

Figure 3.4: Solutions to the mean first passage time equation (Eq 3.3) for different diffusion coefficients. The solid line is the solution for $d = 0.5$ and the dashed line is the solution for $d = 0.1$. The boundary conditions are Neumann at $x = L$ (animals are reflected at $x = L$) and Dirichlet at $x = 0$ (animals are captured at $x = 0$). The other parameter value is $L = 1$.

same as the diffusion coefficient of the corresponding space use equation. Second, the mean first passage time equation must be solved on a finite domain. Mean first passage time at the edge of the domain is subject to Neumann (reflecting) conditions and the specified final location is defined using Dirichlet (absorbing) conditions. Third, mean first passage time decreases monotonically (i.e. is strictly decreasing, meaning the slope does not change signs) with distance of the starting location from the specified end location. This means that individuals who begin closer to the end location will on average reach it faster than individuals who start farther away.

Mean first passage time, $w(x)$, is a less common way of thinking about animal movement in ecology, whereas the concept of space use, $u(x,t)$, is prevalent. Nevertheless, mean first passage time may be just as useful for understanding the connection between individual small-scale movement and landscape-level ecological processes. However, equations describing realistic animal movement must incorporate animal response to spatial heterogeneity. For example, instead of considering two animals diffusing at different rates, we can consider one animal moving between two patches with different diffusion coefficients. In the following section I review how more complex animal movement is translated into an equation describing space use and derive a new equation for the corresponding mean first passage time.

3.3 Movement in a heterogeneous environment

The influence of landscape heterogeneity on animal movement is divided into two parts: movement rate and movement direction. Habitat structure may vary, resulting in varying movement rates between habitats (Weins, 2001). For example, wolves are observed to move greater than two times faster on linear features than in the forest (James, 1999) and prairie butterflies move faster in regions between habitat patches than regions in habitat patches (Schultz and Crone, 2001). This spatial variability in movement speed is incorporated into the movement model by allowing the diffusion coefficient to vary in space. Animals may also bias their movement directions relative to landscape features. For example, red fox movements are directionally biased towards the home range centre (Siniff and Jessen, 1969) and male checkerspot butterflies bias their movement in the uphill direction when searching for mates (Turchin, 1991). Directional bias is incorporated into the movement model by adding an advection term, which describes the directed component of movement.

Spatially variable movement rates. We begin by defining movement rules to allow for spatially variable movement rates. Similar to the random walk in a homogeneous landscape animals may move to the right or left with equal probability. However to have spatially variable movement rates, the animal is also allowed to remain still. Thus, animals may move to the right and left with probability $\frac{(1-N(x))}{2}$, where $0 < N(x) < 1$ is the probability of not moving during a time step (Figure 3.5(a)). For the space use equation, the probability of staying still will be associated with the previous location of the animal. Then the master equation becomes

$$u(x,t+\tau) = \left(\frac{1-N(x-\delta,t)}{2}\right)u(x-\delta,t)+\left(\frac{1-N(x+\delta,t)}{2}\right)u(x+\delta,t)+N(x)u(x,t) \tag{3.8}$$

which, using similar techniques as in the homogeneous case, can be translated into the diffusion equation (Appendix 3.E)

$$\frac{\partial u}{\partial t} = \frac{\partial^2}{\partial x^2}[d(x)u], \tag{3.9}$$

with spatially variable diffusion coefficient $d(x) = \lim_{\delta,\tau\to 0}\frac{\delta^2(1-N(x))}{2\tau}$. If $N(x) = 0$ then the probabilities of jumping to the right and left are $1/2$ and Eq 3.9 reduces to the simple diffusion equation (Eq 3.1). Now consider the corresponding mean first

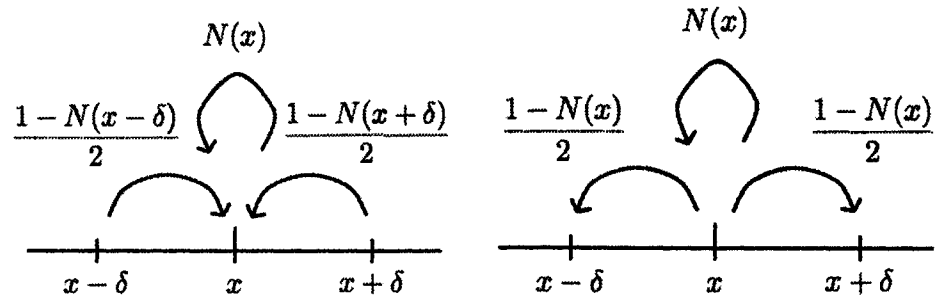

(a) Space use

(b) Mean first passage time

Figure 3.5: Pictorial representation of random walks corresponding to space use and mean first passage time in a one-dimensional heterogeneous landscape with variable diffusion.

passage equation. In this case the probability of not moving is associated with the current location (Figure 3.5(b)). The master equation for the mean first passage time equation is

$$w(x) = \tau + \left(\frac{1 - N(x)}{2}\right) w(x - \delta) + \left(\frac{1 - N(x)}{2}\right) w(x + \delta) + N(x)w(x). \quad (3.10)$$

which corresponds to the diffusion equation (Appendix 3.J)

$$d(x)\frac{\partial^2 w(x)}{\partial x^2} + 1 = 0, \quad (3.11)$$

with spatially variable diffusion coefficient $d(x)$ as given for Eq 3.9. Again if $N(x) = 0$, meaning the animal moves at every time step, the diffusion coefficient simplifies to the original coefficient found by Berg (1993). As with the homogeneous case, the diffusion coefficients for the space use and mean first passage time equations are the same. It is possible to solve Eq 3.11 analytically for simple landscape configurations. For example, if we divide $\Omega = [0, L]$ at $x = a$ into two patches of fast and slow diffusion, subject to boundary conditions $w(0) = 0$ (Dirichlet, absorbing) and $\frac{dw}{dx}(l) = 0$ (Neumann, reflecting), the solution of the mean first passage time equation is (Appendix 3.G, Figure 3.6)

$$w(x) = \begin{cases} \frac{1}{2d_1}\left(2ax - x^2\right) + \frac{x}{d2}\left(l - a\right) & x \in (0, a) \\ \frac{a^2}{2d_1} - \frac{a^2}{2d_2} + \frac{1}{2d_2}\left(2xl - x^2\right) & x \in (a, l). \end{cases} \quad (3.12)$$

We see that if $d_1 = d_2$, then Eq 3.12 reduces to the solution of the homogenous equation (Berg, 1993). Figure 3.6 shows that spatial variation in the diffusion coefficient affects the mean first passage time. For all starting locations, animals moving in the patchy landscape arrive at the end location on average later than animals travelling in the homogeneous landscape with a faster diffusion coefficient, but a sooner than animals in the homogeneous landscape with a slower diffusion coefficient.

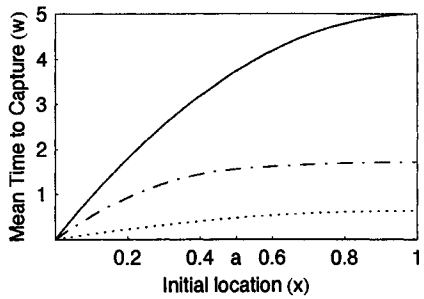

Figure 3.6: Solution of the mean first passage time equation with variable diffusion coefficient (Eq 3.11) in a patchy environment with absorbing boundary conditions at $x = 0$ and reflecting boundary conditions at $x = L$. The solid and dotted lines are the solutions to the homogeneous problem (Eq 3.1) with $d = 0.1$ and $d = 0.8$ respectively. The dot-dashed line is the solution to heterogeneous problem (Eq 3.12) with $d_1 = 0.1, d_2 = 0.8$. The other parameter values are $L = 1, a = 0.5$. The mean first passage time in a heterogeneous landscape is bounded by the mean first passage times in the homogeneous landscapes.

Attraction towards a bias. To incorporate directional bias into the animal movement rules, I allow the probabilities of jumping to the right $R(x)$ and left $L(x)$ to be unequal (Figure 3.7(a)). Because the animal must either move to the right or left, or stay still at each time step, $R(x) + L(x) + N(x) = 1$.

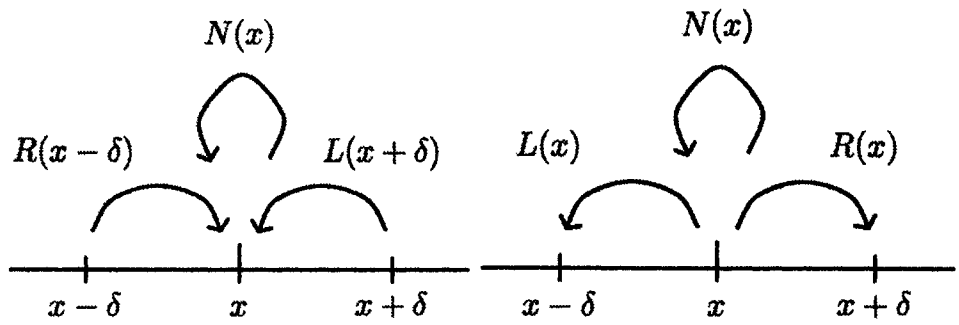

(a) Space use

(b) Mean first passage time

Figure 3.7: Pictorial representation of the random walks corresponding the space use and mean first passage time in a one-dimensional heterogeneous landscape.

These movement rules incorporate both variable movement rates and directions. Again we see that for the space use equation these probabilities depend on the animal's previous location. Under these new assumptions, the master equation for space use becomes

$$u(x, t+\tau) = R(x-\delta, t)u(x-\delta, t) + L(x-\delta, t)u(x+\delta, t) + N(x)u(x, t) \quad (3.13)$$

and using the diffusion approximation, the corresponding advection-diffusion equation is (Appendix 3.H)

$$\frac{du}{dt} = -\frac{\partial}{\partial x}[c(x)u] + \frac{\partial^2}{\partial x^2}[d(x)u], \quad (3.14)$$

where $c(x) = \lim_{\delta,\tau\to 0} \frac{\delta(R(x)-L(x))}{\tau}$ is the spatially variable advection coefficient with units $\frac{\text{distance}}{\text{time}}$ and $d(x) = \lim_{\delta,\tau\to 0} \frac{\delta^2(R(x)+L(x))}{2\tau}$ is the spatially variable diffusion coefficient with units $\frac{\text{distance}^2}{\text{time}}$. If $R(x) = L(x)$ Eq 3.14 simplifies to Eq 3.9. The master equation for the corresponding mean first passage time is (Figure 3.7(b))

$$w(x) = L(x)w(x-\delta,t) + R(x)w(x+\delta,t) + N(x)w(x,t) \tag{3.15}$$

which is translates to the advection-diffusion equation (Appendix 3.I)

$$c(x)\frac{\partial u}{\partial x} + d(x)\frac{\partial^2 w}{\partial x^2} + 1 = 0, \tag{3.16}$$

where $c(x)$ and $d(x)$ are the same advection and diffusion coefficients as for the space use equation (Eq 3.14).

It is possible to solve Eq 3.16 analytically if c and d are constant. On a domain of length L with boundary conditions $w(0) = 0$ and $w(L) = 0$ (homogeneous Dirichlet conditions) Eq 3.9 has solution

$$w(x) = \frac{L(\exp[-c/d(x)] - 1)}{c(\exp[-c/d(L)] - 1)} - \frac{x}{c}. \tag{3.17}$$

Figure 3.8 shows the effect of several movement biases on the mean first passage time.

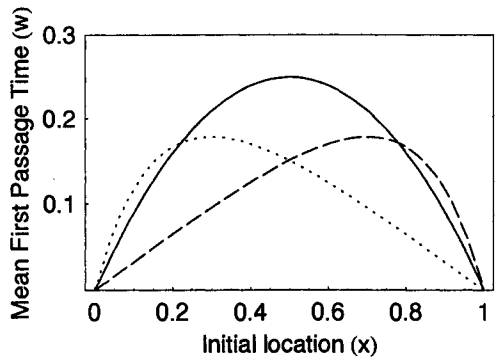

Figure 3.8: Solution of the mean first passage time equation (Eq 3.16) with constant coefficients and homogeneous Dirichlet boundary conditions ($w(x) = 0$ and $w(L) = 0$). The solid line is the solution to the mean first passage time with simple diffusion, $c = 0, d = 0.5$. The dotted and dashed lines are solutions to the mean first passage time with $c = \pm 3$ respectively. The other parameter is $L = 1$. For most starting locations on average individuals moving with advection are captured by a boundary faster than individuals moving according to simple diffusion.

Two observations arise from the derivations of the space use and mean first passage time equations in heterogeneous space. First, comparable to the equations in homogeneous landscapes, the advection and diffusion coefficients are the same

for the corresponding space use and mean first passage time equations. Second, spatial variation in advection and diffusion coefficients affects the mean first passage time, demonstrating how the mean first passage time is able to translate small-scale changes in animal movement due to landscape heterogeneity into differences in ecological processes at the landscape scale.

Variable step length and the redistribution kernel. Before extending the models for movement in a heterogeneous landscape to two dimensions, following Moorcroft and Lewis (2006) I generalize Eqs 3.14 and 3.16 to a more biologically reasonable case where animals may move steps of different lengths in any one time step. Consider the lattice $\{-L, \ldots, -\delta, 0, \delta, \ldots, L\}$, and suppose an animal is located at x. In the next time step the animal can make a jump of size $\pm n\delta$, where $n > 0$ is a movement to the right, $n < 0$ is a movement to the left, and $n = 0$ represents the event the animal stays still. To express the probability of all possible moves we define a redistribution kernel $k(x, x+n\delta, \tau)$, which is a probability mass function describing the probability that an animal jumps from location x to a new location $x+n\delta$ in the next time step τ. Because k incorporates all possible jumps, $\sum_{n=-\infty}^{\infty} k(x, x+n\delta, \tau) = 1$. Using the redistribution kernel, rewrite the master equations for the space use and mean first passage time as

$$u(x, t+\tau) = \sum_{n=-\infty}^{\infty} k(n\delta, x, \tau) u(n\delta, t)\delta, \tag{3.18}$$

and

$$w(x) = \tau + \sum_{n=-\infty}^{\infty} k(x, n\delta, \tau) w(n\delta)\delta. \tag{3.19}$$

Taking the limit as the step size $\delta \to 0$ and using the definition of the integral these equations become

$$u(x, t+\tau) = \int_{-\infty}^{\infty} k(x', x, \tau) u(x', t) dx', \tag{3.20}$$

and

$$w(x) = \tau + \int_{-\infty}^{\infty} k(x, x', \tau) w(x') dx', \tag{3.21}$$

where x is the current location and x' is the location the animal is arriving from (in the case of the space use equation) or going to (in the case of the mean first

passage time equation). We define a new variable for the distance between x and x', $a = x' - x$. Then the redistribution kernel can be rewritten as $K(x, a, \tau)$ where x is the current location and a is the jump distance in time step τ. After applying the diffusion approximation to Eqs 3.20 and 3.21, we obtain Eq 3.14 (Appendix 3.J) where now the advection and diffusion coefficients are given as the first and second infinitesimal moments of the redistribution kernel (Moorcroft and Lewis, 2006),

$$c(x) = \lim_{a,\tau \to 0} \frac{1}{\tau} \int_{-\infty}^{\infty} aK(x, a, \tau)\, da, \tag{3.22}$$

$$d(x) = \lim_{a,\tau \to 0} \frac{1}{2\tau} \int_{-\infty}^{\infty} a^2 K(x, a, \tau)\, da. \tag{3.23}$$

As before the mean first passage time equation is given by Eq 3.16, but with $c(x)$ and $d(x)$ now given by Eqs 3.22-3.23.

These equations incorporate spatially variable diffusion and advection, as well as variable step length. The coefficients are functions of the redistribution kernel, which describes the probability of moving from the current location to any other location. This shows that small-scale animal movements and the distribution of animals and their encounter rates with landscape features are connected through the advection and diffusion coefficients. Given the understanding provided by considering simple cases in a one-dimensional landscape, extending the model to two dimensions becomes a task of algebraic accounting.

3.4 Movement in a two-dimensional heterogeneous environment

Space use. In two dimensions, the redistribution kernel is a two-dimensional probability density function, $k(\mathbf{x}', \mathbf{x}, \tau)$, describing the probability of moving from a previous small rectangle $[\mathbf{x}', \mathbf{x}' + d\mathbf{x}')$ at time t to the current small rectangle $[\mathbf{x}, \mathbf{x} + d\mathbf{x})$ at time $t + \tau$. Let $u(\mathbf{x}, t)$ be probability density function for an animal located at $\mathbf{x} = (x, y)$ at time t. Then the master equation in 2-dimensions is

$$u(\mathbf{x}, t + \tau) = \int k(\mathbf{x}', \mathbf{x}, \tau, t) u(\mathbf{x}')\, d\mathbf{x}'. \tag{3.24}$$

Redefining the redistribution kernel as before to be $K(\mathbf{x}, \mathbf{a}, \tau)$ where $\mathbf{a} = \mathbf{x}' - \mathbf{x}$, and following the method of (Moorcroft and Lewis, 2006), the corresponding advection-diffusion equation is (Appendix 3.K)

$$\frac{\partial u}{\partial t} = -\nabla\cdot[\mathbf{c}(\mathbf{x},t)u] + \frac{\partial^2[d_{xx}(\mathbf{x},t)u]}{\partial x^2} + \frac{\partial^2[d_{xy}(\mathbf{x},t)u]}{\partial x\partial y} + \frac{\partial^2[d_{yx}(\mathbf{x},t)u]}{\partial y\partial x} + \frac{\partial^2[d_{yy}(\mathbf{x},t)u]}{\partial y^2}, \tag{3.25}$$

where $\nabla u = \left[\frac{\partial u}{\partial x}, \frac{\partial u}{\partial y}\right]^T$, $\nabla^2 = \nabla\cdot\nabla u = \frac{\partial^2 u}{\partial x^2} + \frac{\partial^2 u}{\partial y^2}$, and the coefficients are given by

$$\mathbf{c}(\mathbf{x}) = \lim_{\tau\to 0}\frac{1}{\tau}\int \mathbf{a}K(\mathbf{x},\mathbf{a},\tau)\,d\mathbf{a}, \tag{3.26}$$

$$d_{xx}(\mathbf{x}) = \lim_{\tau\to 0}\frac{1}{2\tau}\int_{-\infty}^{\infty} a_1^2 K(\mathbf{x},\mathbf{a},\tau)\,d\mathbf{a}, \tag{3.27}$$

$$d_{xy}(\mathbf{x}) = \lim_{\tau\to 0}\frac{1}{2\tau}\int_{-\infty}^{\infty} a_1 a_2 K(\mathbf{x},\mathbf{a},\tau)\,d\mathbf{a}, \tag{3.28}$$

$$d_{yx}(\mathbf{x}) = d_{xy}(\mathbf{x}), \tag{3.29}$$

$$d_{yy}(\mathbf{x}) = \lim_{\tau\to 0}\frac{1}{2\tau}\int_{-\infty}^{\infty} a_2^2 K(\mathbf{x},\mathbf{a},\tau)\,d\mathbf{a}. \tag{3.30}$$

Mean first passage time. Similarly, let $w(\mathbf{x})$ be the mean first passage time for an individual initially located at $\mathbf{x} = (x, y)$. Writing the master equation as

$$w(\mathbf{x}) = \tau + \int_{-\infty}^{\infty} k(\mathbf{x},\mathbf{x}',\tau)w(\mathbf{x}')\,d\mathbf{x}'. \tag{3.31}$$

and then redefining the redistribution kernel and using the diffusion approximation yields the advection-diffusion equation (Appendix 3.K)

$$\mathbf{c}(\mathbf{x})\cdot\nabla w + d_{xx}(\mathbf{x})\frac{\partial^2 w}{\partial x^2} + d_{xy}(\mathbf{x})\frac{\partial^2 w}{\partial x\partial y} + d_{yx}(\mathbf{x})\frac{\partial^2 w}{\partial y\partial x} + d_{yy}(\mathbf{x})\frac{\partial^2 w}{\partial y^2} + 1 = 0, \tag{3.32}$$

where the spatially dependent advection and diffusion coefficients are given by Eqs 4.2-4.6. The derivation of the space use and mean first passage time equations in two-dimensions preserves the property of similarity between coefficients for both equations that was observed in one-dimension.

Now I consider the interpretation of the mean first passage time in a two-dimensional landscape. The solution to the Eq 3.32 is a surface whose height is the mean time to arrive at a specified location for the first time as a function of the starting location $\mathbf{x}$. The surface gives the mean first passage time for every possible starting location in the domain. While the surface provides a qualitative picture of how the mean first passage time changes throughout the landscape, it may be difficult to use the information without a summary statistic. This is particularly

true if the mean first passage time is being compared across different domains. One possible summary statistic is the spatial average of the mean first passage time throughout the domain,

$$\text{MFPT}_{avg} = \int_{\mathbf{x}\in\Omega} u_0(\mathbf{x})w(\mathbf{x})\, d\mathbf{x}, \tag{3.33}$$

where $u_0(\mathbf{x})$ is the initial probability distribution of the animals is space. If $u_0(\mathbf{x})$ is assumed to be a uniform distribution, MFPT_{avg} is equivalent to the expected mean first passage time from a random starting location (Benichou et al., 2005). If the initial distribution of animals in space is known, the MFPT_{avg} is equivalent to the expected mean first passage time conditional on the initial distribution of animals. Therefore, the mean first passage time surface provides a map of how long it would take to arrive at the specified end location given different starting locations and can be summarized into a metric that facilitates comparison of the mean first passage times among landscapes.

3.5 Influence of home range behaviour on first passage time to prey

The notion of a home range was first proposed by Burt (1943) as "that area traversed by the individual in its normal activities of food gathering, mating, and caring for young." Subsequent analysis of animal locations support Burt's suggestion that movement of non-migratory animals is not random in the landscape, but focused within a home range (Siniff and Jessen, 1969). A simple model for animal movement in a home range was first proposed by Holgate (1971) and further described by Okubo and Levin (2001). The Holgate-Okubo model assumes a centralizing tendency in the animal's movement directions because of the need to care for young located at the den site. During denning many canids, including the red fox (*Vulpes vulpes*), display behaviour that is well-described by this model (Mech and Boitani, 2003; Siniff and Jessen, 1969). The space use equation for the Holgate-Okubo model was mechanistically derived and parameterized by Moorcroft and Lewis (2006) using red fox location data due to Siniff and Jessen (1969). The expected location of the red fox is described by the Fokker-Planck equation

$$\frac{\partial u}{\partial t} = -\nabla \cdot [\mathbf{c}(\mathbf{x})u] + \nabla^2[du], \tag{3.34}$$

with constant diffusion coefficient $d = 0.041$ km^2/hr and advection vector $\mathbf{c}$ pointing

in the direction of the home range centre, which is assumed to be at the origin, with magnitude 0.085 km/h (Figure 3.9(a)). The steady state solution to Eq 3.34 is (Figure 3.9(b))

$$u(x,y) = \frac{c^2}{d^2\pi} E_1[c/d(\sqrt{x^2+y^2})], \tag{3.35}$$

where E_1 is the exponential integral

$$E_1(u) = \int_u^\infty \frac{\exp(-t)}{t}\, dt. \tag{3.36}$$

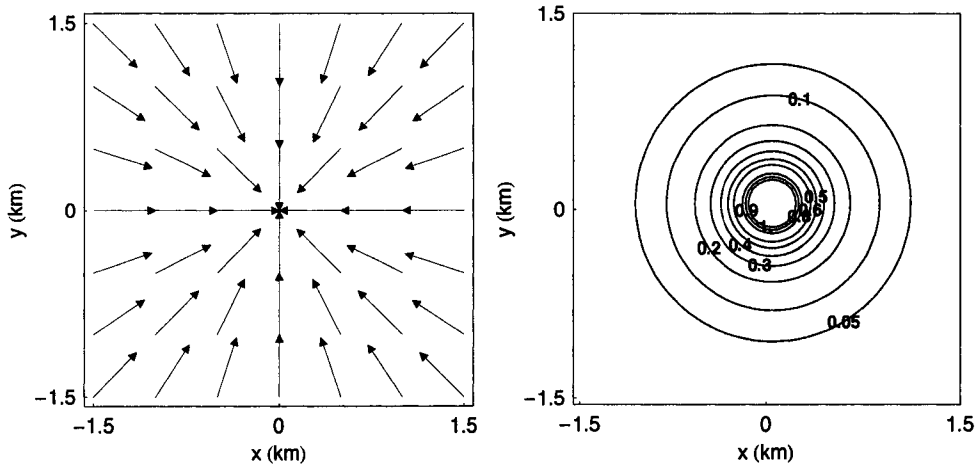

(a) Advection field

(b) Steady state solution

Figure 3.9: Red fox movement with centralizing tendancy. (a) The vector field representing the advection coefficient $\mathbf{c}(\mathbf{x})$ at each point in the domain. (b) The steady state solution to the space use equation for the red fox (Eq 3.34).

Figure 3.9(b) shows that the expected pattern of space use is radially symmetric around the home range centre, and that the individual is more likely to be found close to the home range centre. How might the centralizing tendency in red fox movement affect the time to locate prey as a function of prey distance from the home range centre? To answer this question I compare the mean first passage times of a red fox moving according to the Holgate-Okubo centralizing tendency model to that of one moving randomly.

Following the random walk approach illustrated earlier, the corresponding mean first passage time equation for the Holgate-Okubo model was found to be,

$$\mathbf{c}(\mathbf{x}) \cdot \nabla w + d\nabla^2 w + 1 = 0, \tag{3.37}$$

where previously the coefficients, $\mathbf{c}(\mathbf{x})$ and d, were shown to be the same as those in the space use equation. If $\mathbf{c}(\mathbf{x}) = 0$ Eq 3.37 describes the mean first passage times for movement without a centralizing tendency. To obtain mean first passage time for a red fox moving with and without the centralizing tendency, Eq 3.37 was solved for $\mathbf{c}(\mathbf{x}) \neq 0$ and $\mathbf{c}(\mathbf{x}) = 0$ on a square domain similar in area to the 95% minimum convex polygon for the expected location of the red fox (3 km x 3 km). The edges of the domain were subject to Neuman (reflecting) conditions. Biologically this corresponded to the red fox remaining within its home range. This is different than the centralizing tendency, which impacts movement throughout the domain. Prey were specified at distances of 0, 0.25, 0.5, 0.75, 1, 1.25, and 1.5 km from the home range centre by a disk of radius 10 m with Dirichlet (absorbing) conditions. Solutions were found numerically (Appendix 3.L) and summarized using MFPT_{avg}, where the initial distributions of expected locations were assumed to be the steady state solution of Eq 3.34 for the red fox with centralizing tendency and uniform for the red fox without a centralizing tendency.

The mean first passage time surfaces differ for movement with and without a centralizing tendency (Figure 3.10). The MFPT_{avg} for both models increases with increasing prey distance from home range center (Figure 4.12). For prey near the home range centre, animals with centralizing tendency locate the prey faster, whereas animals without the centralizing tendency locate the prey farther from the home range centre faster. For this choice of parameter values the switch occurs when the prey is 1 km from the home range centre.

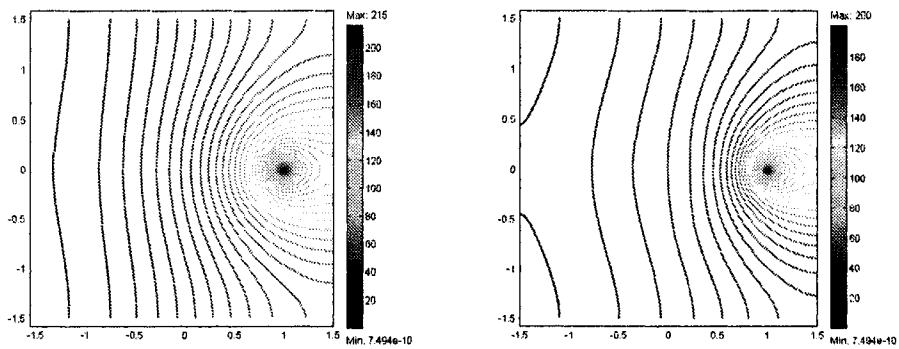

(a) No bias (b) Bias

Figure 3.10: The mean first passage time of a red fox to a prey located 1 km from the den site. Surfaces are solutions to Eq 3.37 (a) with and (b) without the centralizing tendency. Differences in the surfaces are apparent in the height of the far left side of the domain and in the asymmetry near the prey.

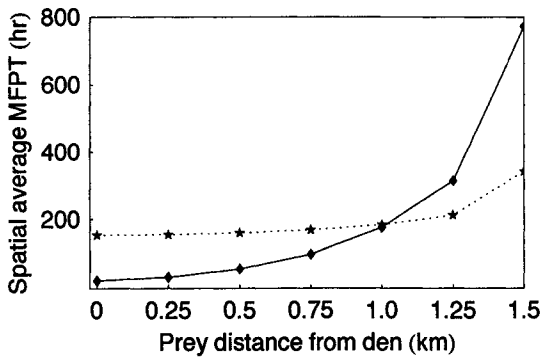

Figure 3.11: Spatially average of the mean first passage time of a red fox to prey assuming movement with (solid line) and without (dotted line) a centralizing tendency.

3.6 Incorporating movement mechanisms into the functional response

The Holling disk equation for the functional response assumes a constant area is searched for new prey per unit time (Holling, 1959). This is consistent with pure directed motion (advection), where displacement of an individual increases linearly with time. Here the size of the region searched scales linearly with the time elapsed. However, for random motion (diffusion) it is the mean squared displacement that increases linear with time. In this case, the size of the area searched scales with the square root of the time elapsed. In other words, to search an area of twice the size requires four times longer. This scaling arises from the fact that Brownian motion allows individuals to move back and forth over regions recently searched, via random switching of direction. In this section I deduce the effect of random versus directed movement behaviour on the functional response. I consider the case where prey are stationary and located randomly in space.

Consider an infinite one-dimensional landscape where prey are distributed according to a Poisson process with intensity λ per unit length (λ is equivalent to N, the expected density of prey). The waiting times, or times between consecutive events, of a Poisson process are exponentially distributed (Taylor and Karlin, 1998). Denote the locations of prey as $\{\ldots, x_{-3}, x_{-2}, x_{-1}, 0, x_1, x_2, x_3, \ldots\}$. Translating this to a Poisson process for prey locations in space indicates the distances between prey, x_i, are exponentially distributed,

$$g(x_i) = \lambda \exp[-\lambda x_i]. \tag{3.38}$$

Without loss of generality, consider the sub-domain $[0, x_1]$, where prey are located at 0 and x_1. Suppose $w(x)$ is the solution to the mean first passage time equation on $[0, x_1]$, given some underlying movement and homogeneous Dirichlet boundary conditions at $x = 0$ and $x_1 = 0$. Then the expected mean first passage time on $[0, x_1]$, assuming a uniform distribution of starting locations, is

$$E[w(x)|x_1] = \frac{1}{x_1} \int_0^{x_1} w(x)\, dx. \tag{3.39}$$

Now, the expected mean first passage time over all sub-domains is

$$E[w(x)] = \int_0^{\infty} E[w(x)|x_1] g(x_1)\, dx_1. \tag{3.40}$$

Then the rate at which predators encounter prey as a function of prey density is given by $E[w(x)]^{-1}$. This method is used to derive functional responses for predators undergoing pure advection, simple diffusion, and a mixture of advection and diffusion.

Pure advection. The mean first passage time equation for pure advection is given by Eq 3.16, where $d = 0$ and c is constant. For this case, the solution is

$$w(x) = \frac{L - x}{c}. \tag{3.41}$$

Substituting Eq 3.41 into Eq 3.39 the expected mean first passage time for a fixed x_1 is

$$\frac{1}{x_1}\int_0^{x_1} \frac{x_1 - x}{c} = \frac{x_1}{2c}, \tag{3.42}$$

and the expected mean first passage time is

$$\int_0^{\infty} \lambda e^{-\lambda x_1} \frac{x_1}{2c}\, dx_1 = \frac{1}{2c\lambda}. \tag{3.43}$$

Therefore the encounter rate is $2c\lambda$. This is equivalent to the Holling Type I functional response where $a = 2c$, $f_c(N) = 2cN$.

Simple diffusion. Now consider a predator moving according to simple diffusion. Then $w(x)$ is given by Eq 3.4 and the expected mean first passage time for a fixed x_1 is

$$\frac{1}{x_1}\int_0^{x_1} \frac{x(x_1 - x)}{2d}\, dx = \frac{x_1^2}{12d}, \tag{3.44}$$

and the expected mean first passage time over all x_1,

$$\int_0^{\infty} \lambda e^{-\lambda x_1} \frac{x_1^2}{12d}\, dx_1 = \frac{1}{6d\lambda^2} \tag{3.45}$$

The rate that a single predator encounters prey as a function of prey density λ is $6d\lambda^2$, $f(N) = 6dN^2$ (Figure 3.12).

Including handling time. I extend the results from the above encounter rate calculations to include handling time T_h for predation. Following the argument of Gurney and Nisbet (1998), the average number of prey items ingested by an individual predator per unit time is given by

$$f(N) = \frac{R}{1 + T_h R}, \tag{3.46}$$

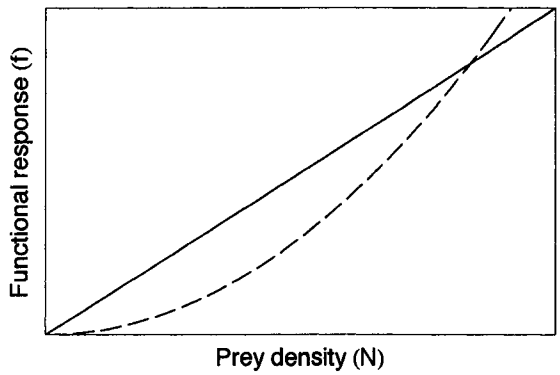

Figure 3.12: Shape of the functional response for underlying movement mechanisms of pure advection (solid) and simple diffusion (dashed) when no handling time is included.

where predators capture prey at an average rate R per unit time. For each underlying movement mechanism, R can be obtained from the encounter rates above (Figure 3.13. Therefore the functional responses with handling time assuming pure advection and simple diffusion are respectively

$$f_c(N) = \frac{2cN}{1 + T_h 2cN}, \tag{3.47}$$

$$f_d(N) = \frac{6dN^2}{1 + T_h 6dN^2}. \tag{3.48}$$

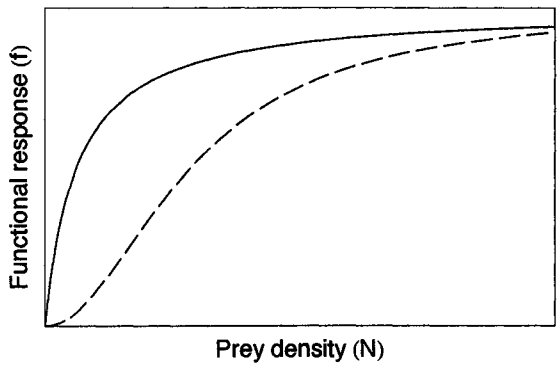

Figure 3.13: Shape of the functional response for different underlying movement mechanisms, pure advection (solid) and simple diffusion (dashed) including handling time.

3.7 Discussion

While advection and diffusion processes have been widely applied in ecology to answer questions about how animals use space (Turchin, 1998; Okubo and Levin, 2001), no similar framework exists for studying animal encounter rates with landscape features. In this chapter I suggest that mean first passage time could provide such a framework. New equations for mean first passage time were derived from first principals. These equations incorporate directed (advective) and random (diffusive) motion in spatially heterogeneous landscapes. The solution to these equations specifies the average time taken to first reach a given location in space. Immediate applications of mean first passage time to predator-prey encounter rates and predator functional response were demonstrated.

Using red fox movement within a home range as an example, I showed that mean first passage time can be used to calculate the effect of detailed movement behaviours on encounter rates between a predator and a single prey item. Mean first passage time analysis revealed that foxes moving with a centralizing tendency found prey near the den site faster, but took longer to find prey near the territory boundary, than randomly moving foxes.

The connection between mean first passage time and predator movement was extended to analyse the effects of random versus directed movement behaviour on functional response. While directed (advective) movement resulted in a linear functional response, equivalent to the Holling type I functional response, random movement produced a quadratic functional response. When handling time was included, directed movement resulted in the traditional Holling Type II functional response, while random movement led to a sigmoidal functional response, similar in shape to the Holling type III functional response. Therefore, mean first passage time analysis demonstrated that random movement could be an alternative biological mechanism to prey refugia or prey switching, which gives rise to the Holling type III functional response.

The underlying movement model for the mean first passage time equation is diffusion-advection. This is a general formulation for random and directed motion of animals (Turchin, 1998). It is an approximation which uses summary statistics $\mathbf{c}(\mathbf{x})$ and $d(\mathbf{x})$ (Eq 4.2-4.6) for complex spatial movement patterns (Holmes et al., 1994). The first advantage of this general formulation for mean first passage time is that it yields an equation that need only be solved once either by analytical (Sections 3.1-3.3) or by numerical methods (Section 3.5). This contrasts with individual-based

simulation of the same process. Obtaining a mean first passage time surface by simulation requires that n realizations of well-defined rules for animal movement be simulated from each possible initial starting location, where n is large enough to provide a reasonable measure of the mean. Whereas this intensive simulation process may be possible for simple problems it becomes intractable for complex animal movement patterns in large heterogeneous domains (Grimm, 1999). The mean first passage time framework developed in this chapter provides an elegant alternative. The second advantage of the general formulation is the ability to model animal movement where the underlying master equation is unknown. If the specific behavioural interactions that give rise to the master equation are known, it would be possible to analyse mean first passage time directly from the master equation without taking the diffusion approximation. However, behavioural mechanisms are rarely known with certainty for ecological processes (Lima and Zollner, 1996; Belisle, 2005). Instead empirical movement data, such as mean move distance and move direction, can be used to calculate summary statistics for animal motion. This approach was demonstrated in the red fox example and is the basis of the model of wolf movement discussed in Chapter 3.

This chapter introduces a new modelling framework for mean first passage time, which compliments the Fokker-Planck equation, and demonstrates two initial applications to predator-prey interactions. Future applications of mean first passage time could include interactions between adjacent territory holders, dispersal and mate finding in heterogeneous landscapes, the effect of environmental heterogeneity on predator-prey encounter rates (Chapter 3), or time to first contact in spatial disease models. Additionally, the framework could be extended to consider moving prey or predators searching using prey-taxis.

Appendix

3.A Solution to the diffusion equation

The solution to Eq 3.1 on a domain of length L for an initial distribution of animals $f(x)$, is found by the method of separation of variables (Haberman, 2003). If animals are absorbed at the edges of the domain then

$$u(x,t) = \sum_{n=1}^{\infty} B_n \sin\left(\frac{n\pi x}{L}\right) \exp\left[-\left(\frac{n\pi}{L}\right)^2 kt\right], \qquad \text{(3.A-1)}$$

where

$$B_n = \frac{2}{L}\int_0^L f(x)\sin\left(\frac{n\pi x}{L}\right)\,dx. \tag{3.A-2}$$

In contrast, if the animals are absorbed at $x = 0$ and reflected at $x = L$, then

$$u(x,t) = \sum_{n=1}^{\infty} D_n \sin\left(\frac{(n-1/2)\pi x}{L}\right)\exp\left[-\left(\frac{(n-1/2)\pi}{L}\right)^2 kt\right] \tag{3.A-3}$$

where

$$D_n = \frac{2}{L}\int_0^L f(x)\sin\left(\frac{(n-1/2)\pi x}{L}\right)\,dx. \tag{3.A-4}$$

3.B Solution to the mean first passage time equation in one-dimensional homogeneous domain without advection

Consider the first passage time equation

$$d\frac{d^2w}{dx^2} + 1 = 0, \tag{3.B-1}$$

on the domain $\Omega = [0, l]$. The solution is found using the method of separation of variables. First, rewrite the equation as

$$\frac{d^2w}{dx^2} = -\frac{1}{d}, \tag{3.B-2}$$

and let $u = \frac{dw}{dx}$. Then

$$\int du = \int -\frac{1}{d}\,dx$$

so

$$u = -\frac{x}{d} + c_1.$$

Integrating again,

$$\int dw = \int \left(-\frac{x}{d} + c_1\right)\,dx.$$

Therefore the general solution to the original differential equation is

$$w(x) = -\frac{x^2}{2d} + c_1 x + c_2. \tag{3.B-3}$$

Consider two types of boundary conditions in order to determine constants c_1, c_2. In the first case $w(0) = w(l) = 0$ (homogeneous Dirichlet conditions). Then $c_1 = \frac{l}{2d}, c_2 = 0$ and

$$w(x) = \frac{1}{2d}(lx - x^2). \tag{3.B-4}$$

In the second case $w(0) = 0$ and $\frac{dw}{dx}(l) = 0$ (mixed Dirichlet and Neumann conditions). Substituting these conditions into Eq 3.B-3, $c_2 = 0$, hence

$$w(x) = \frac{1}{2d}(2lx - x^2). \tag{3.B-5}$$

3.C Random walk to simple diffusion

To arrive at the diffusion equation from a random walk, begin with the master equation

$$u(x, t+\tau) = \frac{1}{2}u(x-\delta, t) + \frac{1}{2}u(x+\delta, t). \tag{3.C-1}$$

Expand $u(x, t+\tau), u(x-\delta, t)$, and $u(x+\delta, t)$ using Taylor series,

$$u(x,t) + \tau\frac{\partial u}{\partial t} = \frac{1}{2}\left\{u(x,t) - \delta\frac{\partial u}{\partial x} + \frac{\delta^2}{2}\frac{\partial^2 u}{\partial x^2}\right\} + \frac{1}{2}\left\{u(x,t) + \delta\frac{\partial u}{\partial x} + \frac{\delta^2}{2}\frac{\partial^2 u}{\partial x^2}\right\} + \text{h.o.t.} \tag{3.C-2}$$

where h.o.t. represents higher order terms. Divide through by τ and rearrange,

$$\frac{\partial u}{\partial t} = \frac{\delta^2}{2\tau}\frac{\partial^2 u}{\partial x^2} + \text{h.o.t.} \tag{3.C-3}$$

By taking the limit as $\delta, \tau \to 0$ we obtain the diffusion equation

$$\frac{\partial u}{\partial t} = d\frac{\partial^2 u}{\partial x^2}, \tag{3.C-4}$$

where $d = \lim_{\delta,\tau\to 0}\frac{\delta^2}{2\tau}$ is the diffusion coefficient.

3.D Random walk to mean first passage time

Using the random walk framework following (Berg, 1993), write the mean first passage time equation as

$$w(x) = \tau + \frac{1}{2}w(x-\delta) + \frac{1}{2}w(x+\delta). \tag{3.D-1}$$

Using Taylor series rewrite the above equation as

$$w(x) = \tau + \frac{1}{2}\left\{w(x) - \delta\frac{dw}{\partial x} + \frac{\delta^2}{2}\frac{d^2w}{dx^2}\right\} + \frac{1}{2}\left\{w(x) + \delta\frac{dw}{dx} + \frac{\delta^2}{2}\frac{d^2w}{dx^2}\right\} + \text{h.o.t.} \tag{3.D-2}$$

Divide through by τ and rearrange to obtain

$$\frac{\delta^2}{2\tau}\frac{d^2w}{dx^2} + 1 + \text{h.o.t.} = 0. \tag{3.D-3}$$

Take the limit as $\delta \to 0$ to arrive at the equation for the mean first passage time

$$d\frac{d^2w}{dx^2} + 1 = 0, \tag{3.D-4}$$

where $d = \lim_{\delta\to 0}\frac{\delta^2}{2\tau}$ is the diffusion coefficient.

3.E Random walk to diffusion with spatially variable diffusion coefficient

Begin with the master equation for the expected location of the individual,

$$u(x,t+\tau) = \left(\frac{1-N(x-\delta,t)}{2}\right)u(x-\delta,t) + \left(\frac{1-N(x+\delta,t)}{2}\right)u(x+\delta,t) + N(x)u(x,t).$$

Simplify and collect terms to rewrite the equation as

$$\begin{aligned} u(x,t+\tau) &= \frac{1}{2}\left(u(x-\delta,t) - N(x-\delta,t)u(x-\delta,t) + u(x+\delta,t)\right. \\ &\quad \left. -N(x+\delta,t)u(x+\delta,t) + N(x)u(x,t)\right). \end{aligned} \tag{3.E-1}$$

Expand $u(x,t+\tau), u(x-\delta,t), u(x+\delta,t), N(x-\delta,t)$, and $N(x+\delta,t)$ using Taylor series, divide by τ, and take the limit as $\delta, \tau \to 0$ to obtain the diffusion equation

$$\frac{\partial u}{\partial t} = \frac{\partial^2}{\partial x^2}(d(x)u),$$

where $d(x) = \lim_{\delta,\tau\to 0}\frac{\delta(1-N(x))}{2\tau}$ is the spatially variable diffusion coefficient.

3.F Random walk to mean first passage time with spatially variable diffusion coefficient

The master equation describing the random walk is

$$w(x) = \tau + \left(\frac{1-N(x)}{2}\right) w(x-\delta) + \left(\frac{1-N(x)}{2}\right) w(x+\delta) + N(x)w(x).$$

Simplify and collect terms to rewrite the equation as

$$w(x) = \tau + \frac{1}{2}\left(w(x-\delta) - N(x)w(x-\delta) + w(x+\delta) - N(x)w(x+\delta) + N(x)w(x)\right).$$

Expand $w(x-\delta)$, and $w(x+\delta)$ using Taylor series, divide by τ, and take the limit as $\delta, \tau \to 0$ to obtain the mean first passage time equation

$$1 + d(x)\frac{\partial^2 w}{\partial x^2} = 0,$$

where $d(x) = \frac{\delta^2(1-N(x))}{2\tau}$ is the spatially variable diffusion coefficient.

3.G Solution to the mean first passage time equation in a patchy environment

Consider the mean first passage time equation in a two-patch heterogeneous environment. Use the method of separation of variables to obtain the following solution

$$w(x) = \int_0^x \int_v^l \frac{1}{d(u)}\, du\, dv. \tag{3.G-1}$$

There are two cases depending on the location of x is in the domain. For the first case, $x \in (0, a)$. Then

$$w(x) = \int_0^x \left(\int_v^a \frac{1}{d_1}\, du + \int_a^l \frac{1}{d_2}\, du\right) dv = \frac{1}{2d_1}(2ax - x^2) + \frac{x}{d_2}(l-a). \tag{3.G-2}$$

For the second case $x \in (a, l)$ and,

$$\begin{aligned} w(x) &= \int_0^a \left(\int_v^a \frac{1}{d_1}\, du + \int_a^l \frac{1}{d_2}\, du\right) dv + \int_a^x \int_v^l \frac{1}{D_2}\, du\, dv \\ &= \frac{a^2}{2d_1} - \frac{a^2}{2d_2} + \frac{1}{2d_2}(2lx - x^2). \end{aligned} \tag{3.G-3}$$

Combining Eqs 3.G-2 and 3.G-3 the complete solution is,

$$w(x) = \begin{cases} \frac{1}{2d_1}\left(2ax - x^2\right) + \frac{x}{d2}\left(l - a\right) & x \in (0, a) \\ \frac{a^2}{2d_1} - \frac{a^2}{2d_2} + \frac{1}{2d_2}\left(2lx - x^2\right) & x \in (a, l) \end{cases} \tag{3.G-4}$$

3.H Random walk to Fokker-Planck equation

The master equation from the random walk is given by

$$u(x, t+\tau) = R(x-\delta, t)u(x-\delta, t) + L(x-\delta, t)u(x+\delta, t) + N(x)u(x, t).$$

Expand $u(x-\delta, t), u(x+\delta, t), R(x-\delta, t)$, and $L(x+\delta, t)$ using Taylor series, divide by τ and take the limit as $\delta, \tau \to 0$ to obtain the Fokker-Planck equation,

$$\frac{du}{dt} = -\frac{\partial}{\partial x}(c(x)u) + \frac{\partial^2}{\partial x^2}(d(x)u),$$

where $c(x) = \lim_{\delta,\tau\to 0} \frac{\delta(R(x)-L(x))}{\tau}$ is the advection coefficient and $d(x) = \lim_{\delta,\tau\to 0} \frac{\delta^2(R(x)+L(x))}{2\tau}$ is the diffusion coefficient.

3.I Random walk to mean first passage time equation including advection and diffusion

The master equation is given by

$$w(x) = L(x)w(x-\delta, t) + R(x)w(x+\delta, t) + N(x)w(x, t).$$

Expand $u(x-\delta)$ and $u(x+\delta)$ using Taylor series, divide by τ and take the limit as $\delta \to 0$ to obtain the mean first passage time equation,

$$c(x)\frac{\partial}{\partial x}(w) + d(x)\frac{\partial^2}{\partial x^2}(w) + 1 = 0,$$

where $c(x) = \lim_{\delta,\tau\to 0} \frac{\delta(R(x)-L(x))}{\tau}$ is the advection coefficient and $d(x) = \lim_{\delta,\tau\to 0} \frac{\delta^2(R(x)+L(x))}{2\tau}$ is the diffusion coefficient.

3.J Incorporating variable step length

Space use. Begin with the master equation

$$u(x,t+\tau)=\int_{-\infty}^{\infty}k(x',x,\tau)u(x',t)dx'.$$

Write $x'=x-a$ and the redistribution kernel as $K(x-a,a,\tau)$, where a is the directed length of the move. The equation becomes

$$u(x,t+\tau)=\int_{-\infty}^{\infty}K(x-a,a,\tau)u(x-a,t)da.$$

Expand $u(x,t+\tau),u(x-a,t)$, and $K(x-a,a,\tau)$ using Taylor series,

$$u(x,t)+\tau\frac{\partial u}{\partial t}=\int_{-\infty}^{\infty}\left\{[K(x,a,\tau)u(x)]-a\frac{\partial}{\partial x}[K(x,a,\tau)u(x,t)]\right.$$
$$\left.+\frac{a^2}{2}\frac{\partial^2}{\partial x^2}[K(x,a,\tau)u(x,t)]+\text{h.o.t.}\right\}da.$$

Divide by τ and use the fact that $\int_{-\infty}^{\infty}K(x,a,\tau)u(x)da=u(x)$ to obtain

$$\frac{\partial u}{\partial t}=\int_{-\infty}^{\infty}\left\{-\frac{a}{\tau}\frac{\partial}{\partial x}[K(x,a,\tau)u(x,t)]+\frac{a^2}{2\tau}\frac{\partial^2}{\partial x^2}[K(x,a,\tau)u(x,t)]+\text{h.o.t.}\right\}da.$$

Switch the order of integration and differentiation and take the limit as $\delta,\tau\to 0$ to rewrite the equation as

$$\frac{\partial u}{\partial t}=-\frac{\partial}{\partial x}(c(x)u)+\frac{\partial^2}{\partial x^2}(d(x)u)$$

where

$$c(x)=\lim_{\delta,\tau\to 0}\frac{a}{\tau}\int_{-\infty}^{\infty}K(x,a,\tau)\,da,$$
$$d(x)=\lim_{\delta,\tau\to 0}\frac{a^2}{2\tau}\int_{-\infty}^{\infty}K(x,a,\tau)\,da.$$

Mean first passage time. Begin with the master equation

$$w(x)=\tau+\int_{-\infty}^{\infty}k(x,x',\tau)w(x')dx'.$$

Let $x'=x+a$ and define a new redistribution kernel as $K(x,a,\tau)$, where a is the directed length of the move and the equation becomes

$$w(x)=\tau+\int_{-\infty}^{\infty}K(x,a,\tau)w(x+a)da.$$

Expand $w(x+a)$ using Taylor series,

$$w(x) = \tau + \int_{-\infty}^{\infty} K(x,a,\tau)\left\{w(x) + a\frac{\partial}{\partial x}w(x) + \frac{a^2}{2}\frac{\partial^2}{\partial x^2}w(x) + \text{h.o.t.}\right\}\, da.$$

Divide by τ and use the fact that $\int_{-\infty}^{\infty} K(x,a,\tau,t)\, da = 1$ to obtain

$$\int_{-\infty}^{\infty} K(x,a,\tau)\left\{-a\frac{\partial u}{\partial x}w(x) + \frac{a^2}{2}\frac{\partial^2}{\partial x^2}w(x) + \text{h.o.t.}\right\}\, da + 1 = 0.$$

Because the derivatives are independent of a it is possible to remove them from the integral. Take the limit as $\delta, \tau \to 0$ and the equation becomes

$$c(x)\frac{\partial w}{\partial x} + d(x)\frac{\partial^2 w}{\partial x^2} + 1 = 0$$

where

$$c(x) = \lim_{\delta,\tau\to 0} \frac{a}{\tau}\int_{-\infty}^{\infty} K(x,a,\tau)\, da,$$

$$d(x) = \lim_{\delta,\tau\to 0} \frac{a^2}{2\tau}\int_{-\infty}^{\infty} K(x,a,\tau)\, da.$$

3.K Extension from one- to two-dimensions

Space use. Let $\mathbf{x} = (x,y)$. Then the master equation is

$$u(\mathbf{x}, t+\tau) = \int u(\mathbf{x}', t)k(\mathbf{x}', \mathbf{x}, \tau)\, d\mathbf{x}'.$$

Re-write $\mathbf{x}' = \mathbf{x} - \mathbf{a}$ and define a new redistribution kernel $K(\mathbf{x}-\mathbf{a}, \mathbf{a}, \tau)$, where $\mathbf{a}$ is the vector representing the move. The equation becomes

$$u(\mathbf{x}, t+\tau) = \int u(\mathbf{x}-\mathbf{a}, t)K(\mathbf{x}-\mathbf{a}, \mathbf{a}, \tau)\, d\mathbf{a}.$$

Expland $u(\mathbf{x}, t+\tau), u(\mathbf{x}-\mathbf{a}, t)$ and $K(\mathbf{x}-\mathbf{a}, \mathbf{a}, \tau)$ using the two-dimensional Taylor series to obtain

$$
\begin{aligned}
&u(\mathbf{x},t)+\tau\frac{\partial}{\partial t}u(\mathbf{x},t)= \\
&\int\Big\{u(\mathbf{x},t)K(\mathbf{x},\mathbf{a},\tau)-a_1\frac{\partial}{\partial x}[u(\mathbf{x},t)K(\mathbf{x},\mathbf{a},\tau)] \\
&-a_2\frac{\partial}{\partial y}[u(\mathbf{x},t)K(\mathbf{x},\mathbf{a},\tau)]+\frac{(a_1)^2}{2}\frac{\partial^2}{\partial x^2}[u(\mathbf{x},t)K(\mathbf{x},\mathbf{a},\tau)] \\
&+\frac{a_1a_2}{2}\frac{\partial^2}{\partial x\partial y}[u(\mathbf{x},t)K(\mathbf{x},\mathbf{a},\tau)]+\frac{a_2a_1}{2}\frac{\partial^2}{\partial y\partial x}[u(\mathbf{x},t)K(\mathbf{x},\mathbf{a},\tau)] \\
&+\frac{(a_2)^2}{2}\frac{\partial^2}{\partial y^2}[u(\mathbf{x},t)K(\mathbf{x},\mathbf{a},\tau)]+\text{h.o.t.}\Big\}\,d\mathbf{a} \qquad \text{(3.K-1)}
\end{aligned}
$$

Divide by τ, and use the fact that $\int K(\mathbf{x},\mathbf{a},\tau)u(\mathbf{x},t)d\mathbf{a} = u(\mathbf{x},t)$ to rearrange. Taking the limit as $\tau \to 0$ gives the Fokker-Planck equation

$$
\frac{\partial u}{\partial t} = -\nabla\cdot[c(\mathbf{x},t)u]+\frac{\partial^2[d_{xx}(\mathbf{x},t)u]}{\partial x^2}+\frac{\partial^2[d_{xy}(\mathbf{x},t)u]}{\partial x\partial y}+\frac{\partial^2[d_{yx}(\mathbf{x},t)u]}{\partial y\partial x}+\frac{\partial^2[d_{yy}(\mathbf{x},t)u]}{\partial y^2}, \qquad \text{(3.K-2)}
$$

where

$$
\begin{aligned}
c(\mathbf{x},t) &= \lim_{\tau\to 0}\frac{1}{\tau}\int \mathbf{a}K(\mathbf{x},\mathbf{a},\tau)\,d\mathbf{a}, && \text{(3.K-3)}\\
d_{xx}(\mathbf{x},t) &= \lim_{\tau\to 0}\frac{1}{2\tau}\int a_1^2K(\mathbf{x},\mathbf{a},\tau)\,d\mathbf{a}, && \text{(3.K-4)}\\
d_{xy}(\mathbf{x},t) &= \lim_{\tau\to 0}\frac{1}{2\tau}\int a_1a_2K(\mathbf{x},\mathbf{a},\tau)\,d\mathbf{a}, && \text{(3.K-5)}\\
d_{yx}(\mathbf{x},t) &= d_{xy}(\mathbf{x}), && \text{(3.K-6)}\\
d_{yy}(\mathbf{x},t) &= \lim_{\tau\to 0}\frac{1}{2\tau}\int a_2^2K(\mathbf{x},\mathbf{a},\tau)\,d\mathbf{a}, && \text{(3.K-7)}
\end{aligned}
$$

Mean first passage time. From the random walk the master equation is

$$
w(\mathbf{x}) = \tau + \int k(\mathbf{x},\mathbf{x}',\tau)w(\mathbf{x}')\,d\mathbf{x}'.
$$

Re-write $\mathbf{x}' = \mathbf{x}+\mathbf{a}$ and define a new redistribution kernel $K(\mathbf{x},\mathbf{a},\tau)$, where $\mathbf{a}$ is a vector representing the move. The equation becomes

$$
w(\mathbf{x}) = \tau + \int k(\mathbf{x},\mathbf{a},\tau)w(\mathbf{x}+\mathbf{a})\,d\mathbf{a}.
$$

Expland $w(\mathbf{x}+\mathbf{a})$ using the two-dimensional Taylor series the equation to obtain

$$w(\mathbf{x}) = \tau + \int k(\mathbf{x}, \mathbf{a}, \tau) \left\{ w(\mathbf{x}) + a_1 \frac{\partial}{\partial x} w(\mathbf{x}) + a_2 \frac{\partial}{\partial y} w(\mathbf{x}) + \frac{a_1^2}{2} \frac{\partial^2}{\partial x^2} w(\mathbf{x}) \right.$$
$$\left. + \frac{a_1 a_2}{2} \frac{\partial^2}{\partial x \partial y} w(\mathbf{x}) + \frac{a_2 a_1}{2} \frac{\partial^2}{\partial y \partial x} w(\mathbf{x}) + \frac{a_2^2}{2} \frac{\partial^2}{\partial y^2} w(\mathbf{x}) \right\} d\mathbf{a}.$$

Divide by τ, and using the fact that $\int K(\mathbf{x}, \mathbf{a}, \tau) w(\mathbf{x}) d\mathbf{a} = w(\mathbf{x})$, rearrange and take the limit as $\tau \to 0$ to obtain the mean first passage time equation

$$c(\mathbf{x}) \cdot \nabla w + d_{xx}(\mathbf{x}) \frac{\partial^2 w}{\partial x^2} + d_{xy}(\mathbf{x}) \frac{\partial^2 w}{\partial x \partial y} + d_{yx}(\mathbf{x}) \frac{\partial^2 w}{\partial y \partial x} + d_{yy}(\mathbf{x}) \frac{\partial^2 w}{\partial y^2} + 1 = 0$$

where

$$c(\mathbf{x}) = \lim_{\tau \to 0} \frac{1}{\tau} \int \mathbf{a} K(\mathbf{x}, \mathbf{a}, \tau) \, d\mathbf{a}, \tag{3.K-8}$$

$$d_{xx}(\mathbf{x}) = \lim_{\tau \to 0} \frac{1}{2\tau} \int a_1^2 K(\mathbf{x}, \mathbf{a}, \tau) \, d\mathbf{a}, \tag{3.K-9}$$

$$d_{xy}(\mathbf{x}) = \lim_{\tau \to 0} \frac{1}{2\tau} \int a_1 a_2 K(\mathbf{x}, \mathbf{a}, \tau) \, d\mathbf{a}, \tag{3.K-10}$$

$$d_{yx}(\mathbf{x}) = d_{xy}(\mathbf{x}), \tag{3.K-11}$$

$$d_{yy}(\mathbf{x}) = \lim_{\tau \to 0} \frac{1}{2\tau} \int a_2^2 K(\mathbf{x}, \mathbf{a}, \tau) \, d\mathbf{a}, \tag{3.K-12}$$

3.L Numerical Method

The spatially heterogeneous mean first passage time problem was solved using COMSOL Multiphysics. The landscape was defined in COMSOL using the draw tools. The model was defined using the PDE, coefficient form (stationary analysis) application mode. The general pde in this form is

$$\begin{cases} \nabla \cdot (-c\nabla u - \alpha u + \gamma) + \beta \cdot \nabla u + au = f & \text{in } \Omega \\ \mathbf{n} \cdot (c\nabla + \alpha u - \gamma) + qu = g - h^T \mu & \text{on } \partial\Omega \\ hu = r & \text{on } \partial\Omega \end{cases} \tag{3.L-1}$$

where Ω is the computational domain, $\partial\Omega$ is the boundary, and $\mathbf{n}$ is the outward normal on $\partial\Omega$. The second equation is the generalized Neumann boundary condition and the third equation is the generalized Dirichlet boundary condition. To adapt the

general equation for the mean first passage time equation I specified the coefficients as follows

$$\begin{aligned} d_a,\ \alpha,\ \gamma,\ a &= 0 \\ f &= 1 \\ \beta &= [\,-CX(x,y)\ \ -CY(x,y)\,] \\ \\ c &= d \end{aligned}$$

where $CX(x,y)$ and $CY(x,y)$ are MATLAB functions that compute the spatially dependent advection coefficients and d is the constant diffusion coefficient. The insulating boundary condition on the exterior boundaries is specified using the generalized Neumann boundary condition ($q = g = 0$) and the absorbing boundary condition on the interior boundary is specified using the generalized Dirchlet boundary condition ($h = 1$ and $r = 0$). Therefore the mean first passage time problem is stated as

$$\begin{cases} \nabla \cdot (c(\mathbf{x})\nabla u) + \beta(\mathbf{x}) \cdot \nabla u + 1 = 0 & \text{in } \Omega \\ \mathbf{n} \cdot (c\nabla u) = 0 & \text{on } \partial\Omega_{\text{ext}} \\ u = 0 & \text{on } \partial\Omega_{\text{int}} \end{cases} \tag{3.L-2}$$

Sample code.

1. Example m-file the advection coefficient vector

```
%
% First Passage Time paper: Red fox example
% functin cx defines the x component of the advection vector
%
function cx = CX(x,y)
global pde
%
% compute scalar speed of advection
%%c = pde.c;
c = 0.085;
```

```
%
% initialize cx and find size sx, required later to reshape cx
%
cx = zeros(length(x),1);
sx = size(x);
%
% loop through each mesh point (x,y) and compute cx
%
for i=1:length(x)
    % find direction of unit vector pointing to homerange center
    % (which is at (0,0))
    xdir = -x(i) / norm([x(i) y(i)]);
    % multiply by scalar speed of advection
    cx(i) = c*xdir;
end
%
% reshape cx for FEMLAB
%
cx = reshape(cx,sx);


%
% First Passage Time paper: Red fox example
% functin cy defines the y component of the advection vector
%
function cy = CY(x,y)
global pde
%
% compute scalar speed of advection
%%c = pde.c;
c = 0.085;
%
% initialize cx and find size sx, required later to reshape cx
%
cy = zeros(length(y),1);
sy = size(y);
```

```
%
% loop through each mesh point (x,y) and compute cx
%
for i=1:length(y)

    % find direction of unit vector pointing to homerange center
    % (which is at (0,0))
    ydir = -y(i) / norm([x(i) y(i)]);
    % multiply by scalar speed of advection
    cy(i) = c*ydir;
end
%
% reshape cy for FEMLAB
%
cy = reshape(cy,sy);
```

Literature cited

Belisle, M. 2005. Measuring landscape connectivity: the challenge of behavioral landscape ecology. Ecology **86**:1988–1995.

Benichou, O., M. Coppey, M. Moreau, P.-H. Suet, and R. Voituriez. 2005. Optimal Search Strategies for Hidden Targets. Physical Review Letters **94**.

Berg, H. 1993. Random Walks in Biology. Princeton University Press.

Brownlee, J. 1911. The mathematica theory of random migration and epidemic distribution. Proceedings of the Royal Society of Edinburgh **31**:262–289.

Burt, W. 1943. Territoriality and Home Range Concepts as Applied to Mammals. Journal of Mammalogy **24**:346–352.

Crist, T., D. Guertin, J. Wiens, and B. Milne. 1992. Animal Movement in Heterogeneous Landscapes: An Experiement with Eleodes Beetles in Shortgrass Prairie. Functional Ecology **6**:536–544.

Fauchauld, P., and R. Tveraa. 2003. Using first passage time in the analysis of area-restricted search and habitat selection. Ecology **84**:282–288.

Frair, J., E. Merrill, D. Visscher, D. Fortin, H. Beyer, and J. Morales. 2005. Scales of movement by elk (Cervus elaphus) in response to heterogeneity in forage resources and predation risk. Landscape Ecology **20**:273–287.

Grimm, V. 1999. Ten years of individual-based modelling in ecology: what have we learned and what could we learn in the future? Ecological Modelling **115**:129–148.

Gurney, W., and R. Nisbet. 1998. Ecological Dynamics. Oxford University Press.

Haberman, R. 2003. Applied Partial Differential Equations. Prentice Hall.

Holgate, P., 1971. Random walk models for animal behavior. Pages 1–12 *in* G. Patil, E. Pielou, and W. Waters, editors. Statistical Ecology, volume 2. Penn. State Univ. Press.

Holling, C. 1959. The components of predation as revealed by a study of small mammal predation of the European pine sawfly. The Canadian Entomologist **91**.

Holmes, E., M. Lewis, J. Banks, and R. Veit. 1994. Partial differential equations in ecology: spatial interactions and population dynamics. Ecology **75**:17–29.

James, A., 1999. Effects of Industrial Development on the Predator-Prey Relationship Between Wolves and Caribou in Northeastern Alberta. Ph.D. thesis, Universtiy of Alberta.

Johnson, A., B. Wiens, and T. Crist. 1992. Animal movements and population dynamics in heterogeneous landscapes. Landscape Ecology **7**:63–75.

Kareiva, P., A. Mullen, and R. Southwood. 1990. Population Dynamics in Spatially Complex Environments: Theory and Data [and Discussion]. Philosophical Transactions: Biological Sciences **330**:175–190.

Kareiva, P., and G. Odell. 1987. Swarms of Predator Exhibit "Preytaxis" if Individual Predators Use Area-Restricted Search. The American Naturalist **130**:233–270.

Lewis, M., and J. Murray. 1993. Modelling territoriality and wolf-deer interactions. Letters to Nature **366**:738–740.

Lima, S., and P. Zollner. 1996. Towards a behavioral ecology of ecological landscapes. TREE **11**:1310–135.

Mech, D., and L. Boitani. 2003. Wolves: Behavior, Ecology, and Conservation. University of Chicago Press.

Moorcroft, P., and M. Lewis. 2006. Mechanistic Home Range Analysis. Princeton University Press.

Okubo, A., and S. Levin. 2001. Diffusion and Ecologica Problems. Springer.

Pearson, K. 1905. The problem of the random walk. Nature **72**:294–294.

Pearson, K., and J. Blakeman, 1906. A mathematical theory of random migration. *in* Mathematica contributions to the theory of evolution-XV. Drapers' Company Research Mem. Biometric Series III, Dept. Appl. Math., Univ. College, Univ. London.

Redner, S. 2001. A Guide to First-Passage Processes. Cambridge University Press.

Schultz, C., and E. Crone. 2001. Edge-mediated dispersal behavior in a prairie butterfly. Ecology **82**:1879–1892.

Siniff, D., and C. Jessen. 1969. A Simulation Model of Animal Movement Patterns. Advanced Ecological Research **6**:185–219.

Skellam, J., 1955. The Number of Man and Animals, Chapter the mathematical approach to population dynamics, pages 31–46 . Oliver and Boyde, London.

Skellam, J. 1991. Random dispersal in theoretical populations (reprinted from Biometrika, Vol 38, PG 196-218, 1953). Bulletin of Mathematical Biology **53**:135–165.

Solomon, M. 1949. The natural control of animal populations. Journal of Animal Ecology **18**:1–35.

Taylor, H., and S. Karlin. 1998. An Introduction to Stochastic Modeling. Academic Press.

Tewksbury, J., D. Levey, N. Haddad, S. Sargen, J. Orrock, A. Weldon, B. Danielson, J. Brinkerhoff, E. Damschen, and P. Townsend. 2002. Corridors affect plants, animals, and their interactions in fragmented landscapes. PNAS **99**:12923–12926.

Turchin, P. 1991. Translanting foraging movements in heterogeneous environments into the spatial distribution of foragers. Ecology **72**:1253–1266.

Turchin, P. 1998. Quantitative Analysis of Movement. Sinaur Associates, Inc Publishers.

Weins, J., 2001. Dispersal, Chapter the landscape context of dispersal, pages 96–109. Oxford University Press.

Whittington, J., C. St. Clair, and G. Mercer. 2005. Spatial responses of wolves to roads and trails in mountain valleys. Ecological Applications **15**:543 – 553.

Chapter 4

The effect of linear features on mean first passage time: implications for predator-prey interactions

4.1 Introduction

To understand predator-prey interactions in a spatial context, it is critical to unravel the links among spatial heterogeneity, animal movement, and predation rate. The relationship between the number of prey consumed per predator and the prey density is known as the functional response (Solomon, 1949; Holling, 1959). The functional response couples prey and predator populations by connecting prey death rate and predator birth rate, and therefore lends insight into predator-prey dynamics. A major component of the functional response is search time, the time taken by a predator to locate a prey (Bell, 1991). Search time depends in turn on animal movement, which is influenced by spatial heterogeneity (Weins, 2001). The effect of animal movement behaviour on search time, and therefore the functional response, is not well-understood. In this chapter I demonstrate, through a case study of wolf-ungulate interactions in the central east slopes of the Rocky mountains (Alberta, Canada), how spatial heterogeneity affects wolf movement behaviour, and subsequently wolf functional response.

Spatial heterogeneity in both the abiotic components of the landscape (e.g. terrain structure) and the spatial distribution of prey can impact predator movement (Jalkotzy et al., 1997; James, 1999; Linke et al., 2005) and predator search time (Bell,

1991; Cuddington and Yodzis, 2002). Spatial heterogeneity affects animal movement rate and direction (Weins, 2001), and therefore animal mobility. Using spatially explicit, individual-based population models, McCauley et al. (1993) showed that increased mobility led to increased encounter rates between predators and prey. Conversely, spatial structures that impeded animal movement altered the dynamics of predator-prey systems (De Roos et al., 1991) and led to a reduction in predation rates (Cuddington and Yodzis, 2002). Predator search time is also a function of prey spatial distribution (Bell, 1991). Cain (1985) found that in a stochastic simulation model herbivores found uniformly dispersed plants more easily than clumped plants.

To associate spatial heterogeneity with predator movement, I break the predator's movement path into distributions of move distances and move directions (Turchin, 1998), and consider how these distributions vary in relation to landscape features. Small-scale individual movement responses are linked to search time using the mean first passage time (MFPT) framework developed in Chapter 2. Defined generally, MFPT is the average time taken to reach a site, or set of sites, for the first time (Berg, 1993; Redner, 2001). MFPT has been used in spatial ecology as an alternative metric to mean squared displacement (Johnson et al., 1992), as a method for distinguishing between movement behaviours (Fauchauld and Tveraa, 2003; Frair et al., 2005), and as a measure of search efficiency along a foraging path (Bailey and Thompson, 2006). In the context of predators searching for prey, MFPT is the average time required for a moving predator to locate a stationary prey. I use MFPT as a proxy for search time.

Connecting spatial heterogeneity and its affect on animal movement to functional response is crucial for understanding predator-prey dynamics in patchy or fragmented landscapes. One such landscape is the central east slopes of the Rockies, which are highly developed by the forestry and energy industries. This area is home to several ungulates species, including moose (*Alces alces*), elk (*Cervus elaphus*), mule deer (*Odocoileus hermionus*), and white-tailed deer (*Odocoileus virginianus*), whose main predator is the gray wolf (*Canis lupus*). An increasingly common type of spatial heterogeneity here is created by seismic lines, long, narrow, linear stretches of forest, cleared for energy exploration (Timoney and Lee, 2001). These linear features negatively impact most species by increasing habitat fragmentation, disturbances, and mortality, and decreasing habitat quality, but they may benefit predators, who enjoy increased travel efficiency along the low human-use linear features (Jalkotzy et al., 1997). Wolves both avoid and use linear features, depending on the linear

feature density and level of human use (Thurber et al., 1994; James, 1999; Callaghan, 2002; Whittington et al., 2005). When wolves used linear features as travel corridors (James and Stuart-Smith, 2000), they moved up to 2.8 times further per unit time on linear features than in the forest (James, 1999). Consequently, linear features were associated with higher predation risk for caribou (*Rangifer tarandus*) (James and Stuart-Smith, 2000) and elk (Frair et al., 2005). Edmonds and Bloomfield (1984); Bergerud and Elliot (1986) hypothesized that increasing densities of linear features would affect predator-prey dynamic between wolves and ungulates by increasing the mobility of wolves.

Here I test this hypothesis by asking whether increasing linear feature density in the central east slopes of the Rockies could alter the predator-prey interactions between wolves and ungulates. To address this question I develop a new method for linking spatial heterogeneity and movement to the functional response, which is an integrated empirical and modeling approach. From high-frequency GPS location data I quantify the movement response of wolves to linear features in the central east slopes. Using a MFPT model, parameterized by wolf movement data, I determine how search time changes with increasing linear feature densities and prey distribution, and conclude with a discussion of how this will affect the functional response and predator-prey dynamics.

4.2 Theoretical framework for investigation

The formal framework for investigating the connections among spatial heterogeneity, movement response, search time, and functional response is developed here. The MFPT in a spatially heterogeneous landscape can be written as the partial differential equation

$$\underbrace{\mathbf{c}(\mathbf{x}) \cdot \nabla w}_{\text{Advection}} + \underbrace{d_{xx}(\mathbf{x})\frac{\partial^2 w}{\partial x^2} + d_{xy}(\mathbf{x})\frac{\partial^2 w}{\partial x \partial y} + d_{yx}(\mathbf{x})\frac{\partial^2 w}{\partial y \partial x} + d_{yy}(\mathbf{x})\frac{\partial^2 w}{\partial y^2}}_{\text{Diffusion}} + 1 = 0, \tag{4.1}$$

where the coefficients

$$\mathbf{c}(\mathbf{x}) = \lim_{\tau \to 0} \frac{1}{\tau} \int \mathbf{a} K(\mathbf{x}, \mathbf{a}, \tau)\, d\mathbf{a}, \tag{4.2}$$

$$d_{xx}(\mathbf{x}) = \lim_{\tau \to 0} \frac{1}{2\tau} \int_{-\infty}^{\infty} a_1^2 K(\mathbf{x}, \mathbf{a}, \tau)\, d\mathbf{a}, \tag{4.3}$$

$$d_{xy}(\mathbf{x}) = \lim_{\tau \to 0} \frac{1}{2\tau} \int_{-\infty}^{\infty} a_1 a_2 K(\mathbf{x}, \mathbf{a}, \tau)\, d\mathbf{a}, \tag{4.4}$$

$$d_{yx}(\mathbf{x}) = d_{xy}(\mathbf{x}), \tag{4.5}$$

$$d_{yy}(\mathbf{x}) = \lim_{\tau \to 0} \frac{1}{2\tau} \int_{-\infty}^{\infty} a_2^2 K(\mathbf{x}, \mathbf{a}, \tau)\, d\mathbf{a}. \tag{4.6}$$

specify the spatially variable movement behaviour of the predator. Here $\mathbf{x}$ is the current location of the predator, $\mathbf{a}$ is a vector describing the distance and direction of the next move, and K is the redistribution kernel, which is a probability density function describing the potential movement of the individual (Moorcroft and Lewis, 2006). Eq 4.1 includes random (diffusive) and directed (advective) motion which together give rise to animal movement. For example, far from landscape features wolves may move in a random fashion, but their movement may become more directed as they interact with landscape features. The solution to Eq 4.1 is a three-dimensional surface $w(\mathbf{x})$, where the height is the MFPT for a predator located at $\mathbf{x}$. This surface provides a picture of how MFPT varies in space, and is conveniently summarized by the spatial average of the MFPT, which is the expected MFPT for a randomly located predator. Thus, MFPT provides a way of calculating predator search time which incorporates the influence of spatial heterogeneity on animal movement.

To understand how search time contributes to the functional response, we return to the original derivation of the Holling disk equation (Holling, 1959). Holling (1959) assumed that prey were randomly distributed in the landscape at some density N and that predators searched a constant area per unit time. Therefore, the number of prey encountered by a predator was

$$N_e = aT_sN \tag{4.7}$$

where a is the encounter rate (number of prey encountered by a single predator per unit of time searching) and T_s is the time spent searching. To obtain the disk equation Holling (1959) showed that the time spent searching could be written as

$$T_s = T_t - T_cN_e - T_mfN_e, \tag{4.8}$$

where T_t is the total time, T_c is the time spent chasing prey encountered, and T_m is the time spent manipulating the fraction f of prey encountered that are caught. Assuming that f is constant we can combine T_c and T_m into an overall prey handling time, T_h, so that Eq 4.8 becomes

$$T_s = T_t - N_e T_h. \tag{4.9}$$

Substituting T_s into Eq 4.7, solving for N_e and dividing by the total time we obtain the Holling disk equation, or Holling type II functional response,

$$f(N) = \frac{aN}{1 + aT_h N}. \tag{4.10}$$

From the shape of the curve (Figure 4.1), we can see that at low prey densities the functional response is dominated by the encounter rate (a), while at high prey densities it is governed by the handling time (T_h). A direct connection exists between the encounter rate and the search time (MFPT),

$$a = \frac{1}{N \cdot \mathrm{MFPT}}, \tag{4.11}$$

which highlights how the functional response is affected by predator movement via search time.

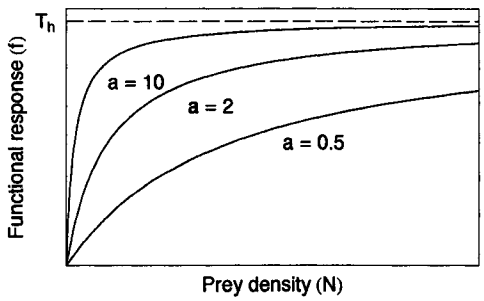

Figure 4.1: The shape of the Type II functional response for different values of encounter rate a.

4.3 Methods

4.3.1 Study area

The study area, consisting of approximately 15,000 km^2 of foothill and mountainous landscape, is located in the central east slopes of the Rocky mountains, Alberta, Canada (52°27'N, 115°45'W). Elevation of the area ranged from 500-1500 m. The average daily mean temperature was -7.5°C in winter (January/February, 2005) and 1°C in spring (March/April, 2005). Total snowfall was 54 cm in winter and 24 cm in spring. The area consists predominantly of forest (68.7%), interspersed with wet and dry meadows (7.1%), areas of harvested forest (4.3%), bare soil/rock (12%), water (2.1%), regeneration areas (< 1%), and urban area (4.1%) (Frair et al., 2005). Development by energy and forestry sectors has led to increased anthropogenic disturbance, including construction of linear features. Here I focus exclusively on a subset of linear features, seismic lines required for oil and gas exploration. At the time of the study there were > 25000 km of linear features present in the landscape, with densities varying from 0.18 km/km^2 near the western boarder to 4.4 km/km^2 near Rocky Mountain House (mean = 1.8 km/km^2). Linear features experienced human use year-round for hunting, trapping, snowmobiling, off-roading, and hiking. The area supports populations of moose (*Alces alces*), mule and white-tailed deer (*Odocoilues hemionus* and *Odocoiles virginianus*), and elk (*Cervus elaphus*), as well as their main predator, wolves (*Canis lupus*). Wolf populations were estimated at 5-7 wolves per 100 km^2 (Clarkson et al., 1984; Schmidt and Gunson, 1985).

4.3.2 Data

As part of a larger study, four wolves from three packs were captured in December 2005 via helicopter netgunning (University of Alberta Protocols #391305 and #353112) and fitted with Lotek GPS_3300 collars (Lotek Engineering, Newmarket, Ontario). Collars were programmed to collect locations at 5 minute intervals during the winter of 2005 (Appendix 4.A) and recorded locations on 90% of fix attempts. Data were downloaded upon retrieval via a remote-release mechanism (3 wolves) or recapture (1 wolf). Data from wolves were considered to be independent because they were either from different packs (i.e. wolves 230, and 234) or the data were collected during different time periods (i.e. wolves 232 and 233). Wolves occupied territories across a gradient of linear feature densities from 1.73-3.60 km/km^2.

4.3.3 Quantitative description of movement

Calculation of movement variables. Two movement variables were used to describe wolf movement. To quantify move distance I calculated the straight-line distance ($\rho : \rho \leq 0$) between the current and next consecutive wolf location (Figure 4.2(a)),

$$\rho = \sqrt{(x_t - x_{t+1})^2 + (y_t - y_{t+1})^2}. \tag{4.12}$$

Although locations contained GPS measurement error, all move distances were used to avoid introducing bias. Movement direction relative to the nearest linear feature was quantified using the relative move direction ($\xi : -\pi \leq \xi < \pi$). The relative move direction was defined as defined the angle between the 'beeline' move direction of the animal (Turchin, 1998) and the direction from the current location towards the linear feature,

$$\xi = \text{sgn}(\mathbf{x} \cdot \mathbf{y}^{\perp}) \cos^{-1}\left(\frac{\mathbf{x} \cdot \mathbf{y}}{\|\mathbf{x}\|\|\mathbf{y}\|}\right), \tag{4.13}$$

where the variables are as defined in Figure 4.2(b), $\cdot$ represents the vector dot product, and $\|\cdot\|$ is the norm. Note that ξ is defined everywhere, as it is the direction towards the centre of the linear feature. In the context of animal movement, $\xi = \pm\pi/2$ represent moves along the linear feature, $\xi = 0$ represents moves towards the linear feature, and $\xi = \pm\pi$ represent moves away from the linear feature. GPS measurement error may result in incorrect inference of move direction between locations that are less than 5 standard deviations of the GPS error kernel apart (Jerde and Visscher, 2005; Hurford, 2005). To avoid incorrect inference only those relative move directions with corresponding move distances greater then 55 m (Chapter 2) were used.

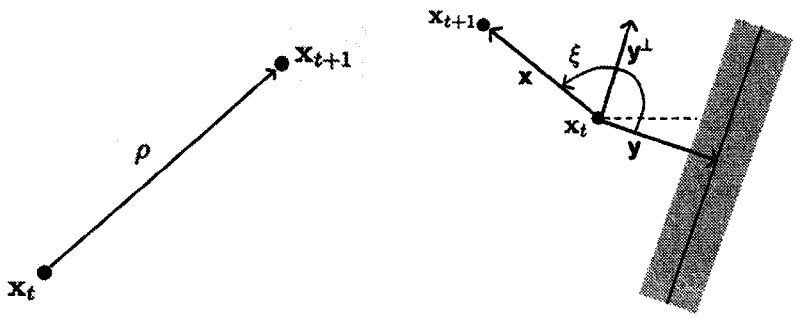

(a) Move distance (b) Relative Move direction

Figure 4.2: Movement variables used to quantify wolf response to linear features. (a) ρ is the distance between two consecutive wolf locations. (b) ξ is the angle between the 'beeline' move and the direction of the nearest linear feature.

Temporal autocorrelation in moves. Animal move directions may be temporally correlated over short times (Turchin, 1998). The relevant way of computing correlation between angles from a non-normal population is using the statistic $(\rho_{aa})_s$, which is obtained from the ranks of circular measurements, and is analogous to the Spearman rank correlation coefficient (Mardia, 1975; Zar, 1996). I tested the null hypothesis that move directions were uncorrelated ($H_0 : (\rho_{aa})_s = 0$) against the alternate hypothesis that move directions were correlated ($H_1 : (\rho_{aa})_s \neq 0$), using a non-parametric correlation procedure (Mardia, 1975; Zar, 1996). Because of large sample sizes ($n > 1500$) the power of the test was large, and therefore rejection of the null hypothesis was likely even for small deviations of $(r_{aa})_s$ from zero (Royall, 1997). Move directions were statistically correlated (Appendix 4.B). A common approach for eliminating correlation is to subsample the data at a longer time interval. I chose not to take this approach, as I was interested in wolf movement over a short-time scale. Because the correlation was small, I did not consider the correlation in subsequent analysis. However, this may have led to underestimation of the mean move distance (Kareiva and Shigesada, 1983).

Classification of locations. To understand how distance to linear feature affected movement variables, wolf locations were classified into three categories: on, near, or far from linear features. Linear features were assumed to have an average width of 5 m and were buffered by an additional 24.5 m to account for GPS measurement error in wolf locations. The size of the buffer was chosen using the method outlined in Chapter 1. Locations within the GPS error buffer were classified on the linear feature. Locations between the GPS error buffer and the range at which wolves perceived linear features were classified near. Because animal perceptual range is not well-understood (Lima and Zollner, 1996), I used two distances in the analysis. The first represented the distance at which linear features might be visible to wolves (50 m) and the second represented a distance at which wolves stopped responding to linear features (200 m) (Whittington et al., 2005). Locations beyond the wolf's perceptual range were classified as far from a linear feature.

Differences in movement distances. Move distances of canids are well-described by an exponential distribution (Moorcroft and Lewis, 2006). Therefore, I assumed the distribution of move distances ρ followed an exponential distribution

$$f(\rho) = \frac{1}{\alpha} \exp\left[-\rho/\alpha,\right] \tag{4.14}$$

where α is the expected move distance. The maximum likelihood estimate for α

is $\hat{\alpha}_{MLE} = \bar{p}$. To test whether the distribution of distances travelled by wolves differed as a function of distance from a linear feature 90% confidence intervals for $\hat{\alpha}_{MLE}$, obtained with non-parameteric bootstraping (Efron and Tibshirani, 1993), were compared among distance classes.

Movement along linear features. Using locations on linear features, I tested whether wolves on linear features tended to continue along the linear feature in the next move. The von Mises distribution is commonly used for animal movement directions (Fisher, 1993; Moorcroft and Lewis, 2006). It is a symmetric unimodal distribution similar to the circular normal distribution. The probability density function is written as

$$f(\phi) = \frac{1}{2\pi I_0(\kappa)} \exp\left[\kappa \cos(\phi - \phi')\right], \tag{4.15}$$

where I_0 is the Bessel function of the first kind, $-\pi \leq \phi' \leq \pi$ is the mean direction, and $\kappa > 0$ is the concentration parameter defining the degree of non-uniformity of the distribution. In the limits, as $\kappa \to 0$ the distribution converges to the uniform distribution and as $\kappa \to \infty$ the distribution tends to a delta function centred on the mean direction. A bivariate von Mises distribution can be written as a combination of two von Mises distributions,

$$f(\phi) = \frac{p}{2\pi I_0(\kappa_1)} \exp\left[\kappa_1 \cos(\phi - \phi_1)\right] + \frac{(1-p)}{2\pi I_0(\kappa_2)} \exp\left[\kappa_2 \cos(\phi - \phi_2)\right], \tag{4.16}$$

where ϕ_1, ϕ_2, and κ_1, κ_2 are the mean directions and concentration parameters of the univariate distributions, and $0 \leq p \leq 1$. I assumed the distribution of relative move directions on linear features ξ followed a bivariate von Mises distribution

$$f(\xi; \kappa) = \frac{1}{4\pi I_0(\kappa)} \exp[\kappa \cos(\xi + \pi/2)] + \frac{1}{4\pi I_0(\kappa)} \exp[\kappa \cos(\xi - \pi/2)], \tag{4.17}$$

and tested the null hypothesis $H_0 : \kappa = 0$ against the alternate hypothesis $H_1 : \kappa > 0$ using the parametric bootstrap likelihood ratio (PBLR) test (Barnard, 1963; Dennis and Taper, 1994). The PBLR was used in this case because the parameter of interest, κ, is bounded by 0 and therefore the likelihood ratio test does not follow the Chi-squared distribution (Barnard, 1963).

Movement towards linear features. I used locations classified as near linear features to determine if wolves near linear features biased their next move towards the linear feature. The distribution of relative move directions was assumed to be

$$g(\xi;\kappa) = \frac{1}{2\pi I_0(\kappa)} \exp[\kappa \cos(\xi)], \tag{4.18}$$

and the null hypothesis $H_0 : \kappa = 0$ was tested against the alternate hypothesis $H_1 : \kappa > 0$ using the parametric bootstrap likelihood ratio test (Barnard, 1963; Dennis and Taper, 1994). I repeated the same test on locations far from linear features to determine whether wolves beyond the perceptual range moved randomly with respect to linear features.

4.3.4 Mean first passage time analysis

Predator search time under different scenarios was assessed using mean first passage time methods (Chapter 2). The mean first passage time for each scenario was summarized using the spatial average of the mean first passage time,

$$\text{MFPT}_{avg} = \frac{1}{A} \int_{\Omega} w(\mathbf{x})\, \mathbf{x}, \tag{4.19}$$

where Ω is a landscape or area A and w is the mean first passage time from initial location x. Biologically MFPT_{avg} can be interpreted as the expected search time of a randomly located wolf. Definitions of animal movement, landscape configuration, and prey locations are required to parameterize the mean first passage time model 4.1. I considered combinations of four wolf movement behaviours, eleven landscapes of varying linear feature density, and four prey distributions.

Wolf movement behaviour. Four models of wolf response to linear features were considered. In the no response model (NR), wolves did not alter their movement in response to linear features. Although this model may be biologically unreasonable (Thurber et al., 1994; James, 1999; Whittington et al., 2004, 2005), it provides a baseline for comparison. The anisotropic diffusion model (AD) incorporated faster movement rates on linear features, as well as the tendency to continue along linear features. The anistotropic diffusion and bias model (AD+BIAS) was an extension of AD, where wolves near linear feature biased their movements towards the linear feature. The final model was a modification of AD+BIAS that arose from an observation of wolf movement. In this case movements near linear features were biased towards linear features, but were also shorter. This model is referred to as the anisotropic diffusion and bias with reduced diffusion model (AD+BIAS+RD). The wolf responses were incorporated into the models by the advection and diffusion coefficients. Formulae for the coefficients of each model were derived following the

method of Moorcroft and Lewis (2006) (Appendices 4.C and 4.D).

Linear feature density. Geographical locations of linear features were mapped to a resolution of 5 m using Indian Remote sensing satellite imagery. Landscapes were created based on a section of the study area near Rocky Mountain House with linear feature density of 3.8 km/km^2 (Figure 4.3). To create landscapes of lower linear feature densities, while controlling for the configuration of the linear features, I randomly selected linear features to be removed from the landscape, such that landscapes of approximately 0, 20, 40, 60, and 80 % of the original linear feature density were obtained. Landscapes of approximately 120, 140, 160, 180, and 200% of the original linear feature density where generated by combining the original landscape with each of the new lower density landscapes rotated by 90°.

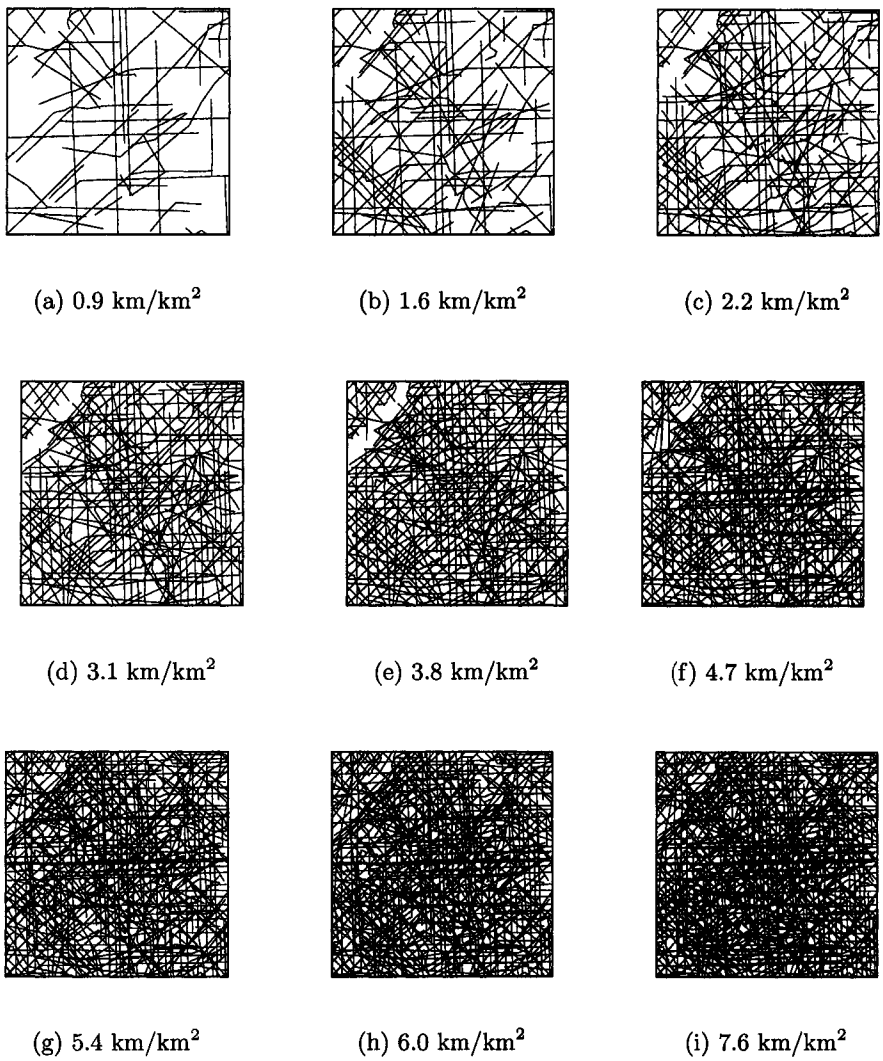

(a) 0.9 km/km^2 (b) 1.6 km/km^2 (c) 2.2 km/km^2

(d) 3.1 km/km^2 (e) 3.8 km/km^2 (f) 4.7 km/km^2

(g) 5.4 km/km^2 (h) 6.0 km/km^2 (i) 7.6 km/km^2

Figure 4.3: Landscapes of varying linear feature densities. The original landscape is shown in (e). Landscapes of lower and higher linear features densities were created by removing randomly selected linear features or combining the original landscape with each reduced landscape rotated by 90°.

Prey distribution. Prey were represented as disks or radius 100 m. The choice of radius will not affect relative comparison of mean first passage times among models. One hundred prey were placed in each landscape according to distributions that were random, clumped, near (within 200 m) and far (beyond 200 m) from linear features (Figure 4.4).

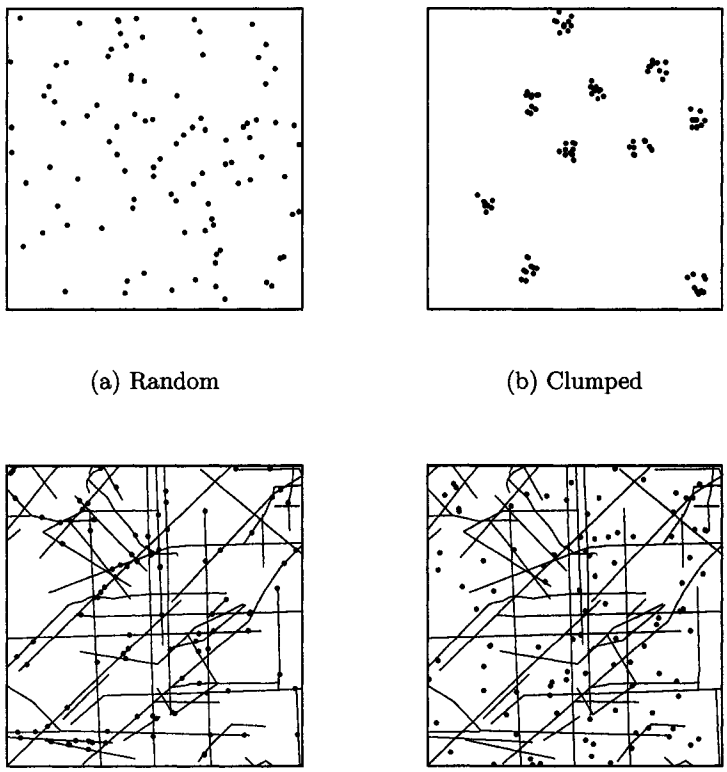

(a) Random (b) Clumped

(c) Near: 0.9 km/km^2 (d) Far: 0.9 km/km^2

Figure 4.4: Prey distributions. Each landscape contains 100 prey placed in the landscape (a) randomly, (b) clumped, (c) near (within 200 m), or far (beyond 200 m) from linear features. One example is shown for the landscape with 0.9 km/km^2 where prey are distributed near and far from linear features.

4.3.5 Functional response

The functional response was calculated using Eqs 4.10 and 4.11. To comply with the assumption of randomly distributed prey (Holling, 1959), mean first passage time was calculated from model scenarios where prey were randomly distributed. Wolves had movement behaviour described by model AD and landscapes with linear feature densities of 0, 3.1, and 7.6 km/km^2 were used. I compared functional responses between linear feature densities using a ratio of Holling Type II functional responses (Holling, 1959),

$$g(N) = \frac{(a_{LF}N)/(1 + a_{LF}T_hN)}{(aN)/(1 + aT_hN)}, \tag{4.20}$$

where N is the prey density, T_h is the handling time (defined by Holling (1959) as the combined chasing and manipulation times), and a_{LF}, a are the encounter rates for landscapes with and without linear features. A handling time of $T_h = 48$ hrs was assumed, but had no effect on the comparison among linear feature densities. Ratios greater than 1 indicated wolves killed more prey per unit of time in landscapes with linear features than without linear features.

4.4 Results

4.4.1 Quantitative description of wolf movement

Effect of location on movement distance. The mean distance moved by wolves on linear features ranged from 100-190 m, and was farther than in other parts of the landscape (Figure 4.5). While wolves 230, 232, and 234 had shorter move distances far from linear features, wolf 233 showed the opposite trend, with shorter move distances near linear features. Mean move distances of wolves far from linear features were similar among all wolves, ranging from 50-100m.

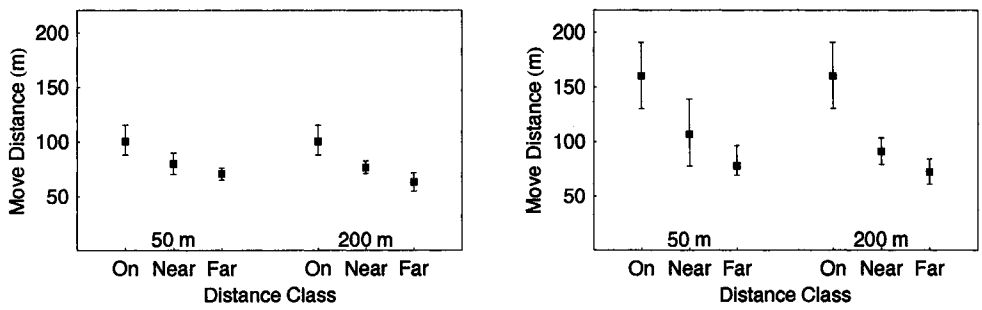

(a) Wolf 230

(b) Wolf 232

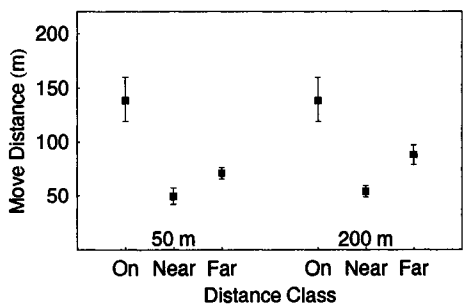

(c) Wolf 233

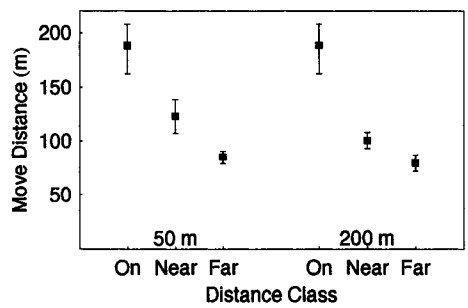

(d) Wolf 234

Figure 4.5: Mean move distance of wolves at different distances from linear features. Near and far were defined using perceptual ranges of 50 m and 200 m. Bars are 90% non-parametric bootstrapped confidence intervals.

Movement along linear features. When on linear features, three of the four wolves (230, 233, and 234) had distributions of relative move directions that differed from the uniform distribution (Table 4.1, Figure 4.6). These wolves selected movement directions along the linear feature more often then any other direction. However, wolf 232 had a uniform distribution of relative move directions, suggesting it moved randomly with respect to the nearest linear feature.

Table 4.1: Results of the parametric bootstrap likelihood ratio test for moves on linear features. The null hypothesis for the test is $f(\xi;\kappa = 0)$ and the alternate hypothesis is $f(\xi;\kappa = 0)$. Number of bootstrap samples = 2000.

Wolf	$\hat{\kappa}_{MLE}$	LRT statistic	Critical value	p-value	Conclusion
230	1.43	0.009	0.457	<0.001	Reject H_0
232	0.61	0.902	0.428	0.31	Do no reject H_0
233	1.76	0.004	0.406	<0.001	Reject H_0
234	1.54	0.003	0.419	<0.001	Reject H_0

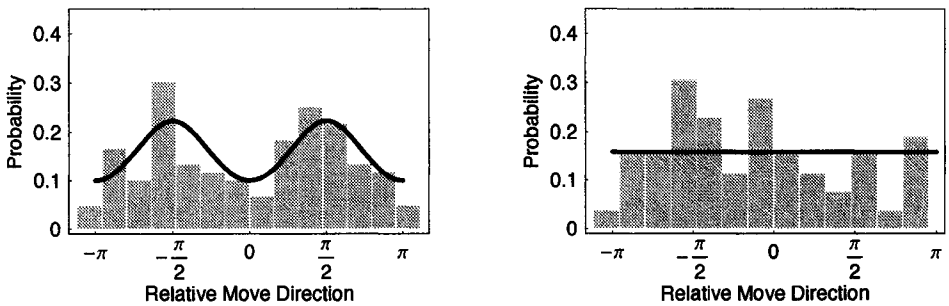

(a) Wolf 230

(b) Wolf 232

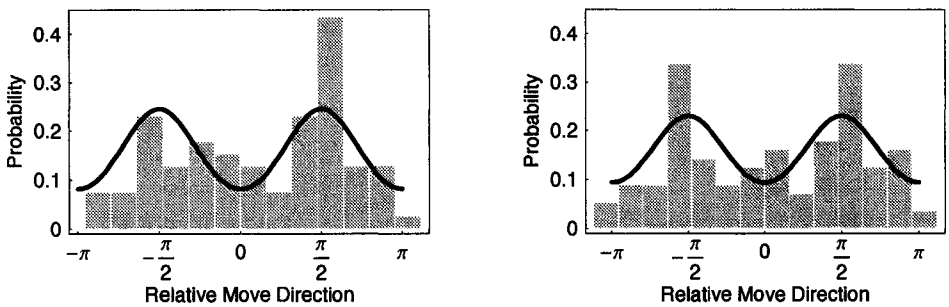

(c) Wolf 233

(d) Wolf 234

Figure 4.6: Distribution of relative move directions of wolves on linear features. Bars represent the empirical distribution, solid lines are the maximum likelihood fit of the model chosen using the PBLR test. Wolves 230, 232, and 234 (panel a,c, and d) had distributions of relative move directions that varied from uniform, while wolf 230 (panel b) had a uniform distribution of relative move directions.

Movement towards linear features. Wolf 233 had a non-uniform distribution of relative move directions within 50 and 200 m of a linear feature (Table 4.2 and Figures 4.7, 4.8). The single mode of the distributions corresponded to movements towards linear features, suggesting a bias to move towards linear features when near them (both within 50 and 200 m). All other wolves had uniform distributions of move distances within 50 and 200 m of a linear feature and displayed no bias to move towards linear features when near them.

Table 4.2: Parametric bootstrap likelihood ratio test for moves near linear features. The null hypothesis for the test is $g(\xi;\kappa = 0)$ and the alternate hypothesis is $g(\xi;\kappa = 0)$. Number of bootstrap samples = 2000.

Wolf	$\hat{\kappa}_{MLE}$	LRT statistic	Critical value	p-value	Conclusion
Within 50 m:					
230	0.	1.003	0.434	0.82	Do not reject H_0
232	0.	1.001	0.427	0.60	Do not reject H_0
233	0.34	0.078	0.452	0.01	Reject H_0
234	0.04	0.959	0.412	0.38	Do not reject H_0
Within 200 m:					
230	0.01	0.990	0.453	0.43	Do not reject H_0
232	0.	1.007	0.464	0.96	Do not reject H_0
233	0.24	0.040	0.432	0.003	Reject H_0
234	0.01	0.990	0.430	0.43	Do not reject H_0

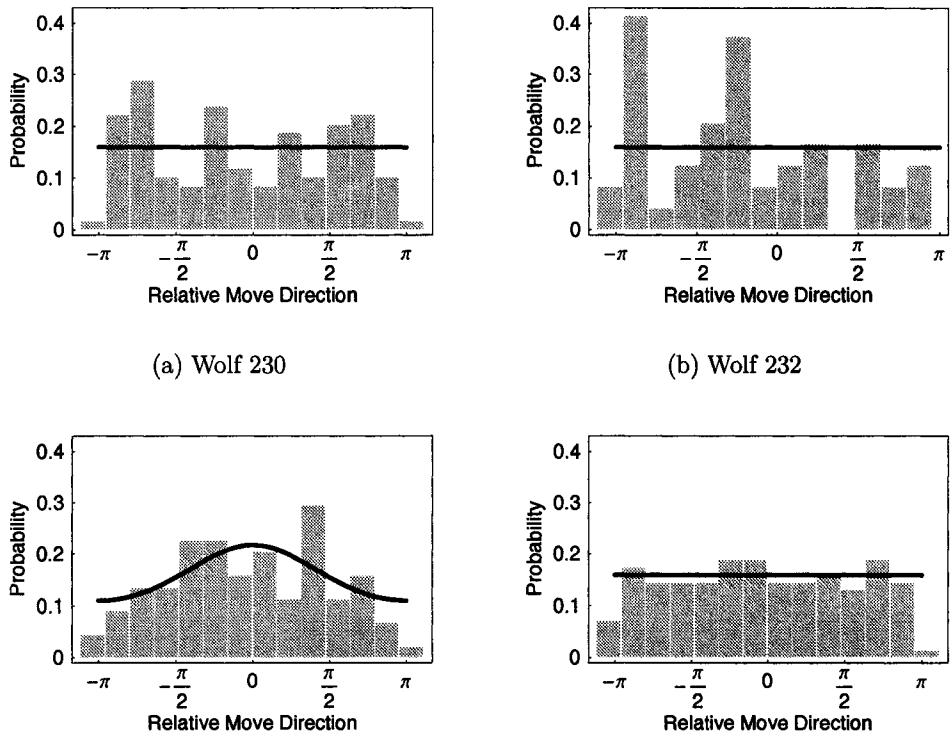

(a) Wolf 230

(b) Wolf 232

(c) Wolf 233

(d) Wolf 234

Figure 4.7: Distribution of relative move directions of wolves within 50 m of a linear feature. Bars represent the empirical distribution, solid lines are the maximum likelihood fit of the model chosen using the PBLR test. Wolf 233 (panel c) displayed a bias to move towards the linear feature, while wolves 230, 232, and 234 (panels a, b, and d) did not.

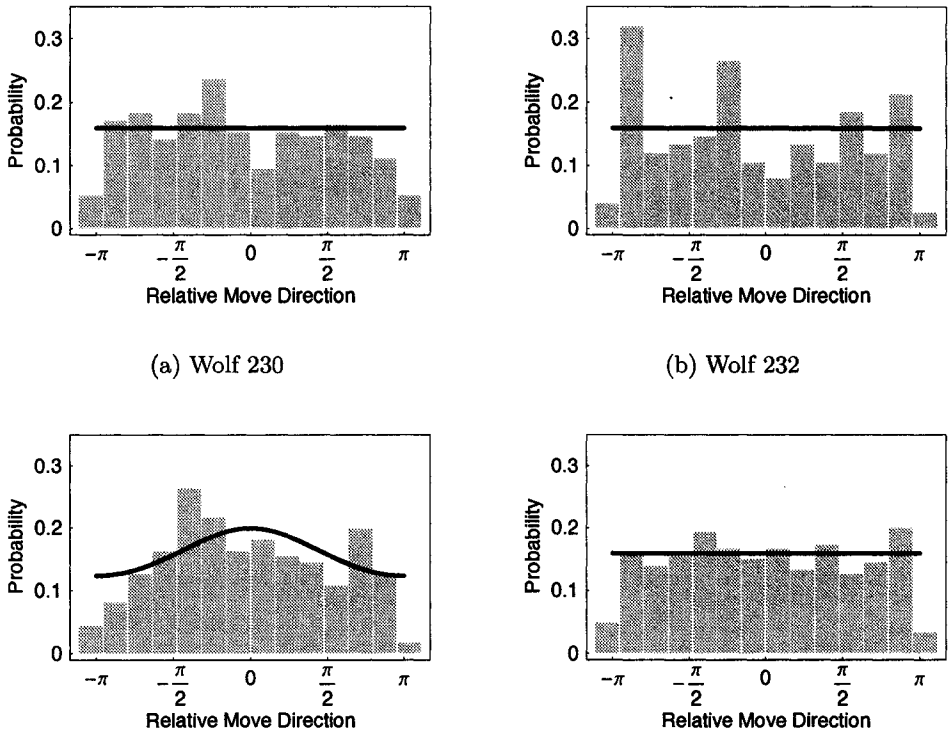

(a) Wolf 230

(b) Wolf 232

(c) Wolf 233

(d) Wolf 234

Figure 4.8: Distribution of relative move directions of wolves within 200 m of a linear feature. Bars represent the empirical distribution, solid lines are the maximum likelihood fit of the model chosen using the PBLR test. Wolf 233 (panel 3) displayed a bias to move towards the linear feature, while wolves 230, 232, and 234 (panels a, b, and d) did not.

The distribution of relative move directions of wolves far from linear features did not differ from a random distribution (Table 4.3 and Figures 4.9, 4.10). Therefore wolves did not bias their movements towards linear features when they were beyond either 50 and 200 m.

Table 4.3: Parametric bootstrap likelihood ratio test for moves far from linear features. The null hypothesis for the test is $g(\xi; \kappa = 0)$ and the alternate hypothesis is $g(\xi; \kappa = 0)$. Number of bootstrap samples = 2000.

Wolf	$\hat{\kappa}_{MLE}$	LRT statistic	Critical value	p-value	Conclusion
Beyond 50 m:					
230	0.081	0.601	0.420	0.18	Do not reject H_0
232	0.	1.01	0.419	0.86	Do not reject H_0
233	0.083	0.575	0.428	0.15	Do not reject H_0
234					
Beyond 200 m:					
230	0.081	0.862	0.459	0.29	Do not reject H_0
232	0.041	0.952	0.447	0.37	Do not reject H_0
233	0.018	0.990	0.445	0.42	Do not reject H_0
234	0.	1.	0.460	0.48	Do not reject H_0

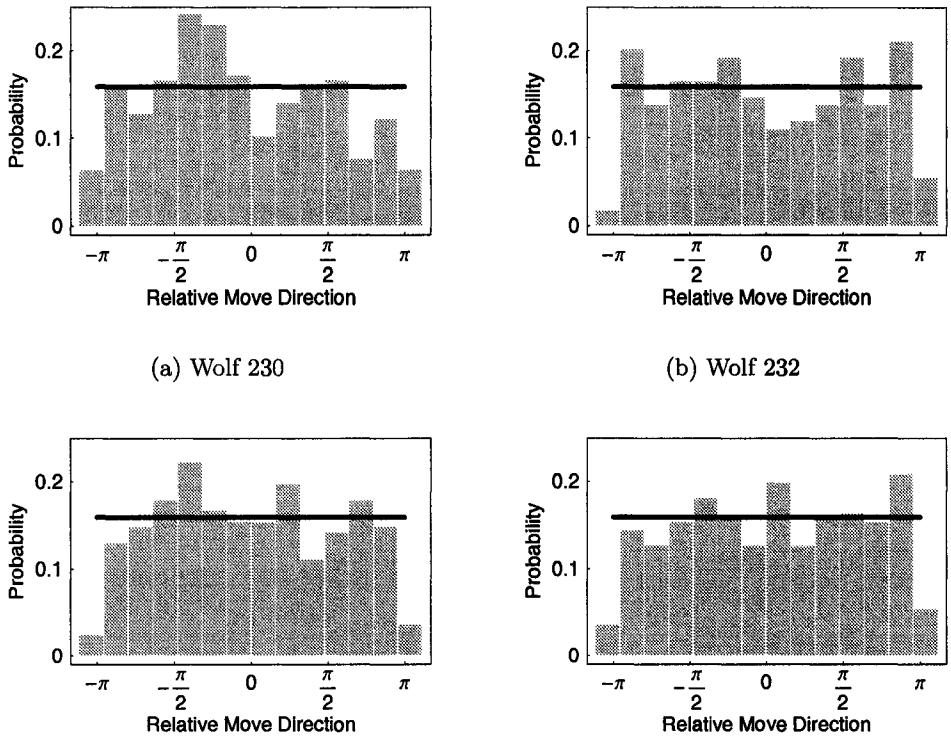

(a) Wolf 230

(b) Wolf 232

(c) Wolf 233

(d) Wolf 234

Figure 4.9: Distribution of relative move directions of wolves beyond 50 m of a linear feature. Bars represent the empirical distribution, solid lines are the maximum likelihood fit of the model chosen using the PBLR test. All wolves had uniform distributions of relative move directions.

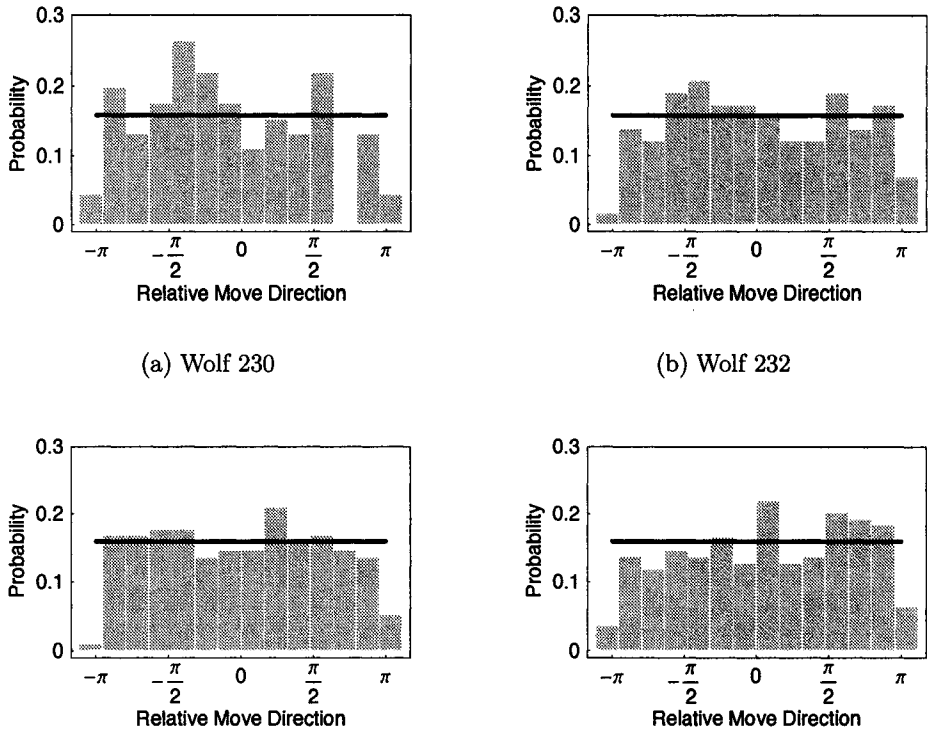

(a) Wolf 230

(b) Wolf 232

(c) Wolf 233

(d) Wolf 214

Figure 4.10: Distribution of relative move directions of wolves beyond 200 m of a linear feature. Bars represent the empirical distribution, solid lines are the maximum likelihood fit of the model chosen using the PBLR test. All wolves had uniform distributions of relative move directions.

4.4.2 Mean first passage time analysis

The mean first passage time model was parameterized using the movement data from wolf 233 and a perceptual range of 50 m (Table 4.4).

Table 4.4: Movement parameters for wolf 233. Near was defined using a perceptual range of 50 m. Four models were considered: NR = no response, AD = anisotropic diffusion on linear features, AD+BIAS extends AD to include bias towards linear features, and AD+BIAS+RD is the AD+BIAS model with reduced diffusion near linear features. Parameters were estimated from the distributions of move distance and move direction using maximum likelihood.

	Parameters		
Model	$\overline{\rho}$ (km)	$\overline{\rho^2}$ (km^2)	κ
NR:			
	0.071	0.017	0
AD:			
On	0.139	0.043	1.76
Off	0.071	0.017	0
AD+BIAS:			
On	0.139	0.043	1.76
Near	0.071	0.017	0.34
Far	0.071	0.017	0
AD+BIAS+RD:			
On	0.139	0.043	1.76
Near	0.049	0.012	0.34
Far	0.071	0.017	0

Mean first passage time surfaces had local differences. For example, surface height, location and presence of peaks, and steepness of gradients differed among mean first passage time surfaces for different wolf movement behaviours, linear feature densities, and prey distributions (Figure 4.11).

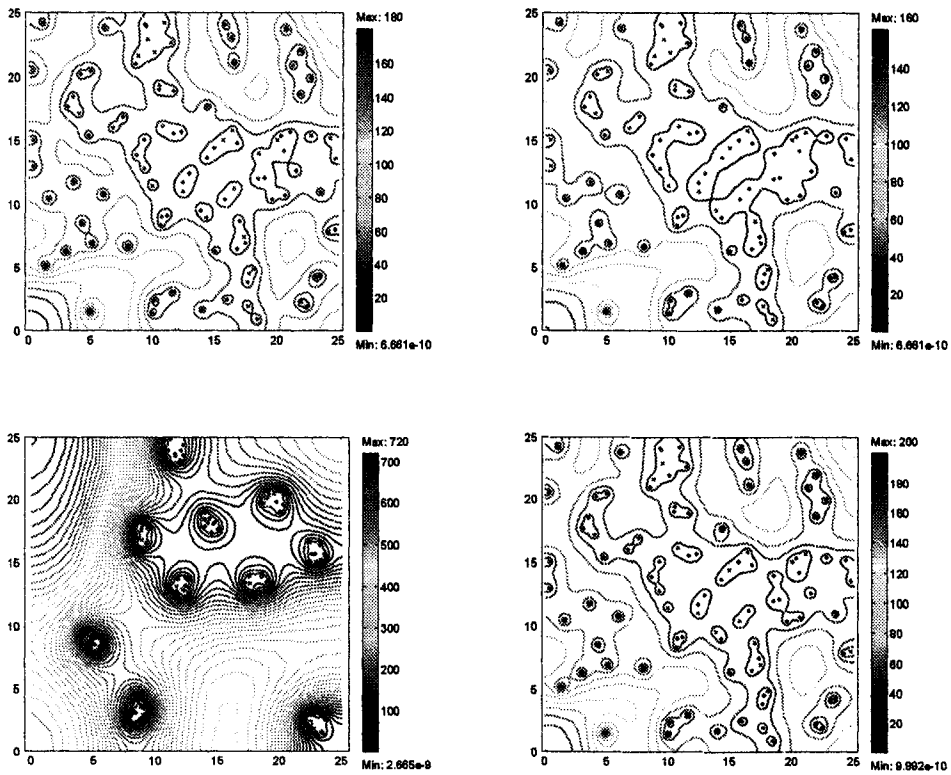

Figure 4.11: MFPT surfaces showing local variation. The model scenarios are (a) AD movement with linear feature density of 3.1 km/km^2 and randomly distributed prey, (b) AD movement with linear feature density of 7.6 km/km^2 and randomly distributed prey, (c) AD movement with linear feature density of 3.1 km/km^2 and clumped prey, and (d) AD+BIAS+RD movement with linear feature density of 3.1 km/km^2 and randomly distributed prey. The movement models are denoted by AD for anisotropic diffusion and AD+BIAS+RD for anisotropic diffusion and bias, with reduced diffusion near linear features. In each case the contours represent a different of 20 hr, however please note the different vertical scales.

Mean first passage time decreased linearly with increasing linear feature density (Figure 4.12). While mean first passage times for landscapes where prey were distributed near and far from linear features are more variable, due to stochasticity in prey locations, the general trend remains decreasing. When prey were clumped mean first passage times were approximately 6 times longer than for all other prey distributions considered. In contrast, mean first passage times for randomly distributed prey and prey distributed near and far from linear features were similar. Wolves that responded to linear features had shorter mean first passage times than those that did not (model NR). There was no difference between wolf movement with and without bias towards linear features (models AD and AD+BIAS). However, wolves with bias and reduced movement rates near linear features (model AD+BIAS+RD) found prey consistently more slowly than other wolves responding to linear features.

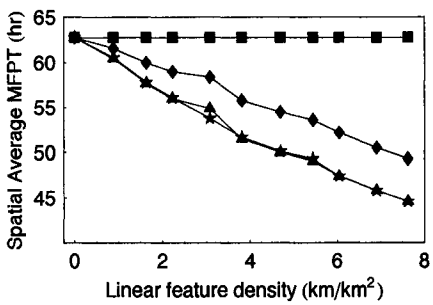

(a) Random prey distribution

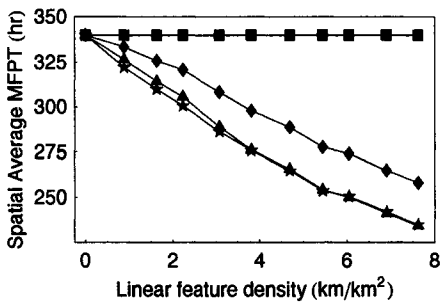

(b) Clumped prey distribution

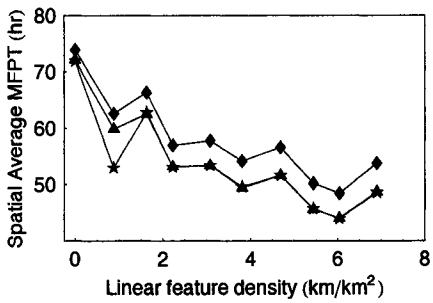

(c) Prey distributed near linear features

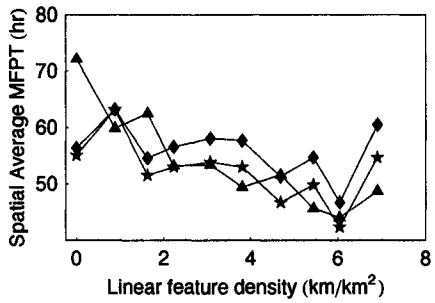

(d) Prey distributed far from linear features

Figure 4.12: Spatial averages of the mean first passage time for varying wolf responses and linear feature densities when prey (n=100) distributions are (a) random and (b) clumped, (c) near, and (d) far from linear features in a landscape 626 km^2. Wolf responses are NR (square), AD (star), AD+BIAS (triangle), and AD+BIAS+RD (diamond). Note the different vertical scales.

4.4.3 Functional response

In landscapes with linear features the wolf's functional response saturated more quickly than in landscape without linear features (Figure 4.13(a)). At low prey densities, wolves in landscapes with linear feature densities of 3.1 and 7.6 km/km^2 killed approximately 1.2 and 1.4 times more prey than wolves in landscapes with no linear features (Figure 4.13(b)). The relative increase in kill rates was larger at low prey densities and became negligible at high prey densities.

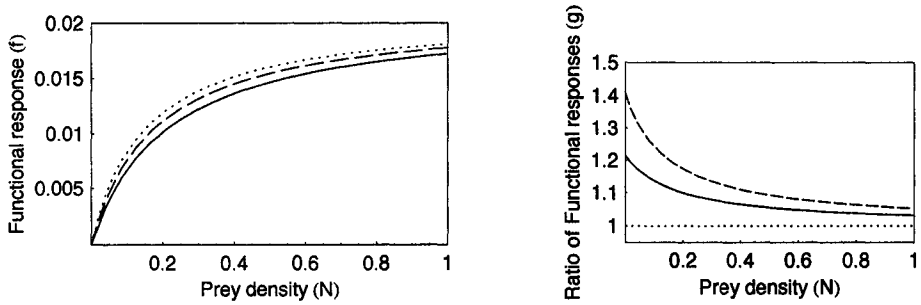

(a) Functional Response

(b) Ratio of functional responses

Figure 4.13: Illustration of the effect of linear features on a Holling type II functional response for a wolf. The change in the rate of approach to the saturation is shown in (a) for linear feature densities of 0 (solid), 3.1 (dashed) and 7.6 (dotted) km/km^2. Panel (b) shows the ratio of the functional response of wolves in landscapes with linear features to landscapes without linear features, where linear feature density is 3.1 (solid) and 7.6 (dashed) km/km^2.

4.5 Discussion

In this chapter I investigated how spatial heterogeneity can influence predator-prey dynamics. Specifically, I determined how changing the linear feature density in the landscape affected the functional response of wolves using data from the central east slopes of the Rocky mountains (Alberta, Canada). The approach was to use mean first passage time analysis, which incorporated observed wolf movement behaviour and landscape heterogeneity, to understand the effect of increasing linear feature density on search time. Search time was then connected to the functional response through the encounter rate.

Empirical data showed that linear features altered wolf movement. Differences in mean distance moved per unit time of wolves as a function of distance from linear features were consistent with differences observed by James (1999) (Figure 4.5). However, the tendency of wolves to continue along linear features when on them had not previously been shown (Figure 4.6). While wolves have been shown to alter their direction with respect to linear features when near them (Callaghan, 2002), I observed bias towards linear features for only one out of four wolves (Figures 4.7 and 4.8). One explanation is that the wolves observed did not bias their movement towards linear features. Alternatively, inference of such fine-scale directional response from GPS location data may not be possible (Callaghan (2002) relied on movement paths obtained through snow-tracking), or grouping individual move directions into distributions swamped weak directional biases.

Analysis of wolf movement using mean first passage time models, parameterized with empirical movement data, showed that increasing linear feature density led to decreased mean first passage time. Therefore, wolves found prey faster in landscapes containing higher densities of linear features. The observed decrease in search time is caused by increased predator mobility due to increased mean move distances of wolves on linear features, as well as their tendency to continue along linear features once they are on them (Figures 4.5 and 4.6). This finding is supported by spatially-explicit individual-based predator-prey models which showed increased predator mobility would led to increased encounter rates with prey (i.e. decreased search time) (McCauley et al., 1993). Because wolves are widely foraging predators that rely on covering large areas in search of prey (Pianka, 1966; Mech and Boitani, 2003) and searching success is linked to predator mobility (Bell, 1991), the MFPT model presented here provides the first empirically-based evidence for the hypothesis that linear features would affect predator-prey dynamics (Edmonds and Bloomfield,

1984; Bergerud and Elliot, 1986). Although linear feature configuration was not considered here, it is likely the natural interconnected arrangement of linear features in the landscape influenced the results. It is expected that in landscapes with similar densities of parallel, rather than intersecting linear features, MFPT would decrease at a slower rate.

Decreasing MFPT (i.e. increasing encounter rate) resulted in an increased predator functional response (Eq 4.11, Figure 4.1), as suggested by McCauley et al. (1993). Therefore, for a constant prey density, wolves in landscapes with higher linear feature densities had higher per capita kill rates, assuming constant predation sucess. For the parameter estimates and range of linear feature densities considered here, the model estimated a 1.4 times increase in the number of prey killed by a single predator per unit time at low prey densities (Figure 4.13). The effect of linear features on kill rate was reduced as prey densities increased. One possible explanation is that mobility constrains searching success more at low rather than high prey densities when prey are randomly distributed (Cain, 1985). For example, at low prey densities prey are spaced further apart, therefore the relative benefits of increased mobility are greater than at high prey densities when prey are closer together. For extremely high prey densities, search time becomes insignificant and the functional response is dominated by handling time (Holling, 1959). In this case, the increased encounter rate facilitated by linear features would have relatively little effect. However, at low prey densities, when the functional response is driven by search time, the effect of linear features on predator mobility is expected to be relatively large. One possible consequence of this increased functional response would be a numerical increase in the wolf population and subsequent depletion of ungulate populations. Therefore, in terms of conservation, increasing linear feature density will have a larger relative impact on predator-prey dynamics when the prey is at risk (i.e. low density), as is the case for caribou in Alberta (Dzus, 2001). In general, any mechanism that increases or decreases encounter rate, such as increased mobility, will lead to an increase or decrease in the functional response.

The spatial distribution of prey also affected the functional response via the encounter rate. The MFPT was longer when prey were aggregated than when they were distributed randomly, near, or far from linear features (Figure 4.12). These results are consistent with simulations done by Cain (1985), who showed that herbivores found uniformly dispersed plants more easily than clumped plants. However, as linear feature density increased, the proportionate decrease in MFPT

was the same for each prey distribution. For non-random prey distributions the Holling disk equation cannot be used to calculate the effect of increasing linear feature density on the prey consumption rate (Holling, 1959). However, because the proportionate change in MFPT was similar among prey distributions, the change in predator-prey functional response is also expected to be similar. Thus for example, the wolf's functional response to elk, which tend to aggregate (Hebblewhite and Pletscher, 2002) and moose, which tend to be more dispersed across the landscape (Schwartz and Franzmann, 1998), would have the same relative change with increasing linear feature density. The variation in absolute MFPT among different prey distributions suggests the time required for predators to find prey in their landscape is a function of both spatial heterogeneity affecting predator movement and heterogeneity in prey distribution. MFPT provides a combined measure of both of these types of heterogeneity.

There was no difference in MFPT for prey distributed near and far from linear features. This result followed from the effect of wolf bias towards linear features on MFPT. Specifically, addition of bias towards linear features to the wolf's movement response did not affect the MFPT (Figure 4.12). However, when the bias was coupled with shorter mean move distances near linear features, as was observed for wolf 233 (Figures 4.5, 4.7, and 4.8), MFPT was longer. Because bias alone did not alter MFPT, the observed difference in this case can be explained solely by the decreased movement rate near the linear features.

The finding that MFPT did not decrease when bias was included in the movement behaviour was unexpected, particularly when prey were distributed near linear features. Consider first the insignificant effect of bias. A possible explanation for why the addition of bias did not change the MFPT is that the direction of the bias changes over a small spatial range throughout the landscape. For example, wolves located within a radius of 100 m may experience different bias directions, depending on the direction of the nearest linear feature. Therefore, due to the local nature of the bias, the overall effect on the MFPT is small. Alternatively, because the behavioural mechanism underlying a wolf's bias towards linear features is not well-understood, I took at behaviourally-minimalistic approach to modelling wolf bias (Lima and Zollner, 1996). This approach dictates that movement models include only behavioural traits that are likely to be of most importance for describing animal movement. As indicated by Lima and Zollner (1996), the informed decisions required of the researcher about what behaviour should be included constitute a major

challenge of this approach. To further explore the effects of movement bias on MFPT and predator-prey interactions, it would be important to understand the underlying mechanism for the potential bias. Perhaps it is a function of extrinsic factors such as local prey density, or current state of the linear feature (i.e. presence of humans, deep snow) not considered here. More complex still, perhaps intrinsic details, such as level of hunger, behavioural state (travelling, hunting, territorial defence, mating), or spatial memory (i.e. knowledge of areas of high prey density or cognitive maps of linear feature locations) are essential for making correct biological inferences. Untangling the important aspects of the mechanism underlying wolf use of linear features would require a large amount of data, as well as extensive and creative model analysis. I now return to the insignificant effect of prey distributed near or far from linear features. This resulIt was contrary to studies suggesting predation risk for caribou and elk increased near linear features (James and Stuart-Smith, 2000; Frair et al., 2005). It is possible that while encounter rates are similar throughout the landscape, wolves have a higher capture success rate near linear features. In the Holling type II functional response, capture success is assumed to be 100%, and therefore this mechanistic difference would not be captured in my analysis. Additionally, James and Stuart-Smith (2000) found that wolves were significantly closer to linear features than expected, and therefore perhaps calculating the average MFPT under the assumption of a uniform distribution of predator starting locations is not appropriate.

This study found that increasing linear feature density led to decreased search time and increased predator functional response, particularly at low prey densities. This result has specific implications for the effects of linear features on wolf-ungulate dynamics and management in the central east slopes of the Rocky mountains (Alberta, Canada). I also developed and illustrated a new application of MFPT for investigating the effects of spatial heterogeneity on predator movement, search time, and predator-prey dynamics. While alternate searching strategies (Zollner and Lima, 1999; Bailey and Thompson, 2006), the cost of searching (Cain, 1985), and population dynamics (e.g. numerical response of predators) (McCauley et al., 1993) were not considered here, I acknowledge the potential of the integration of these subjects with the mean first passage time method. This framework could be more generally applied to similar ecological questions about the impact of spatial heterogeneity on dispersal, mate-finding, and resource acquisition.

Appendix

4.A Wolves monitored for the winter 2005

Table 4.5: Wolves monitored during the winter of 2005.

Wolf	Pack	Dates	N	Linear feature density km/km^2
230	Radial Lake	Jan 29, Feb 2 & 26, Mar 2,26, & 30	5345	2.44
232	Blackstone	Jan 22 & 26, Feb 19 & 23, Mar 19 & 23	6477	1.73
233	Blackstone	Feb 5 & 9, Mar 5 & 9, Apr 2 & 6	5076	1.73
234	Prairie Creek	Jan 29, Feb 2 & 26, Mar 2,26, & 30	5109	3.60

4.B Temporal correlation in move direction

Table 4.6: Circular correlation coefficients for move directions (5-min). Results of a non-parametric angular-angular correlation test of the null hypothesis $H_0 : (\rho_{aa})_s = 0$ against the alternative $H_1 : (\rho_{aa})_s \neq 0$, where r_{aa} is analogous to the Spearman rank correlation coefficient.

Wolf	n	$(r_{aa})_s$	Test Statistic	p-value
230	3174	-0.10	-3.840	< 0.001
232	2002	-0.16	-4.668	< 0.001
233	3094	-0.12	-4.284	< 0.001
234	1551	-0.09	-3.533	< 0.001

4.C Movement in a landscape with linear features

I derive general formulas for the diffusion and advection coefficients of the first passage time equation given univariate and bivariate von Mises distributions of relative move directions. The derivation follows the method of Moorcroft and Lewis (2006). In the derivation I make use of the following:

1. The trigonometric identities,

$$\cos(\phi) = \frac{x' - x}{|\mathbf{x} - \mathbf{x}'|}$$

$$\sin(\phi) = \frac{y' - y}{|\mathbf{x} - \mathbf{x}'|}.$$

$$\cos^2(\phi) = \frac{1 + \cos(2\phi)}{2}$$

$$\sin^2(\phi) = \frac{1 - \cos(2\phi)}{2}$$

$$\sin(\phi)\cos(\phi) = \frac{\sin(2\phi)}{2}$$

$$\cos(2\phi) = \cos(2(\phi - \phi') + 2\phi') = \cos(2(\phi - \phi'))\cos(2\phi') - \sin(2(\phi - \phi'))\sin(2\phi')$$

$$\sin(2\phi) = \sin(2(\phi - \phi') + 2\phi') = \sin(2(\phi - \phi'))\cos(2\phi') + \sin(2\phi')\cos(2(\phi - \phi'))$$

2. If $K(\theta)$ is a von Mises distribution with concentration parameter κ then

$$\int_{-\pi}^{\pi} \cos(n\theta) K(\theta)\, d\theta = \frac{I_n(\kappa)}{I_0(\kappa)}.$$

3. The first and second moments of the distribution of move distances are defined to be

$$\overline{\rho} = \int_0^{\infty} \rho f(\rho)\, d\rho \quad \text{and} \quad \overline{\rho^2} = \int_0^{\infty} \rho^2 f(\rho)\, d\rho.$$

4. The series expansions of the modified Bessel functions:

$$I_0(\kappa) = 1 + \frac{1}{4}\kappa^2 + \text{h.o.t.}$$

$$I_1(\kappa) = \frac{1}{2}\kappa + \text{h.o.t.}$$

$$I_2(\kappa) = \frac{1}{8}\kappa^2 + \text{h.o.t.}$$

K is a univariate von Mises distribution

$$K = K(\phi - \phi') = \frac{1}{2\pi I_0(\kappa)} \exp[\kappa \cos(\phi - \phi')]$$

Diffusion

$$\begin{aligned}
d_{xx}(\mathbf{x}) &= \lim_{\tau \to 0} \frac{1}{2\tau} \int (x' - x)^2 k(\mathbf{x}, \mathbf{a}, \tau)\, d\mathbf{a} \\
&= \lim_{\tau \to 0} \frac{1}{2\tau} \int_0^\infty \rho^2 f(\rho)\, d\rho \int_{-\pi}^{\pi} \cos^2(\phi) K(\phi - \phi')\, d\phi \\
&= \lim_{\tau \to 0} \frac{1}{4\tau} \int_0^\infty \rho^2 f(\rho)\, d\rho \left(1 + \cos(2\phi') \int_{-\pi}^{\pi} \cos(2(\phi - \phi')) K(\phi - \phi')\, d\phi\right) \\
&= \lim_{\tau \to 0} \frac{\overline{\rho^2}}{4\tau} \left(1 + \cos(2\phi') \frac{I_2(\kappa)}{I_0(\kappa)}\right)
\end{aligned}$$

$$\begin{aligned}
d_{yy}(\mathbf{x}) &= \lim_{\tau \to 0} \frac{1}{2\tau} \int (y' - y)^2 k(\mathbf{x}, \mathbf{a}, \tau)\, d\mathbf{a} \\
&= \lim_{\tau \to 0} \frac{1}{2\tau} \int_0^\infty \rho^2 f(\rho)\, d\rho \int_{-\pi}^{\pi} \sin^2(\phi) K(\phi - \phi')\, d\phi \\
&= \lim_{\tau \to 0} \frac{1}{4\tau} \int_0^\infty \rho^2 f(\rho)\, d\rho \left(1 - \cos(2\phi') \int_{-\pi}^{\pi} \cos(2(\phi - \phi')) K(\phi - \phi')\, d\phi\right) \\
&= \lim_{\tau \to 0} \frac{\overline{\rho^2}}{4\tau} \left(1 - \cos(2\phi') \frac{I_2(\kappa)}{I_0(\kappa)}\right)
\end{aligned}$$

$$\begin{aligned}
d_{xy}(\mathbf{x}) &= \lim_{\tau \to 0} \frac{1}{2\tau} \int (x' - x)(y' - y) k(\mathbf{x}, \mathbf{a}, \tau)\, d\mathbf{a} \\
&= \lim_{\tau \to 0} \frac{1}{2\tau} \int_0^\infty \rho^2 f(\rho)\, d\rho \int_{-\pi}^{\pi} \sin(\phi)\cos(\phi) K(\phi - \phi')\, d\phi \\
&= \lim_{\tau \to 0} \frac{1}{4\tau} \int_0^\infty \rho^2 f(\rho)\, d\rho \left(\sin(2\phi') \int_{-\pi}^{\pi} \cos(2(\phi - \phi')) K(\phi - \phi')\, d\phi\right) \\
&= \lim_{\tau \to 0} \frac{\overline{\rho^2}}{4\tau} \left(\sin(2\phi') \frac{I_2(\kappa)}{I_0(\kappa)}\right)
\end{aligned}$$

$$d_{yx}(\mathbf{x}) = d_{xy}(\mathbf{x}).$$

Advection

To find the advection coefficient I make use of a geometric interpretation of the dot product. The dot product of $\mathbf{c}$ and $\mathbf{v}$, where $\mathbf{v} = [\cos(\phi', \sin\phi']$ is unit vector

pointing in the direction ϕ', can be interpreted as the length of the projection of $\mathbf{c}$ onto the vector $\mathbf{v}$ (Figure). The

$$\begin{aligned}
\mathbf{c}(\mathbf{x}) \cdot \mathbf{v}(\mathbf{x}) &= \lim_{\tau \to 0} \frac{1}{\tau} \int (\mathbf{x}' - \mathbf{x}) k(\mathbf{x}, \mathbf{a}, \tau)\, d\mathbf{a} \\
&= \lim_{\tau \to 0} \frac{1}{\tau} \int_0^{\infty} \rho f(\rho)\, d\rho \int_{-\pi}^{\pi} \cos(\phi - \phi') K(\phi - \phi')\, d\phi \\
&= \lim_{\tau \to 0} \frac{\overline{\rho} \kappa}{2\tau} \qquad (4.C\text{-}1)
\end{aligned}$$

Multiplying $\mathbf{c}$ by a unit vector perpendicular to $\mathbf{v}$, $\mathbf{v}^{\perp} = [-\sin\phi', \cos\phi']$ I find,

$$\begin{aligned}
\mathbf{c}(\mathbf{x}) \cdot \mathbf{v}^{\perp}(\mathbf{x}) &= \lim_{\tau \to 0} \frac{1}{\tau} \int (\mathbf{x}' - \mathbf{x}) k(\mathbf{x}, \mathbf{a}, \tau)\, d\mathbf{a} \\
&= \lim_{\tau \to 0} \frac{1}{\tau} \int_0^{\infty} \rho f(\rho)\, d\rho \int_{-\pi}^{\pi} \sin(\phi - \phi') K(\phi - \phi')\, d\phi x v \\
&= 0
\end{aligned}$$

because K is even. Therefore since there is no advection in the direction perpendicular to ϕ' the vectors $\mathbf{c}$ and $\mathbf{v}$ are collinear and the formula for the scalar speed is given by equation 4.C-1.

K is a bivariate von Mises distribution

$$K = \frac{1}{2} K(\phi - \phi_1) + \frac{1}{2} K(\phi - \phi_2)$$

Diffusion

$$
\begin{aligned}
d_{xx}(\mathbf{x}) &= \lim_{\tau\to 0}\frac{1}{2\tau}\int (x'-x)^2 k(\mathbf{x},\mathbf{a},\tau)\,d\mathbf{a} \\
&= \lim_{\tau\to 0}\frac{1}{2\tau}\int_0^\infty \rho^2 f(\rho)\,d\rho \int_{-\pi}^{\pi}\cos^2(\phi)\left(\frac{1}{2}K(\phi-\phi_1)+\frac{1}{2}K(\phi-\phi_2)\right)\,d\phi \\
&= \lim_{\tau\to 0}\frac{1}{4\tau}\int_0^\infty \rho^2 f(\rho)\,d\rho\left(1+\cos(2\phi_1)\int_{-\pi}^{\pi}\cos(2(\phi-\phi_1))\frac{1}{2}K(\phi-\phi_1)\right. \\
&\quad \left.+\cos(2\phi_2)\int_{-\pi}^{\pi}\cos(2(\phi-\phi_2))\frac{1}{2}K(\phi-\phi_2)\,d\phi\right) \\
&= \lim_{\tau\to 0}\frac{\overline{\rho^2}}{4\tau}\left(1+\left(\frac{1}{2}\cos(2\phi_1)+\frac{1}{2}\cos(2\phi_2)\right)\left(\frac{I_2(\kappa)}{I_0(\kappa)}\right)\right)
\end{aligned}
$$

$$
\begin{aligned}
d_{yy}(\mathbf{x}) &= \lim_{\tau\to 0}\frac{1}{2\tau}\int (y'-y)^2 k(\mathbf{x},\mathbf{a},\tau)\,d\mathbf{a} \\
&= \lim_{\tau\to 0}\frac{1}{2\tau}\int_0^\infty \rho^2 f(\rho)\,d\rho \int_{-\pi}^{\pi}\cos^2(\phi)\left(\frac{1}{2}K(\phi-\phi_1)+\frac{1}{2}K(\phi-\phi_2)\right)\,d\phi \\
&= \lim_{\tau\to 0}\frac{1}{4\tau}\int_0^\infty \rho^2 f(\rho)\,d\rho\left(1-\cos(2\phi_1)\int_{-\pi}^{\pi}\cos(2(\phi-\phi_1))\frac{1}{2}K(\phi-\phi_1)\right. \\
&\quad \left.-\cos(2\phi_2)\int_{-\pi}^{\pi}\cos(2(\phi-\phi_2))\frac{1}{2}K(\phi-\phi_2)\,d\phi\right) \\
&= \lim_{\tau\to 0}\frac{\overline{\rho^2}}{4\tau}\left(1-\left(\frac{1}{2}\cos(2\phi_1)+\frac{1}{2}\cos(2\phi_2)\right)\left(\frac{I_2(\kappa)}{I_0(\kappa)}\right)\right)
\end{aligned}
$$

$$
\begin{aligned}
d_{xy}(\mathbf{x}) &= \lim_{\tau\to 0}\frac{1}{2\tau}\int (x'-x)(y'-y) k(\mathbf{x},\mathbf{a},\tau)\,d\mathbf{a} \\
&= \lim_{\tau\to 0}\frac{1}{2\tau}\int_0^\infty \rho^2 f(\rho)\,d\rho \int_{-\pi}^{\pi}\sin(\phi)\cos(\phi)\left(\frac{1}{2}K(\phi-\phi_1)+\frac{1}{2}K(\phi-\phi_2)\right)\,d\phi \\
&= \lim_{\tau\to 0}\frac{1}{4\tau}\int_0^\infty \rho^2 f(\rho)\,d\rho\left(\sin(2\phi_1)\int_{-\pi}^{\pi}\cos(2(\phi-\phi_1))\frac{1}{2}K(\phi-\phi_1)\right. \\
&\quad \left.+\sin(2\phi_2)\int_{-\pi}^{\pi}\cos(2(\phi-\phi_2))\frac{1}{2}K(\phi-\phi_2)\,d\phi\right) \\
&= \lim_{\tau\to 0}\frac{\overline{\rho^2}}{4\tau}\left(\frac{1}{2}\sin(2\phi_1)+\frac{1}{2}\sin(2\phi_2)\right)\left(\frac{I_2(\kappa)}{I_0(\kappa)}\right)
\end{aligned}
$$

$$
d_{yx}(\mathbf{x}) = d_{xy}(\mathbf{x}).
$$

Advection

The advection coefficient,

$$\mathbf{c}(\mathbf{x}) \cdot \mathbf{v}(\mathbf{x}) \;=\; \lim_{\tau \to 0} \frac{1}{\tau} \int (\mathbf{x}' - \mathbf{x}) k(\mathbf{x}, \mathbf{a}, \tau)\, d\mathbf{a}$$

is the first moment of the redistribution kernel $k(\mathbf{x}, \mathbf{a}, \tau)$. Because the bivariate von Mises distribution is symmetric, the first moment is zero. Therefore the advection coefficient is also zero.

4.D Coefficients of the mean first passage time model

Table 4.7: Coefficients of the mean first passage time model for wolf movement in response to linear features. Models: NR = no response, AD = anisotropic diffusion on linear features, AD+BIAS = AD including bias towards linear features, AD+BIAS+RD = AD+BIAS with reduced diffusion near linear features. Movement parameters estimated from distributions of move distances (ρ) and relative move directions (κ). The direction towards the nearest linear feature is μ.

NR:

$d_{xx}(\mathbf{x}) = d_{yy}(\mathbf{x}) = \lim_{\tau \to 0} \frac{\overline{\rho^2}}{4\tau}$, everywhere
$d_{xy}(\mathbf{x}) = d_{yx}(\mathbf{x}) = 0$
$\mathbf{c}(\mathbf{x}) = \mathbf{0}$

AD:

$$d_{xx}(\mathbf{x}) = \begin{cases} \lim_{\tau \to 0} \frac{\overline{\rho^2}}{4\tau} \left(1 + \left(\frac{1}{2}\cos(2(\mu + \pi/2)) + \frac{1}{2}\cos(2(\mu - \pi/2))\right)\left(\frac{I_2(\kappa)}{I_0(\kappa)}\right)\right), \text{on} \\ \lim_{\tau \to 0} \frac{\overline{\rho^2}}{4\tau}, \text{off} \end{cases}$$

$$d_{yy}(\mathbf{x}) = \begin{cases} \lim_{\tau \to 0} \frac{\overline{\rho^2}}{4\tau} \left(1 - \left(\frac{1}{2}\cos(2(\mu + \pi/2)) + \frac{1}{2}\cos(2(\mu - \pi/2))\right)\left(\frac{I_2(\kappa)}{I_0(\kappa)}\right)\right), \text{on} \\ \lim_{\tau \to 0} \frac{\overline{\rho^2}}{4\tau}, \text{off} \end{cases}$$

$$d_{xy}(\mathbf{x}) = \begin{cases} \lim_{\tau \to 0} \frac{\overline{\rho^2}}{4\tau} \left(\frac{1}{2}\sin(2(\mu + \pi/2)) + \frac{1}{2}\sin(2(\mu - \pi/2))\right)\left(\frac{I_2(\kappa)}{I_0(\kappa)}\right), \text{on} \\ 0, \text{off} \end{cases}$$

$d_{yx}(\mathbf{x}) = d_{xy}(\mathbf{x})$
$\mathbf{c}(\mathbf{x}) = \mathbf{0}$

AD+BIAS/AD+BIAS+RD:

$$d_{xx}(\mathbf{x}) = \begin{cases} \lim_{\tau \to 0} \frac{\overline{\rho^2}}{4\tau} \left(1 + \frac{1}{2}\left(\cos(2(\mu + \pi/2)) + \frac{1}{2}\cos(2(\mu - \pi/2))\right)\left(\frac{I_2(\kappa)}{I_0(\kappa)}\right)\right), \text{on} \\ \lim_{\tau \to 0} \frac{\overline{\rho^2}}{4\tau} \left(1 + \cos(2\mu)\frac{I_2(\kappa)}{I_0(\kappa)}\right), \text{near} \\ \lim_{\tau \to 0} \frac{\overline{\rho^2}}{4\tau}, \text{far} \end{cases}$$

$$d_{yy}(\mathbf{x}) = \begin{cases} \lim_{\tau \to 0} \frac{\overline{\rho^2}}{4\tau} \left(1 - \frac{1}{2}\left(\cos(2(\mu + \pi/2)) + \frac{1}{2}\cos(2(\mu - \pi/2))\right)\left(\frac{I_2(\kappa)}{I_0(\kappa)}\right)\right), \text{on} \\ \lim_{\tau \to 0} \frac{\overline{\rho^2}}{4\tau} \left(1 - \cos(2\mu)\frac{I_2(\kappa)}{I_0(\kappa)}\right), \text{near} \\ \lim_{\tau \to 0} \frac{\overline{\rho^2}}{4\tau}, \text{far} \end{cases}$$

$$d_{xy}(\mathbf{x}) = \begin{cases} \lim_{\tau \to 0} \frac{\overline{\rho^2}}{4\tau} \left(\frac{1}{2}\sin(2(\mu + \pi/2)) + \frac{1}{2}\sin(2(\mu - \pi/2))\right)\left(\frac{I_2(\kappa)}{I_0(\kappa)}\right), \text{on} \\ \lim_{\tau \to 0} \frac{\overline{\rho^2}}{4\tau} \left(\sin(2\mu)\frac{I_2(\kappa)}{I_0(\kappa)}\right), \text{near} \\ 0, \text{far} \end{cases}$$

$d_{yx}(\mathbf{x}) = d_{xy}(\mathbf{x})$

$$\mathbf{c}(\mathbf{x}) = \begin{cases} \lim_{\tau \to 0} \frac{\overline{\rho}}{2\tau} \frac{I_1(\kappa)}{I_0(\kappa)} \mathbf{v}(\mathbf{x}), \text{near} \\ 0, \text{elsewhere} \end{cases}$$

4.E Results for 5-min data

Table 4.8: Movement rates in different regions (5-min)

Wolf	N	Region	Parameter (α)	90% CI
w230	308	On	100.74	(87.44,115.24)
	361	Near<50 m	80.64	(70.56,139.08)
	1017	Near< 100m	76.88	(71.19,82.92)
	959	Far> 50m	71.21	(65.73,76.79)
	303	Far> 100m	63.44	(55.02,71.74)
w232	116	On	160.79	(130.81,191.24)
	152	Near< 50m	107.22	(78.42,139.08)
	512	Near< 100m	91.57	(79.82,103.88)
	754	Far> 50m	78.70	(69.71,88.03)
	394	Far> 100m	72.99	(61.46,84.46)
w233	147	On	138.58	(118.97,160.2)
	373	Near< 50m	49.49	(41.87,57.28)
	952	Near< 100m	53.83	(48.84,59.32)
	1078	Far> 50m	71.19	(65.73,76.50)
	498	Far> 100m	88.15	(78.97,97.38)
w234	155	On	188.76	(163.17,208.29)
	250	Near< 50m	123.74	(107.75,139.27)
	827	Near< 100 m	101.12	(93.71,108.88)
	1191	Far> 50m	85.59	(79.62,91.02)
	614	Far> 100m	80.21	(72.77,87.55)

4.F Numerical method

The spatially heterogeneous mean first passage time problem was solved using COMSOL Multiphysics. Solving a model required three steps (see sample code below for further details). First, the landscape (locations of linear features and prey) was defined in ESRI ArcMap, imported into MATLAB and saved as a .mat file. Second, the PDE data structure was defined and initialized, so that it contained all the information necessary to solve the equation. Finally, the model was defined and solved in COMSOL. The model was defined using the PDE, coefficient form (stationary analysis) application mode. The general pde in this form is

$$\begin{cases} \nabla \cdot (-c\nabla u - \alpha u + \gamma) + \beta \cdot \nabla u + au = f & \text{in } \Omega \\ \mathbf{n} \cdot (c\nabla + \alpha u - \gamma) + qu = g - h^T \mu & \text{on } \partial\Omega \\ hu = r & \text{on } \partial\Omega \end{cases} \tag{4.C-2}$$

where Ω is the computational domain, $\partial\Omega$ is the boundary, and $\mathbf{n}$ is the outward normal on $\partial\Omega$. The second equation is the generalized Neumann boundary condition and the third equation is the generalized Dirichlet boundary condition. To adapt the general equation for the mean first passage time equation I specified the coefficients as follows

$$\begin{aligned} d_a,\ \alpha,\ \gamma,\ a &= 0 \\ f &= 1 \\ \beta &= [\,-look(x,y,5) \ \ -look(x,y,6)\,] \\ c &= \begin{bmatrix} look(x,y,1) & look(x,y,2) \\ look(x,y,3) & look(x,y,4) \end{bmatrix} \end{aligned}$$

where $look(x,y,i)$ is a MATLAB function that looks up the spatially dependent advection and diffusion coefficients in a matrix defined in the PDE data structure. The insulating boundary condition on the exterior boundaries is specified using the generalized Neumann boundary condition ($q = g = 0$) and the absorbing boundary condition on the interior boundary is specified using the generalized Dirchlet boundary condition ($h = 1$ and $r = 0$). Therefore the mean first passage time problem is stated as

$$\begin{cases} \nabla \cdot (c(\mathbf{x})\nabla u) + \beta(\mathbf{x}) \cdot \nabla u + 1 = 0 & \text{in } \Omega \\ \mathbf{n} \cdot (c\nabla u) = 0 & \text{on } \partial\Omega_{\text{ext}} \\ u = 0 & \text{on } \partial\Omega_{\text{int}} \end{cases} \tag{4.C-3}$$

Sample code.

1. Example m-file defining the PDE data structure and initializing the coefficient matrices

```
%
% MATLAB M-file defining the model:
% M1LOPu
%
tic;
global pde

% domain definition
pde.area = [25.020,25.020]; % size of the domain,
% distance in x and y.
pde.delta = 0.03; % grid size for coefficients
load('prey_uniform.mat'); % load the prey locations
pde.prey = P; % location of prey (x,y), radius of perception range
load('points20.mat'); % load the landscape configuration
pde.land = X; % configuration of LFs in the landscape
% grid number, region, direction towards nearest linear feature

% time definition
pde.t = 0.08; % timestep (1/frequency of data)

% movement definition
% on
pde.m1_on = 0.071; % mean move distance
pde.m2_on = 0.017; % mean squared move distance
pde.kappa_on = 0; % concentration parameter
% near
```

```
pde.m1_near = 0.071; % mean move distance
pde.m2_near = 0.017; % mean squared move distance
pde.kappa_near = 0; % concentration parameter
% far
pde.m1_far = 0.071; % mean move distance
pde.m2_far = 0.017; % mean squared move distance
pde.kappa_far = 0; % concentration parameter

% initialize the coefficient matrices
getdxx;
getdxy;
getdyx;
getdyy;
getcx;
getcy;

% initalize the geometry
geominit
pde.s = s;
% save the .m file that defines the pde
save('M1L0Pu','pde')

% clear pde
clear pde
toc;
```

2. Functions to find the advection and diffusion coefficients (getdxx, getdxy, getdyx, getdyy, getcx, and get cy)

```
% function to calculate the coefficient dxx
% Inputs:   info = matrix (Nx3) {ID,Region,AngleTowards}
% Outputs:  dxx = matrix (NxN) with coefficients for each cell
% define the global variables
global pde
% initialize coefficient matrix
n = size(pde.land,1);
```

```
dxx = zeros(1,n);
% loop through each cell and compute the coefficient
for i = 1:n
region = pde.land(i,2);% define switch
% switch cases based on region
switch region
case 1
dxx(i) = (pde.m2_on/(4*pde.t))...
*(1+(besseli(2,pde.kappa_on)/besseli(0,pde.kappa_on))...
*(0.5*cos(2*(pde.land(i,3)-pi/2))...
+ 0.5*cos(2*(pde.land(i,3)+pi/2))));
case 2
dxx(i) = (pde.m2_near/(4*pde.t))...
*(1+(besseli(2,pde.kappa_near)/besseli(0,pde.kappa_near))...
*(cos(2*pde.land(i,3))));
case 3
dxx(i) = pde.m2_far/(4*pde.t);
end
end
pde.dxx = reshape(dxx,sqrt(n),sqrt(n));

% function to calculate the coefficient dxy
% Inputs:   info = matrix (Nx4) {ID,Region,AngleAlong,AngleTowards}
% Outputs:  dxy = matrix (NxN) with coefficients for each cell
% define the global variables
global pde
% initialize coefficient matrix
n = size(pde.land,1);
dxy = zeros(1,n);
% loop through each cell and compute the coefficient
for i = 1:n
region = pde.land(i,2);% define switch
% switch cases based on region
switch region
case 1
dxy(i) = pde.m2_on/(4*pde.t)...
```

```
*(besseli(2,pde.kappa_on)/besseli(0,pde.kappa_on))...
*(0.5*sin(2*(pde.land(i,3)-pi/2))+...
0.5*sin(2*(pde.land(i,3)+pi/2)));
case 2
dxy(i) = pde.m2_near/(4*pde.t)...
*(besseli(2,pde.kappa_near)/besseli(0,pde.kappa_near))...
*(sin(2*pde.land(i,3)));
case 3
dxy(i) = 0;
end
end
pde.dxy = reshape(dxy,sqrt(n),sqrt(n));

% function to calculate the coefficient dyx
% Inputs:   info = matrix (Nx4) {ID,Region,AngleAlong,AngleTowards}
% Outputs:  dyx = matrix (NxN) with coefficients for each cell
% define the global variables
global pde
% initialize coefficient matrix
n = size(pde.land,1);
dyx = zeros(1,n);
% loop through each cell and compute the coefficient
for i = 1:n
region = pde.land(i,2);% define switch
% switch cases based on region
switch region
case 1
dyx(i) = pde.m2_on/(4*pde.t)...
*(besseli(2,pde.kappa_on)/besseli(0,pde.kappa_on))...
*(0.5*sin(2*(pde.land(i,3)-pi/2))...
+ 0.5*sin(2*(pde.land(i,3)+pi/2)));
case 2
dyx(i) = pde.m2_near/(8*pde.t)...
*(besseli(2,pde.kappa_near)/besseli(0,pde.kappa_near))...
*(sin(2*pde.land(i,3)));
case 3
```

```
dyx(i) = 0;
end
end
pde.dyx = reshape(dyx,sqrt(n),sqrt(n));

% function to calculate the coefficient dyy
% Inputs:   info = matrix (Nx3) {ID,Region,AngleTowards}
% Outputs:  dyy = matrix (NxN) with coefficients for each cell
%
% define the global variables
global pde
% initialize coefficient matrix
n = size(pde.land,1);
dyy = zeros(1,n);
% loop through each cell and compute the coefficient
for i = 1:n
region = pde.land(i,2);% define switch
% switch cases based on region
switch region
case 1
dyy(i) = (pde.m2_on/(4*pde.t))...
*(1-(besseli(2,pde.kappa_on)/besseli(0,pde.kappa_on))...
*(0.5*cos(2*(pde.land(i,3)-pi/2))...
+ 0.5*cos(2*(pde.land(i,3)+pi/2))));
case 2
dyy(i) = (pde.m2_near/(4*pde.t))...
*(1-(besseli(2,pde.kappa_near)/besseli(0,pde.kappa_near))...
*(cos(2*pde.land(i,3))));
case 3
dyy(i) = pde.m2_far/(4*pde.t);
end
end
pde.dyy = reshape(dyy,sqrt(n),sqrt(n));

% function to calculate the coefficient cx
% Inputs:   info = matrix (Nx3) {ID,Region,AngleTowards}
```

```
% Outputs:  cx = matrix (NxN) with coefficients for each cell
% define the global variables
global pde
% initialize coefficient matrix
n = size(pde.land,1);
cx = zeros(1,n);
% loop through each cell and compute the coefficient
for i = 1:n
region = pde.land(i,2);% define switch
% switch cases based on region
switch region
case 1
cx(i) = 0;
case 2
cx(i) = (pde.m1_near/(2*pde.t))...
*(besseli(1,pde.kappa_near)/besseli(0,pde.kappa_near))...
*cos(pde.land(i,3));
case 3
cx(i) = 0;
end
end
pde.cx = reshape(cx,sqrt(n),sqrt(n));

% function to calculate the coefficient cy
% Inputs:   info = matrix (Nx3) {ID,Region,AngleTowards}
% Outputs:  cy = matrix (NxN) with coefficients for each cell
% define the global variables
global pde
% initialize coefficient matrix
n = size(pde.land,1);
cy = zeros(1,n);
% loop through each cell and compute the coefficient
for i = 1:n
region = pde.land(i,2);% define switch
% switch cases based on region
switch region
```

```
case 1
cy(i) = 0;
case 2
cy(i) = (pde.m1_near/(2*pde.t))...
*(besseli(1,pde.kappa_near)/besseli(0,pde.kappa_near))...
*sin(pde.land(i,3));
case 3
cy(i) = 0;
end
end
pde.cy = reshape(cy,sqrt(n),sqrt(n));
```

3. The routine to initialize the geometry (domain and prey locations)

```
%
% script that takes a matrix pde.L and converts it into a
% form that can be used to initialize a geometry in FEMLAB
%
% Inputs:
% domain =  a 1 x 2 vector that contains the length and height of
% the rectangular domain.  The corner is assumed to be at (0,0).
% prey =  a 1 x 3 vector specifying the location of the prey
% and the radius of capture.
%
% global structures: pde
%
global pde
domain = pde.area;
prey = pde.prey;
% create the rectangular domain
r1 = rect2(domain(1),domain(2),'base','corner','pos',[0,0]);
%r2 = rect2(3,3,'base','center','pos',[0,0]);
% create a solid
s = solid2(r1);
% create the circles that represents the prey
for i=1:size(prey,1)
```

```
p = circ2(prey(i,3),'base','center','pos',[prey(i,1),prey(i,2)]);
% take the difference of the prey and the rest of the solid
s = s - p;
end
% make it part of the global pde structure
pde.geom = s;
```

4. The look function which looks up the coefficients for COMSOL

```
% function to lookup coefficients in the tables
% Inputs:   x = vector of x coordinates of the nodes
%           y = vector of y coordinates of the nodes
%           c = string representing the coefficient wanted
%
function coeff = look(x,y,c)
% define global variables
global pde
% initialize ans
coeff = zeros(length(x),1);
scoeff = size(x);

for i = 1:length(x)
    % find index for coefficient matrix
    m = ceil((pde.area(1)-y(i))/pde.delta);
    n = ceil(x(i)/pde.delta);
    % define switch
    switch c(i)
        case 1
            coeff(i) = pde.dxx(m,n);
        case 2
            coeff(i) = pde.dxy(m,n);
        case 3
            coeff(i) = pde.dyx(m,n);
```

```
        case 4
            coeff(i) = pde.dyy(m,n);
        case 5
            coeff(i) = pde.cx(m,n);
        case 6
            coeff(i) = pde.cy(m,n);
    end
end
% reshape ans
coeff = reshape(coeff,scoeff);
```

Literature cited

Bailey, H., and P. Thompson. 2006. Quantitative analysis of bottlenosed dolphin movement patterns and their relation to foraging. Journal of Animal Ecology **75**:456–465.

Barnard, G. 1963. Discussion of: The Spectral Analysis of Point Processes (Barlett, MS). Journal of the Royal Statistical Society. Series B (Methodological) **25**:294.

Bell, W. 1991. Searching Behaviour. Animal Behaviour Series, Chapman and Hall, London.

Berg, H. 1993. Random Walks in Biology. Princeton University Press.

Bergerud, A., and J. Elliot. 1986. Dynamics of caribou and wolves in northern British Columbia. Canadian Journal of Zoology **64**:1515–1529.

Cain, M. 1985. Random search by herbivorous insects: a simulation model. Ecology **66**:876–888.

Callaghan, C., 2002. The ecology of gray wolf (canis lupus) habitat use, survival, and persistence in the central rocky mountains, Canada. Ph.D. thesis, University of Guelph.

Clarkson, P., K. Schmidt, and J. Gunson, 1984. Evaluation of wolf-ungulate predation near Nordegg, Alberta: first year progress rep. Technical report, Alberta Fish and Wildlife Division.

Cuddington, K., and P. Yodzis. 2002. Predator-Prey Dynamics and Movement in Fractal Environments. The American Naturalist **160**:119–134.

De Roos, A., E. McCauley, and W. Wilson. 1991. Mobility versus density-limited predator-prey dynamics on different spatial scales. Proceedings of the Royal Society B-Biological Sciences **246**:117–122.

Dennis, B., and M. Taper. 1994. Density -dependence in time-series observations and natural population - estimation and inference. Ecological Monographs **64**:205–224.

Dzus, E., 2001. Status of the Woodland Caribou (Rangifer tarandus caribou) in Alberta. Technical Report 30, Alberta Environment, Fisheries and Wildlife Management Division, and Alberta Conservation Associate, Edmonton.

Edmonds, E., and M. Bloomfield, 1984. A study of woodland caribou (Rangifer tarandus caribou) in west central Alberta, 1979 to 1983. Technical report, Alberta Energy and Natural Resources, Fish and Wildlife Division, Edmonton, Alberta, Canada.

Efron, B., and R. Tibshirani. 1993. An Introduction to the Bootstrap. Chapman and Hall/CRC.

Fauchauld, P., and R. Tveraa. 2003. Using first passage time in the analysis of area-restricted search and habitat selection. Ecology **84**:282–288.

Fisher, N. 1993. Statistical analysis of circular data. Cambridge University Press.

Frair, J., E. Merrill, D. Visscher, D. Fortin, H. Beyer, and J. Morales. 2005. Scales of movement by elk (Cervus elaphus) in response to heterogeneity in forage resources and predation risk. Landscape Ecology **20**:273–287.

Hebblewhite, M., and D. Pletscher. 2002. Effects of elk group size on predation by wolves. Canadian Journal of Zoology **80**:800–809.

Holling, C. 1959. The components of predation as revealed by a study of small mammal predation of the European pine sawfly. The Canadian Entomologist **91**.

Hurford, A., 2005. Wolf movement within and beyond territory boundary. Master's thesis, University of Alberta.

Jalkotzy, M., P. Ross, and M. Nasserden, 1997. The Effects of Linear developments on Wildlife: A Review of Selected Scientific Literature. Technical report, Arc Wildlife Services Ltd.

James, A., 1999. Effects of Industrial Development on the Predator-Prey Relationship Between Wolves and Caribou in Northeastern Alberta. Ph.D. thesis, Universtiy of Alberta.

James, A., and A. Stuart-Smith. 2000. Distribution of caribou and wolves in relation to linear corridors. Journal of Wildlife Management **64**:154–159.

Jerde, C., and D. Visscher. 2005. GPS measurement error influences on movement model parameterization. Ecological Applications **15**:806 - 810.

Johnson, A., B. Wiens, and T. Crist. 1992. Animal movements and population dynamics in heterogeneous landscapes. Landscape Ecology **7**:63–75.

Kareiva, P., and N. Shigesada. 1983. Analyzing Insect Movement as a Correlated Random Walk. Oecologia **56**:234–238.

Lima, S., and P. Zollner. 1996. Towards a behavioral ecology of ecological landscapes. TREE **11**:1310–135.

Linke, J., S. Franklin, F. Huettman, and G. Stenhouse. 2005. Seismic cutlines, changing landscape metrics and grizzly bear landscape use in Alberta. Landscape Ecology **20**:811–826.

Mardia, K. 1975. Statistics for directional data. Journal of the Royal Statistical Society. Series B (Methodological) **37**:349–393.

McCauley, E., W. Wilson, and A. De Roos. 1993. Dynamics of age-structured and spatially structured predator-prey interactions: individual-based models and population-level formulations. The American Naturalist **142**:412–442.

Mech, D., and L. Boitani. 2003. Wolves: Behavior, Ecology, and Conservation. University of Chicago Press.

Moorcroft, P., and M. Lewis. 2006. Mechanistic Home Range Analysis. Princeton University Press.

Pianka, E. 1966. Convexity, desert lizards, and spatial heterogeneity. Ecology **47**:1055–1059.

Redner, S. 2001. A Guide to First-Passage Processes. Cambridge University Press.

Royall, M. 1997. Statistical Evidence. Chapman and Hall.

Schmidt, K., and J. Gunson, 1985. Evaluation of wolf-ungulate predation near Nordegg, Alberta: second year progress rep. Technical report, Alberta Fish and Wildlife Division.

Schwartz, C., and A. Franzmann, editors. 1998. Ecology and Management of the North American Moose. Smithstonian Books.

Solomon, M. 1949. The natural control of animal populations. Journal of Animal Ecology **18**:1–35.

Thurber, J., R. Peterson, T. Drummer, and S. Thomasma. 1994. Gray wolf response to refuge boundaries and roads in Alaska. Wildlife Society Bulletin **22**:61 – 68.

Timoney, K., and P. Lee. 2001. Environmental management in resource-rich Alberta, Canada: first world jurisdiction, third world analogue? Journal of Environmental Management **63**:387 – 405.

Turchin, P. 1998. Quantitative Analysis of Movement. Sinaur Associates, Inc Publishers.

Weins, J., 2001. Dispersal, Chapter the landscape context of dispersal, pages 96–109. Oxford University Press.

Whittington, J., C. St. Clair, and G. Mercer. 2004. Path Tortuosity adn the Permeability of Roads and Trails to Wolf Movement. Ecology and Society **9**.

Whittington, J., C. St. Clair, and G. Mercer. 2005. Spatial responses of wolves to roads and trails in mountain valleys. Ecological Applications **15**:543 – 553.

Zar, J. H. 1996. Biostatistical Analysis 3rd edition. Prentice Hall.

Zollner, P., and S. Lima. 1999. Search strategies for landscape-level interpatch movements. Ecology **80**:1019–1030.

Chapter 5

Concluding Remarks

This thesis was motivated by a need to understand the potential implications of increasing linear feature density for the predator-prey dynamics of wolves and ungulates in the central east slopes of the Rocky mountains (Alberta, Canada). In the concluding remarks I draw connections among chapters and highlight the major contributions of the thesis, while indicating areas for further research.

In Chapter 1 I demonstrated that ignoring GPS measurement error led to location misclassification and subsequent confounded inference about animal use of linear features. To address this problem I developed a new method of rigourously selecting buffers for linear features, which was applied in the analysis of wolf movement on linear features in Chapter 3. This particular method could be extended to address small habitats in general. Understanding the potential for misclassification in these rare habitats would be critical for their conservation and management.

Chapter 2 introduced mean first passage time as an alternate approach to animal movement analysis, which compliments the Fokker-Planck equation for space use. I showed that mean first passage time can be used to answer questions about animal encounter rates with landscape features, and applied the method to understanding how encounter rates between predators and prey were impacted by spatial variation in animal movement due to territoriality (Chapter 2) and landscape heterogeneity created by linear features (Chapter 3). Mean first passage time was calculated using a differential equation, which I mechanistically derived from first principles following the approach of Moorcroft and Lewis (2006). Because of the mechanistic nature of the derivation, the differential equation accounts for movement behaviour in response to landscape heterogeneity and allows empirical data to be directly incorporated into the model. I also used first passage time to extend the Holling disk

equation, deriving new functional responses for animals moving according to pure advection and simple diffusion processes. I showed that diffusive movement with handling time led to a sigmoidal functional response. Therefore, the Holling Type III functional response can be derived from the assumption of diffusive movement, without invoking prey switching or prey refuges arguments. Because of its ability to incorporate spatial variation in animal movement behaviour and distribution of 'capture' locations, mean first passage time has the potential to be applied to many other questions in spatial ecology, such as mate-finding, interactions between territory-holders, or spatial disease dynamics.

In Chapter 3 I proposed and tested with empirical data a mechanism through which linear features may impact wolf-ungulate interactions. I characterized the individual movement response of wolves to linear features using GPS location data and statistical techniques. Wolf response to linear features varied among individuals and additional data would be required to further understand this variation. To connect individual movement to search time for prey I used first passage time analysis. I applied the methods developed in Chapter 2 to demonstrate the potential impact of wolf movement behaviour, increasing linear feature density, and prey distribution on search time. The implication of changing search times for wolf-ungulate encounters was demonstrated using the functional response. I concluded that linear features would increase encounter rates between wolves and ungulates, and predicted that assuming a Holling Type II functional response this would lead to increased consumption of ungulates.

This thesis develops and uses a new theoretical approach, first passage time analysis, to address a question of significant ecological interest, the effect of increasing linear feature density on wolf-ungulate interactions in the central east slopes of the Rockies. It contributes a new equation for animal movement, and opens up the potential for further research of animal movement in spatial heterogeneous landscapes.

Literature cited

Moorcroft, P., and M. Lewis. 2006. Mechanistic Home Range Analysis. Princeton University Press.